

AD \_\_\_\_\_

Award Number: DAMD17-99-1-9559

TITLE: Toxic Neuronal Death by Glyceraldehyde-3-Phosphate  
Dehydrogenase and Mitochondria

PRINCIPAL INVESTIGATOR: William Tatton, Ph.D.

CONTRACTING ORGANIZATION: Mount Sinai School of Medicine  
New York, New York 10029

REPORT DATE: August 2000

TYPE OF REPORT: Annual

PREPARED FOR: U.S. Army Medical Research and Materiel Command  
Fort Detrick, Maryland 21702-5012

DISTRIBUTION STATEMENT: Approved for public release;  
Distribution unlimited

The views, opinions and/or findings contained in this report are those of the author(s) and should not be construed as an official Department of the Army position, policy or decision unless so designated by other documentation.

**REPORT DOCUMENTATION PAGE**Form Approved  
OMB No. 074-0188

Public reporting burden for this collection of information is estimated to average 1 hour per response, including the time for reviewing instructions, searching existing data sources, gathering and maintaining the data needed, and completing and reviewing this collection of information. Send comments regarding this burden estimate or any other aspect of this collection of information, including suggestions for reducing this burden to Washington Headquarters Services, Directorate for Information Operations and Reports, 1215 Jefferson Davis Highway, Suite 1204, Arlington, VA 22202-4302, and to the Office of Management and Budget, Paperwork Reduction Project (0704-0188), Washington, DC 20503

<b>1. AGENCY USE ONLY (Leave blank)</b>		<b>2. REPORT DATE</b> August 2000	<b>3. REPORT TYPE AND DATES COVERED</b> Annual (1 Jul 99 -1 Jul 00)	
<b>4. TITLE AND SUBTITLE</b> Toxic Neuronal Death by Glyceraldehyde-3-Phosphate Dehydrogenase and Mitochondria			<b>5. FUNDING NUMBERS</b> DAMD17-99-1-9559	
<b>6. AUTHOR(S)</b> William Tatton, Ph.D.				
<b>7. PERFORMING ORGANIZATION NAME(S) AND ADDRESS(ES)</b>  Mount Sinai School of Medicine New York, New York 10029 E-MAIL: william.tatton@mssm.edu			<b>8. PERFORMING ORGANIZATION REPORT NUMBER</b>	
<b>9. SPONSORING / MONITORING AGENCY NAME(S) AND ADDRESS(ES)</b>  U.S. Army Medical Research and Materiel Command Fort Detrick, Maryland 21702-5012			<b>10. SPONSORING / MONITORING AGENCY REPORT NUMBER</b>	
<b>11. SUPPLEMENTARY NOTES</b>  Report contains color graphics.				
<b>12a. DISTRIBUTION / AVAILABILITY STATEMENT</b> Approved for public release; distribution unlimited			<b>12b. DISTRIBUTION CODE</b>	
<b>13. ABSTRACT (Maximum 200 Words)</b>  This proposal was designed to examine the role of glyceraldehyde-3-phosphate dehydrogenase (GAPDH), mitochondrial permeability and mitochondrial membrane potential ( $\Delta\Psi_M$ ) in toxic neuronal apoptosis. Mitochondria have been shown to play a critical decisional role in some forms of apoptotic cell death. Determining the signaling pathways for specific forms of toxin induced apoptosis might reveal potential pharmacological targets which could be manipulated to slow or alleviate the apoptosis. To address these issues, we proposed a series of experiments which include an <i>in vitro</i> study of neurons and neuron-like cells that will be immunoreacted to determine specific toxic insults that involve changes in GAPDH levels or subcellular distribution, changes in $\Delta\Psi_M$ and increased mitochondrial membrane permeability with the release of factors that signal for apoptotic degradation. We proposed to examine cell lines of PC12 and 3T3 cells transfected so as to produce inducible GAPDH upregulation. The direct and joint actions of GAPDH and $NAD^+$ will be examined using a cell free system of nuclear, mitochondrial and cytosolic subfractions. Finally we proposed to examine whether GAPDH alters the transcription and/or translation of specific subsets of genes and/or their RNA targets using a lysate system.				
<b>14. SUBJECT TERMS</b> Neurotoxin, Glyceraldehyde-3-Phosphate Dehydrogenase, Apoptosis, Mitochondria, Mitochondrial Membrane Potential, Protein Synthesis Dependence, Fibroblasts, Cell Free System, Inducible Gene Transfection			<b>15. NUMBER OF PAGES</b>  48	
			<b>16. PRICE CODE</b>	
<b>17. SECURITY CLASSIFICATION OF REPORT</b> Unclassified	<b>18. SECURITY CLASSIFICATION OF THIS PAGE</b> Unclassified	<b>19. SECURITY CLASSIFICATION OF ABSTRACT</b> Unclassified	<b>20. LIMITATION OF ABSTRACT</b> Unlimited	

## FOREWORD

Opinions, interpretations, conclusions and recommendations are those of the author and are not necessarily endorsed by the U.S. Army.

N/A Where copyrighted material is quoted, permission has been obtained to use such material.

N/A Where material from documents designated for limited distribution is quoted, permission has been obtained to use the material.

N/A Citations of commercial organizations and trade names in this report do not constitute an official Department of Army endorsement or approval of the products or services of these organizations.

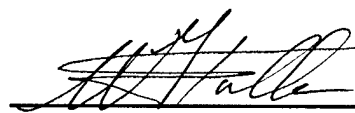
X In conducting research using animals, the investigator(s) adhered to the "Guide for the Care and Use of Laboratory Animals," prepared by the Committee on Care and use of Laboratory Animals of the Institute of Laboratory Resources, national Research Council (NIH Publication No. 86-23, Revised 1985). | WT.

N/A For the protection of human subjects, the investigator(s) adhered to policies of applicable Federal Law 45 CFR 46. | WT.

N/A In conducting research utilizing recombinant DNA technology, the investigator(s) adhered to current guidelines promulgated by the National Institutes of Health.

N/A In the conduct of research utilizing recombinant DNA, the investigator(s) adhered to the NIH Guidelines for Research Involving Recombinant DNA Molecules.

N/A In the conduct of research involving hazardous organisms, the investigator(s) adhered to the CDC-NIH Guide for Biosafety in Microbiological and Biomedical Laboratories. | WT.

  
PI - Signature      Aug. 6/2000  
Date

## Table of Contents

Cover.....	1
SF 298.....	2
Foreword.....	3
Introduction.....	5
Body.....	5
Key Research Accomplishments.....	15
Reportable Outcomes.....	15
Conclusions.....	16
References.....	16
Appendices.....	21

## **(5) Introduction**

This proposal was designed to examine the role of glyceraldehyde-3-phosphate dehydrogenase (GAPDH), mitochondrial permeability and mitochondrial membrane potential ( $\Delta\Psi_M$ ) in apoptotic neuronal death. Mitochondria have been shown to play a critical decisional role in the signaling pathways for some forms of apoptosis. Determining the signaling pathways for toxin induced neuronal apoptosis might reveal signaling proteins, which could serve as pharmacological targets for therapies that slow or alleviate toxic or disease-related apoptosis. To address these issues, we proposed a series of experiments which include an *in vitro* study of neurons and neuron-like cells that will be immunoreacted to determine specific toxic insults that involve changes in GAPDH levels or subcellular distribution, changes in  $\Delta\Psi_M$  and increased mitochondrial membrane permeability with the release of factors that signal for apoptotic degradation. We proposed to examine cell lines of PC12 and 3T3 cells transfected so as to produce inducible GAPDH upregulation. The direct and joint actions of GAPDH and  $NAD^+$  will be examined using a cell free system of nuclear, mitochondrial and cytosolic subfractions. Finally we proposed to examine whether GAPDH alters the transcription and/or translation of specific subsets of genes and/or their RNA targets using a lysate system. At this point, we have successfully addressed a number of the objectives critical to understanding GAPDH mediated apoptosis signaling and are on schedule for the completion of the study by the end of the third year.

## **(6) Body**

### **a) Background To Interpretation Of Progress In Research**

Toxins were originally thought to cause neuronal death through the process of necrosis, which is characterized by neuronal swelling, rupture and the initiation of an inflammatory response caused by the release of cytoplasmic contents. Recent work has shown that a variety of toxins can initiate apoptosis rather than necrosis in neurons (see (Jing et al., 1999; Tatton and Kish, 1997; Tatton et al., 1999) for details and references). Apoptosis is a relatively gradual, multi-step signaling process that culminates in cellular degradation involving cell shrinkage and the fragmentation of the cell into membrane wrapped bodies, which are phagocytosed without inducing inflammation. Accordingly, neurons dying by apoptosis disappear unaccompanied by the extensive tissue damage that accompanies inflammation. The occult nature of apoptotic death made toxic neuronal apoptosis difficult to recognize on standard pathological examination.

Apoptotic signaling events can be divided into three phases: an initiation phase, an effector phase and a degradation phase (Kroemer et al., 1995). The degradation phase is similar for different forms of apoptosis and its demonstration is used to differentiate apoptosis and necrosis. In the nucleus, the degradation phase includes protein (histones and lamins) stripping from DNA, DNA condensation and DNA cleavage by endonucleases. Most work on toxic neuronal apoptosis has been limited to the demonstration of apoptotic degradation and the demonstration that a variety of neuronal toxins can induce nerve cell loss through apoptosis..

Apart from glutamate toxicity, little is known about the signaling events that contribute to the initiation phases and decisional phases of toxic neuronal apoptosis. Various toxins appear to initiate different signaling pathways that lead to apoptotic degradation. The signaling involves series of protein-protein interactions and events in subcellular organelles.

If the signaling pathways for different forms of toxic neuronal apoptosis can be determined, and specific signaling proteins identified, then pharmacological agents targeted to those proteins may interrupt or oppose the signaling process and have the potential to reduce the neurological deficits induced by exposure to the toxin.

**Glyceraldehyde-3-Phosphate Dehydrogenase Signals For Some Neuronal Apoptosis.** Studies using antisense oligonucleotides established that the upregulation of the glycolytic enzyme, glyceraldehyde-3-phosphate dehydrogenase (GAPDH) is a critical signaling event for some forms of neuronal apoptosis (Ishitani and Chuang, 1996; Ishitani et al., 1996a; Saunders et al., 1997). The apoptotic pathways linking GAPDH upregulation to apoptotic degradation are not known.

We and others showed that the dense nuclear accumulation of GAPDH (Carlile et al., 2000; Ishitani et al., 1998; Saunders et al., 1997; Saunders et al., 1999; Sawa et al., 1997; Shashidharan et al., 1999), due at least in part to GAPDH translocation from the cytosol to the nucleus (Shashidharan et al., 1999), accompanies GAPDH upregulation in apoptosis. Although the dense nuclear accumulation appears to serve as a marker for GAPDH dependent apoptosis signaling, the role that the accumulation plays in apoptosis signaling is uncertain. GAPDH nuclear accumulation and upregulation have been reported for a number of forms of apoptosis in cultured

neuronal cells including those initiated in: 1) NGF differentiated PC12 cells by serum and NGF withdrawal (Carlile et al., 2000); 2) cerebellar granule neurons (CGNs) by the DNA toxin, cytosine arabinoside (Chen et al., 1999; Ishitani and Chuang, 1996; Saunders et al., 1997; Saunders et al., 1999); 3) CGNs and cerebrocortical neurons by prolonged maintenance in culture (so called aging) (Ishitani et al., 1996a; Ishitani et al., 1996b); 4) CGNs by reduction of media  $K^+$  levels (Ishitani et al., 1997); 5) COS cells by pro-oxidants (Shashidharan et al., 1999) and 6) CGNs by glutamate excitotoxicity (Eltner, Chalmers-Redman and Tatton, unpublished observations).

### **Possible GAPDH Signaling In Alzheimer's Disease**

Although GAPDH participation in apoptosis in cultured nerve cells has been extensively documented, its participation in neuronal apoptosis in intact animals or in human diseases has not been investigated. Based on the finding of GAPDH in amyloid plaques in the cerebral cortex of patients with Alzheimer's disease (Sunaga et al., 1995), it has been suggested that GAPDH may contribute to neuronal apoptosis in that disease.

### **RNA And Protein-Protein Interactions Of GAPDH**

GAPDH catalyzes the conversion of glyceraldehyde-3-phosphate to 1,3-bisphosphoglycerate in the glycolytic pathway. As part of the conversion, GAPDH converts  $NAD^+$  to the high-energy electron carrier NADH. A number of other possible functions have been attributed to GAPDH including roles in endocytosis, microtubule bundling, viral pathogenesis, mRNA regulation, tRNA export, DNA replication, and DNA repair (see (Sirover, 1999) for a review). GAPDH can bind to tubulin *in vitro* (Huitorel and Pantaloni, 1985; Volker and Knull, 1997) and GAPDH also binds to the 5'-UTR and 3'-UTR regions of mRNA (i.e. to the AU rich portions of RNA) (Nagy and Rigby, 1995). AU rich RNA, particularly AUUUA sequences form stem-loops that bind to the Rossman fold region of GAPDH, the site of its glycolytic activity (see (Borden, 1998)).

We reported that GAPDH co-immunoprecipitates with a translational control protein, promyelocytic leukemia (PML) protein (Carlile et al., 1998), in so-called PML nuclear bodies (Bloch et al., 1999; Matera, 1999). The studies showed that the presence of RNA was necessary for PML/GAPDH binding. PML overexpression has been shown to induce apoptosis in some cells (Chen et al., 1997; Quignon et al., 1998; Wang et al., 1998a; Wang et al., 1998b; Zhong et al., 2000). Hence GAPDH may facilitate apoptosis through a PML dependent action on translation. GAPDH may also influence translational regulation by interacting with hammerhead ribozymes (Sioud and Jespersen, 1996). Other work has suggested that nuclear GAPDH may modulate transcription in neurons (Morgenegg et al., 1986). Accordingly, GAPDH apoptosis signaling might involve actions on either transcriptional or translational mechanisms.

Both nitric oxide (NO) and superoxide radicals have been shown to release GAPDH from AU-rich RNA binding (Beckman and Koppenol, 1996; Brune and Lapetina, 1995; Brune and Lapetina, 1996; Itoga et al., 1997; Mohr et al., 1996). Similarly,  $NAD^+$  can release GAPDH from AU-rich RNA binding (Gabbieri et al., 1996; McDonald and Moss, 1994; Nagy and Rigby, 1995). Since AU-rich RNA bound GAPDH cannot carry out the glycolytic conversion of  $NAD^+$  to NADH, increased  $NAD^+$  may free GAPDH from RNA and then be converted to NADH. Similarly, NO and superoxide radical levels may influence the proportion of GAPDH available for glycolysis. A variety of evidence suggests that GAPDH cannot signal for apoptosis when it is bound to RNA (see our findings in (Carlile et al., 2000)). Both NO and superoxide radical can initiate neuronal apoptosis. Hence, part of the pro-apoptotic action of superoxide radical and NO might result from the freeing of GAPDH from RNA binding and thereby making GAPDH available for apoptosis signaling.

### **Mitochondria In Some Apoptosis Signaling**

There is increasing evidence that mitochondria play a critical decisional role in some forms of apoptosis (see (Loeffler and Kroemer, 2000; Nicholls and Budd, 2000; Susin et al., 1998) for detailed reviews), including those initiated in neurons by withdrawal of trophic factors (Wadia et al., 1998), glutamate excitotoxicity (Ankarcrona et al., 1995; Ankarcrona et al., 1996; Montal, 1998) or exposure to mitochondrial complex I toxins (see (Cassarino et al., 1999; Chalmers-Redman et al., 1999)).

Mitochondria are central to oxidative phosphorylation, but they also contribute to generation of reactive oxygen species (ROS), control of intracellular  $Ca^{2+}$  levels, and apoptosis signaling (see (Ankarcrona et al., 1995; Ankarcrona et al., 1996; Cassarino et al., 1999; Chalmers-Redman et al., 1999; Montal, 1998; Nicholls and Budd, 2000; Tanneti et al., 1998; Wadia et al., 1998)). Mitochondria are double membraned organelles. Four

multi-protein respiratory complexes (MtCxs I to IV), ATP synthase and the adenine nucleotide transporter (ANT) are located within the inner mitochondrial membrane and are involved in oxidative phosphorylation. Other components involved in the transfer of the electrons necessary for oxidative phosphorylation are ubiquinone and holocytochrome C (cytC). Sequential extraction of electron energy provides for outward proton pumping at MtCxs I, III, and IV. The resulting proton concentration gradient causes an electrochemical potential across the inner mitochondrial membrane, reflected by a pH gradient and a potential difference, termed the mitochondrial membrane potential ( $\Delta\Psi_M$ ).  $\Delta\Psi_M$  drives the phosphorylation of ADP to ATP by ATP synthase (Kaim and Dimroth, 1999) and decreases in  $\Delta\Psi_M$  can be an early marker for some forms of mitochondrially dependent apoptosis signaling (see (Susin et al., 1998) for a review).

### **Altered Mitochondrial Membrane Permeability Due To Opening Of A Mitochondrial Membrane Megapore Appears Critical To Some Apoptosis Signaling Pathways**

The mitochondrial permeability transition pore complex (PTPC) involves proteins and factors in the mitochondrial matrix, the intermembranous space, and the outer membrane (see (Crompton, 1999; Tatton et al., 1999) for more details). Proteins known to participate in the PTPC include: a) the ANT, which exchanges ADP and ATP between the mitochondrial matrix and the extra-mitochondrial cytosol; b) a putative chaperone, cyclophilin D (cyD); c) a porin molecule localized to the outer mitochondrial membrane, a possible voltage dependent anion channel (VDAC); d) hexokinase-2, a glycolytic enzyme; e) creatine kinase, which reversibly converts ATP plus creatine to phosphocreatine + ADP; f) a peripheral benzodiazepine binding protein; g) BAX and related pro-apoptotic proteins like BAD; and h) BCL-2 or BCL-X<sub>L</sub>, which are anti-apoptotic proteins.

The protein-protein interactions between the components of the PTPC are controversial. The PTPC can be defined as a voltage-dependent, cyclosporin A (CSA) sensitive, high conductance membrane channel (Bernardi et al., 1998) and appears to open in two states: a transient, low conductance, ion selective state and a sustained, high conductance, non-selective state. The high conduction state allows passage of solutes up to 1.5 kD (see (Fall and Bennett, 1999) for details). Sustained opening of the PTPC or other high conductance increases in inner mitochondrial membrane permeability result in  $\Delta\Psi_M$  dissipation due to proton influx. The proton influx can be accompanied by the efflux of Ca<sup>2+</sup>, metabolites, and other small molecules from the mitochondrial matrix. Furthermore, osmotic swelling of mitochondria may produce mitochondrial membrane fracture, which also dissipates  $\Delta\Psi_M$ . As well as PTPC opening decreasing  $\Delta\Psi_M$ , PTPC conformation is influenced by  $\Delta\Psi_M$ . High  $\Delta\Psi_M$  favors PTPC closure, while decreased  $\Delta\Psi_M$  increases the probability of PTPC opening (Scorrano et al., 1997b). Ca<sup>2+</sup> binding to the matrix side of the PTPC is a requirement for pore opening. In our studies, we view  $\Delta\Psi_M$  as an indicator of mitochondrial membrane permeability. That is, decreased  $\Delta\Psi_M$  indicates increased membrane permeability.

PTPC closure results from the binding of CSA to cyD, which prevents cyD from interacting with the ANT (Halestrap et al., 1997; Nicolli et al., 1996; Scorrano et al., 1997a; Woodfield et al., 1998). The direct binding of bongkreikic acid to the ANT also facilitates PTPC closure. We and others previously used CSA to serve as an indicator of PTPC participation in different forms of apoptosis (see (Cassarino et al., 1998; Chalmers-Redman et al., 1999)). Because of the actions of CSA on other proteins than CyD such a calmodulin, that approach did not unambiguously implicate the PTPC in the genesis of apoptosis. In our current experiments, we now use bongkreikic acid to eliminate that ambiguity.

### **BCL-2 Family Members Act On Mitochondrial Membrane Permeability**

Members of the BCL-2 family of proteins mediate part of their pro- or anti-apoptotic actions by localizing to mitochondrial membranes, in part through the PTPC binding (see (Marzo et al., 1998b)). The association of BCL-2 or BCL-X<sub>L</sub> with the PTPC facilitates PTPC closure and maintenance of  $\Delta\Psi_M$  (Kroemer et al., 1997; Zamzami et al., 1998; Zamzami et al., 1996a). A BCL-2 family member, BAD forms heterodimers with BCL-2 or BCL-X<sub>L</sub> and inactivates the anti-apoptotic actions of BCL-X<sub>L</sub> and possibly BCL-2 (Kelekar et al., 1997; Korsmeyer, 1999; Yang et al., 1995; Zha et al., 1997). Binding of BAX dimer to the ANT increases mitochondrial permeability, possibly by PTPC opening (Marzo et al., 1998a; Marzo et al., 1998b).

We have shown that decreases in  $\Delta\Psi_M$  is a feature of apoptosis caused by NGF and serum withdrawal in cultured neural cells (Wadia et al., 1998) and similar early decreases in  $\Delta\Psi_M$  have been reported for apoptosis initiated by a wide variety of toxic insults (see (Susin et al., 1998) for a detailed review). In general, those

apoptotic decreases in  $\Delta\Psi_M$  indicate increases in mitochondrial membrane permeability. Not all forms of apoptosis, however, involve decreases in  $\Delta\Psi_M$  and increased mitochondrial membrane permeability. For example, apoptosis induced by the general kinase inhibitor, staurosporine in cultured hippocampal cells (Krohn et al., 1999) did not involve  $\Delta\Psi_M$  decreases, while staurosporine induced apoptosis in P6 cells did involve early apoptosis decreases in  $\Delta\Psi_M$  (Heiskanen et al., 1999).

The release of factors from mitochondria due to increased mitochondrial membrane permeability has been shown to induce apoptotic nuclear degradation. Two mitochondrial factors that signal for apoptotic degradation, cytC (Kantrow and Piantadosi, 1997; Li et al., 1997; Liu et al., 1996), and apoptosis initiation factor (AIF), a 50 kD flavoprotein (Susin et al., 1999a; Susin et al., 1999b) have been identified. The mechanisms underlying their apoptotic release are controversial. Both factors normally reside in the inter-mitochondrial space in contact with the inner mitochondrial membrane. It has been proposed that increased permeability of the outer mitochondrial membrane consequent on PTPC opening induces osmotic swelling of the mitochondria and fracture of the membranes are responsible (see (Loeffler and Kroemer, 2000)). Others have suggested the opening of pores in the outer membrane directly by proteins like BAX or the loss of BCL-2 from mitochondrial membranes are responsible.

After its release, cytC interacts with Apaf-1 (Bratton et al., 2000; Li et al., 1997; Zou et al., 1997), dATP/ATP and procaspase 9 to form a complex known as the apoptosome, in which procaspase 9 is converted to caspase 9. Caspase 9 then converts procaspase 3 to active caspase 3. The apoptosome seems to function as a multi-caspase activating complex (see (Bratton et al., 2000)). Activated caspase 3 in turn activates DNA fragmentation factor (also termed caspase-activated Dnase (CAD)) (Liu et al., 1997), an endonuclease activator that enables DNA cleavage and also cleaves other proteins such as lamin, and fodrin (Zou et al., 1997). AIF induces DNA loss, peripheral chromatin condensation and digestion of chromatin into 50 kbp-fragments (Susin et al., 1999b). The caspase-3 inhibitor ZVAD-Fmk inhibits chromatin condensation induced by AIF. Pro-caspase 2 and 9, have been found in the intermembranous space of mitochondria and the microinjection of the caspases can induce apoptotic nuclear degradation (Susin et al., 1999a). Initial studies were interpreted to show that the release of cytC is independent of PTPC opening and decreased  $\Delta\Psi_M$  (Finucane et al., 1999; Kluck et al., 1997; Yang et al., 1997). The interpretations of those studies have been found to be complicated by technical considerations related to the measurement of  $\Delta\Psi_M$  (see (Bernardi et al., 1999) for details). Similar to earlier findings in isolated mitochondria (Zamzami et al., 1996a; Zamzami et al., 1996b), studies of mitochondria *in situ* have shown that PTPC opening and decreased  $\Delta\Psi_M$  can be associated with the induction of apoptotic degradation in a number of models (Narita et al., 1998; Rigobello et al., 1999) including apoptosis induced by the PD-like toxin MPP<sup>+</sup> (Cassarino et al., 1999). Examination of individual mitochondria *in situ* using laser confocal scanning microscopy (LCSM) has shown that decreased  $\Delta\Psi_M$  can accompany cytC release into the cytosol (Heiskanen et al., 1999). Accordingly, although the mechanisms responsible for the release of apoptotic degradation factors from mitochondria are not completely resolved, increased inner membrane permeability, in part due to PTPC opening, appears to be a factor. The increased inner membrane permeability seems to contribute to a decrease in  $\Delta\Psi_M$ .

Mitochondrial BCL-2 can block the release of the mitochondrial factors that signal for apoptotic degradation, possibly due to its capacity to facilitate PTPC closure and maintain  $\Delta\Psi_M$  (see (Crompton, 1999) for a detailed and recent review of the role of the PTPC in cell death). BCL-X<sub>L</sub> has a similar capacity (Gross et al., 1999). Mitochondrial BAX is necessary for cytC release in some systems (Bradham et al., 1998; Pastorino et al., 1998; Pastorino et al., 1999). Caspase-activated BID also facilitates cytC release (Gross et al., 1999). Accordingly, the demonstration of increases in mitochondrial BAX levels, increased extra-mitochondrial cytC levels, decreased mitochondrial BCL-2 or BCL-X<sub>L</sub> levels, decreased  $\Delta\Psi_M$  and caspase 3 activation can together serve as markers of mitochondrially dependent apoptosis signaling.

## **b) Report Of Progress**

### **Progress In Experimental Series 1.**

**Objective 1a. Development Of Methods To Identify Neurons Undergoing Apoptotic Degradation With Certainty.** The use of *in situ* end labeling (ISEL, also termed as TUNEL labeling) of nuclear DNA to demonstrate



cells that have undergone apoptotic degradation is prone to either false negatives or false positives (see (Tatton and Rideout, 1999) for details). In order to avoid false identification of apoptotic neurons, we have jointly employed three separate *in situ* measures of nuclear degradation as illustrated in figure 1: 1) the demonstration of DNA chromatin condensation using the DNA binding dye, YOYO-1; 2) demonstration of DNA fragmentation using *in situ* end labeling (ISEL) of cut DNA with BODIPY-dUTP; and 3) demonstration of histone margination using immunoreaction with anti-histone antibodies (the details of our use of the three methods are presented in (Wadia et al., 1998)). The joint demonstration of the multiple markers of apoptotic degradation in the same nuclei greatly increases confidence in the finding of apoptotic degradation (Tatton, 2000; Tatton and Kish, 1997; Tatton et al., 1998).

We have also examined the temporal relationships between histone margination, nuclear chromatin condensation and nuclear DNA cleavage in cerebellar granule neuron (CGn) apoptosis caused by exposure to glutamatergic excitotoxins, or to reduced  $K^+$  levels. We found that DNA condensation occurs in four stages: stage 1) condensation of DNA around the outer border of the nucleus (examples labeled 1 in figure 1B1); stage 2) DNA condensation spreads to involve the whole nucleus (examples labeled 2 in figure 1B1 and B2); stage 3) shrinkage of the condensed DNA with the appearance of cracks or breaks in the nuclei (examples labeled 3 in 1B1 and B2); and stage 4) the formation nuclear fragments into multiple spherical nuclear bodies of condensed DNA (not shown). As shown in figure 1D1, histone margination surrounds the areas of condensed DNA in stages 1 and 2. DNA fragmentation, as revealed by ISEL in figure 1B2, appears during stage 2 and gradually becomes co-extensive with DNA condensation (figure 1B2). The staging allows us to precisely determine the temporal relations between apoptotic nuclear nuclear degradation and GAPDH signaling events in individual cells.

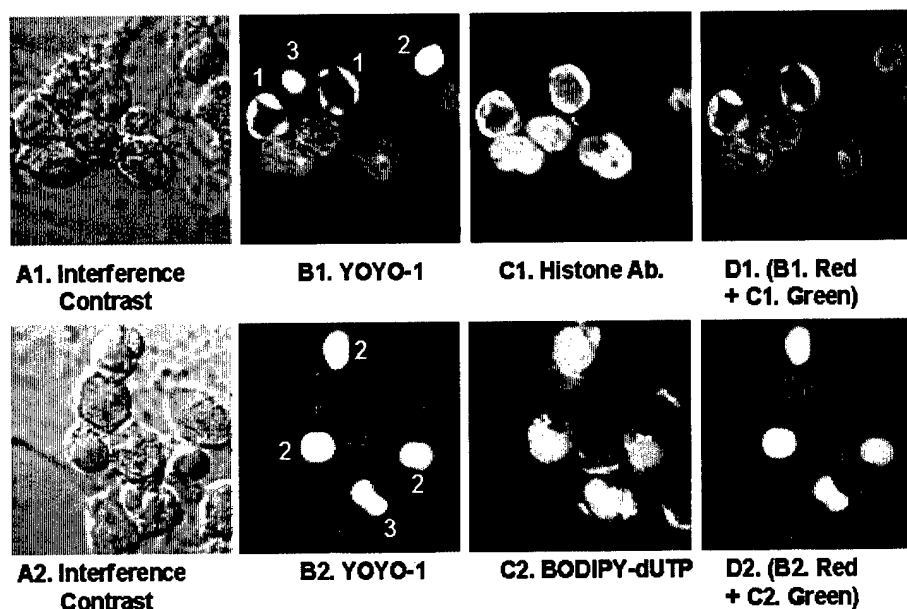


**Figure 1** – LCSM images of CGNs 12 hours after exposure to  $5 \times 10^{-5}$  M NMDA. Each horizontal row of images was taken for an identical image field. DNA chromatin condensation revealed with YOYO-1 binding to DNA (B1 and B2), and DNA fragmentation revealed with ISEL using BODIPY-dUTP (C2), is accompanied by the nuclear margination of histone immunoreaction (C1). Nuclei without evidence of DNA condensation or fragmentation show a pattern of histone immunoreaction that extends across the whole nucleus. In apoptotic nuclei, the histone immunoreaction surrounds the fragmented and condensed DNA but does not co-localize with either (D1). Examination of a large number of cells has shown that DNA condensation proceeds according to 4 stages (examples of stages 1, 2 and 3 are shown in B1 and B2). In the right hand panels of each row, D1 and D2, the images in B1 or B2 and C1 or C2 have been colored red and green respectively and then digitally added. Regions in the added images that are red or green indicate no spatial overlap while yellow -green, yellow or orange coloration indicate varying levels of spatial overlap. The added figures show that histone margination surrounds condensed DNA areas in stage 1 and stage 2 but not in stage 3. DNA fragmentation is not evident until stage 2 and is co-extensive with condensed DNA.

Apoptosis Initiating Agent or Treatment	Concentration , Dosage or Pressure Range	Cell Type	Intact Animal (IA) or In Culture (IC)	Upregulation On LCSM Immunocyt.	Upregulation On Western Blots
Serum and NGF Withdrawal	na	Rat NGF Differentiated PC12 Cells	IC	Yes	Yes
Glutamate	5 x 10 <sup>-4</sup> to 5 x 10 <sup>-5</sup> M	Rat CGNs (7 days in culture)	IC	Yes	nd
NMDA	5 x 10 <sup>-4</sup> to 5 x 10 <sup>-5</sup> M	Rat CGNs (7 days in culture)	IC	Yes	nd
Cytosine Arabinoside	200 µM	Rat CGNs (7 days in culture)	IC	Yes	nd
Reduced Media K <sup>+</sup>	25 mM reduced to 5 mM	Rat CGNs (7 days in culture)	IC	Yes	nd
Nitric Oxide Donor	200 µM	Human Fibroblasts	IC	Yes	nd
Nitric Oxide Donor	200 µM	Rat NGF Differentiated PC12 Cells	IC	Yes	nd
C2 -Ceramide	5 – 20 µM	Rat NGF Differentiated PC12 Cells	IC	Yes	nd
MPP <sup>+</sup>	100-250 µM	Rat NGF Differentiated PC12 Cells	IC	Yes	Yes
Rotenone	10-50 nM	Rat NGF Differentiated PC12 Cells	IC	Yes	Yes
H <sub>2</sub> O <sub>2</sub>	0.15-1.0 mM	Rat NGF Differentiated PC12 Cells	IC	No	No
Staurosporine	2 µM	Rat NGF Differentiated PC12 Cells	IC	No	No
Increased IOP	20-28 mm Hg	Rat RGns	IA	Yes	nd
Glaucoma	na	Human RGns	IA	Yes	nd
Parkinson's Disease	na	Human SNc Neurons	IA	Yes	nd

**Table 1 – Participation of GAPDH Upregulation In Different Forms Of Apoptosis.** Abbreviations: na- not applicable, nd – not yet determined

**Objective 1b. Apoptosis Models That Involve GAPDH Upregulation And Nuclear Accumulation.** GAPDH upregulation has previously been shown in apoptosis initiated in cultured CGNs by exposure to the DNA damaging agent cytosine arabinoside, the reduction of media K<sup>+</sup> levels and after prolonged maintenance in culture (so called aging). We showed similar upregulation of GAPDH in NGF differentiated PC12 cells after serum and NGF withdrawal (Carlile et al., 2000). It is not known whether GAPDH participation is limited to those few forms of apoptosis or widely involved. In order to begin to determine the importance of GAPDH in apoptosis signaling, we have examined a number of apoptosis models *in vitro* and *in vivo* and have examined nervous tissue in two human diseases in which neurons degenerate (see table 1). The studies have demonstrated GAPDH upregulation in apoptosis initiated in cultured rat NGF differentiated PC12 cells, primary cultures of rat cerebellar granule neurons, cultured human fibroblasts, rat retinal ganglion neurons (RGns), human neuromelanin containing substantia nigra compacta neurons (SNc) in PD postmortem brain and human retinal

ganglion neurons. The apoptosis initiating insults that involved GAPDH upregulation and nuclear accumulation included glutamate, n-methyl d-aspartate (NMDA), nitric oxide (NO), the mitochondrial respiratory complex I inhibitors, MPP<sup>+</sup> and rotenone, ceramide and cytosine arabinoside. The pro-oxidant H<sub>2</sub>O<sub>2</sub> or the general kinase inhibitor, staurosporine have not initiated GAPDH upregulation in the models we have examined to date, even though they initiated the typical stigmata of apoptotic degradation. As illustrated in figure 3 for the nitric oxide donor SNAP and for NGF and serum withdrawal in (Carlile et al., 2000), appended, the GAPDH upregulation was associated with GAPDH nuclear accumulation in a proportion of the early apoptotic cells. In each of the models or disease states in which we have found GAPDH upregulation, a proportion of the cells have shown dense GAPDH nuclear accumulation.

We also found GAPDH upregulation in retinal ganglion neurons exposed to increased intra-ocular pressure (IOP) as a model of glaucoma (see (Mittag et al., 2000) for details of our demonstration of mitochondrially-dependent apoptosis in the glaucoma model and figure 2, which presents an example of GAPDH upregulation in the glaucoma model RGns). In terms of neuronal degeneration in human disease, we have found evidence of GAPDH upregulation in postmortem nervous tissue from Parkinson's disease substantia nigra (see (Tatton, 2000)) and in retina from glaucoma patients.

These findings suggest that GAPDH contributes to signaling in a number of , but not all, forms of apoptosis, including apoptosis induced by excitotoxins, DNA damaging agents, lipid toxins like ceramide and mitochondrial toxins and may also contribute to apoptosis in some human neuronal degenerative conditions.

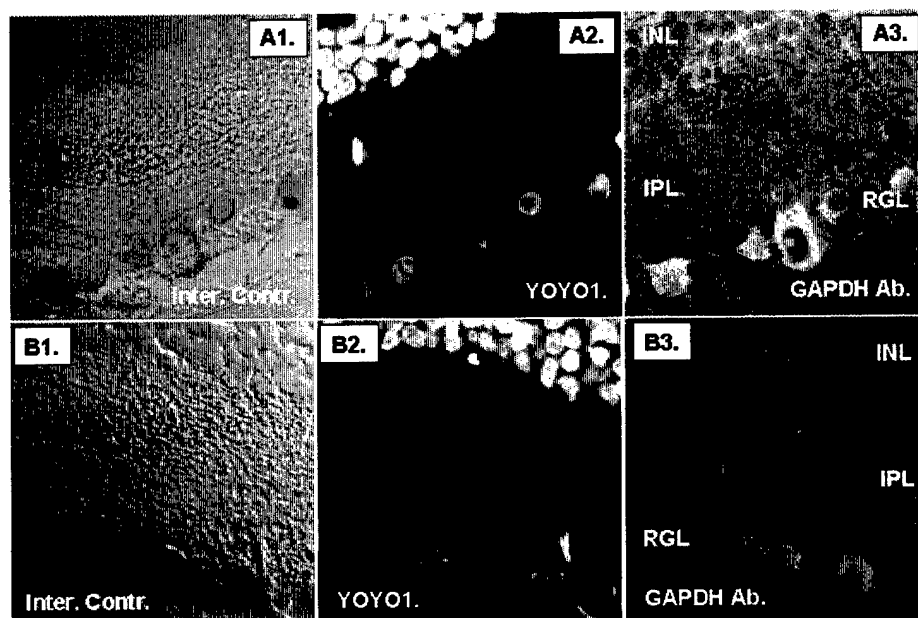


**Figure 2** – In the glaucoma model, IOP was induced in one eye, but not the other, which served as a control. A1, A2 and A3 and B1, B2 and B3 present LCSM images taken for identical image fields. A1-A3 show retinal cross sections for an eye exposed to increased IOP for 3 weeks while B1-B3 are sections from the contralateral eye in the same animal. As shown in A2 RGns frequently showed chromatin condensation in the retinas exposed to increased IOP (see (Mittag et al., 2000) for details), while control retina did not present evidence of apoptotic degradation. The RGns with evidence of apoptotic degradation were usually adjacent to RGns with increased GAPDH immunofluorescence (compare A3 and B3). Abbreviations: Inter. Contr.- Interference Contrast; Ab. – antibody; INL – inner nuclear layer; IPL – inner plexiform layer, RGL- retinal ganglion cell layer.

**Objective 1c. Timing of GAPDH Upregulation/ Nuclear Accumulation Relative To Increased Mitochondrial Membrane Permeability And Apoptotic Nuclear Degradation.** In order to determine the timing of GAPDH upregulation/nuclear accumulation relative to the onset of apoptotic degradation and increases in mitochondrial membrane permeability, we jointly examined GAPDH upregulation/nuclear accumulation and decreased  $\Delta\Psi_M$  in four different models of apoptosis: 1) cultured CGns exposed to the DNA damaging toxin, cytosine arabinoside; 2) cultured CGns exposed to the excitotoxins, glutamate or NMDA; 3) NGF differentiated PC12 cells after serum and NGF withdrawal, and 4) NGF differentiated PC12 cells exposed to the mitochondrial

complex I toxins, MPP<sup>+</sup> and rotenone. In each model, we used a combination of western blotting for cell lysates and immunocytochemistry with laser scanning confocal microscopy (see (Carlile et al., 2000) for examples of our joint use of those methods) together with LCSM measures of  $\Delta\Psi_M$  (see (Wadia et al., 1998) for those methods).

Each model showed increased levels of GAPDH immunoreactivity accompanied by GAPDH nuclear accumulation suggesting that GAPDH contributes to those forms of apoptosis signaling. Timing studies showed that GAPDH upregulation and GAPDH nuclear accumulation precede decreased  $\Delta\Psi_M$  in accord with a model in which ***GAPDH signaling is upstream to increased mitochondrial membrane permeability in apoptosis signaling***. That is, GAPDH upregulation precedes decreased  $\Delta\Psi_M$  and therefore increased mitochondrial membrane permeability, which in turn precedes the appearance of apoptotic nuclear degradation.

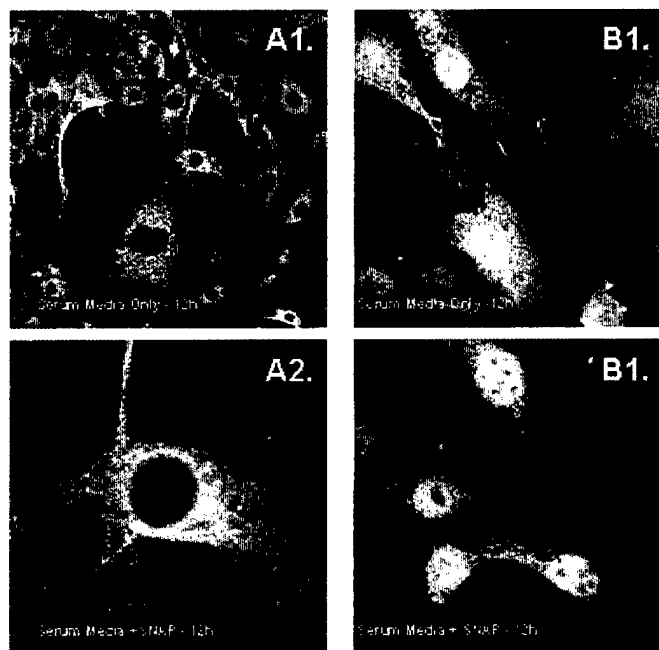


**Figure 3 - 3T3 Fibroblasts Showing GAPDH Nuclear Accumulation After Exposure To An NO Donor.** Figures show laser confocal microscope images of 3T3 fibroblast immunoreacted with a GAPDH antibody. Control cells exposed to vehicle only - low power A1 and high power. Cells exposed to SNAP (200 μM), an NO donor - intermediate power in B1 and B2.

## Progress In Experimental Series 2.

**2a. GAPDH Upregulation Induces Increased Mitochondrial Membrane Permeability And Facilitates Apoptotic Nuclear Degradation.** To directly determine whether GAPDH upregulation is upstream to apoptotic decreases in  $\Delta\Psi_M$  and signaling for apoptotic nuclear degradation, we induced GAPDH upregulation using an inducible expression system. We have produced seven PC12 cell clones that overexpress GAPDH under the control a tetracycline expression (tet-low) system (for details of our use of the system see (Sugrue et al., 1997; Sugrue et al., 1999)). The rat brain GAPDH cDNA that we previously cloned to produce a green fluorescent protein-GAPDH fusion protein was used with the tet-low system (see (Shashidharan et al., 1999) for details of the cDNA). The PC12 cell clones stably overexpressed GAPDH in response to a sudden decrease in media tetracycline (tet) concentration (see figure 4). The model has the advantage that we can first proliferate the cells in the presence of high tet levels and once the cells are differentiated, we can induce the overexpression of GAPDH by reducing tet levels.

To date, we have only examined one of the clones after neuronal differentiation by NGF and serum. According to western blots for cell lysates (see (Carlile et al., 2000) for details of the cell lysate preparation and blotting methods), GAPDH levels begin to increase 1-2 hours after tet reductions and become maximal at 6-12 hours. Western blots for clone I showed 200-600% increases in GAPDH immunodensity after tet withdrawal for

12 hours (see figure 4A). We have obtained comparable estimates of tet induced-low increased GAPDH protein using LCSM measurements of GAPDH immunofluorescence. The LCSM immunocytochemical analysis revealed a 225% increase in average GAPDH immunofluorescence in the cytoplasm and a 178% increase in average GAPDH immunofluorescence levels in the nuclei at 6 hours after the tet withdrawal (see immunofluorescence distributions in figure 5). The levels of increase in GAPDH induced by tet-low were similar in magnitude of those which we found in the NGF-differentiated PC12 cells entering apoptosis at 6 hours and 24 hours after serum and NGF withdrawal (see figure 3 in (Carlile et al., 2000), appended).

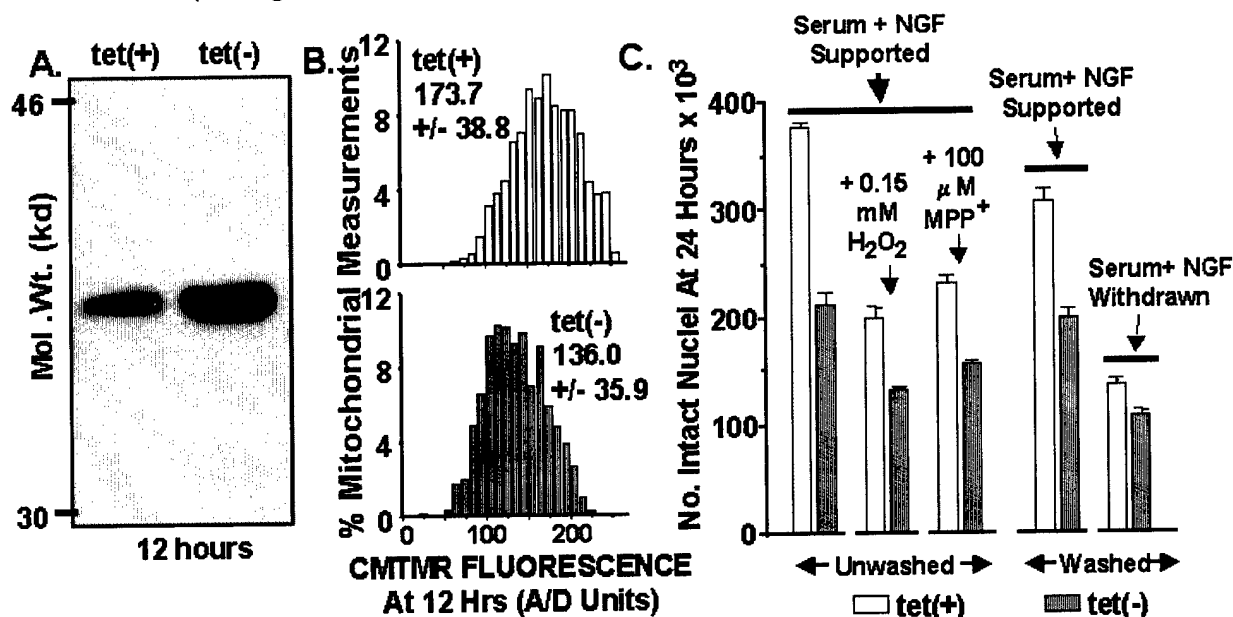


**FIGURE 4** –PC12 cells were differentiated in minimum essential media (MEM) with serum and NGF plus high tet concentrations (tet(+)) for 5 days in order to neuronally-differentiate the cells (see (Carlile et al., 2000; Tatton et al., 1994; Wadia et al., 1998) for details of our methods). After 6-24 hours in tet(-) (i.e media without tet), GAPDH immunoreaction on western blots was increased compared to that for tet(+) cells as shown in the western blot of panel A. By 12 hours, cells in MEM with serum and NGF without tet showed a increase in GAPDH of 2-6 times compared to the tet(+) cells. LCSM was used to measure CMTMR fluorescence as an estimate of  $\Delta\Psi_M$  and as an indicator of mitochondrial membrane permeability at 12 hours after placement in tet(-) and compared to that for cells maintained in tet(+). As shown in panel B, the  $\Delta\Psi_M$  distributions for cells in tet(-) were decreased ( $p < .001$ ) compared to those for cells maintained in tet(+). On the sixth day, (24 hours in tet(-)), three groups of cells in MEM with serum and NGF were exposed to: 1) added MEM as a control, 2) 0.15 mM H<sub>2</sub>O<sub>2</sub> (concentrations of 0.10-0.25 μM H<sub>2</sub>O<sub>2</sub> induce apoptosis in the cells, see below) or 3) 100 μM MPP<sup>+</sup> (see (Chalmers-Redman et al., 2000) for details of our initiation of apoptosis in the neuronally-differentiated PC12 cells with the mitochondrial toxin, MPP<sup>+</sup>). The three groups of cells were matched with three groups that were maintained in tet(+). Two further groups in either tet(+) or tet(-) were washed repeatedly to remove the trophic support offered by serum factors and NGF (see (Wadia et al., 1998) for details of the apoptosis initiated by this procedure). One group was returned to MEM with serum and NGF as a control and the other was placed in MEM only. The tet(-) cells showed decreased survival in response to H<sub>2</sub>O<sub>2</sub>, MPP<sup>+</sup> and serum+NGF withdrawal compared to the tet(+) cells ( $p$ 's < .01). The data shows that the increased GAPDH expression: 1) induces spontaneous apoptosis in about 25% of the cells; 2) increases the vulnerability of the remaining cells to apoptosis induced by to H<sub>2</sub>O<sub>2</sub>, MPP<sup>+</sup> and serum+NGF withdrawal and 3) decreases  $\Delta\Psi_M$  and therefore likely increases mitochondrial membrane permeability.

We compared  $\Delta\Psi_M$  in the NGF differentiated PC12 cells with and without GAPDH upregulation induced by the removal of tet (figures 4A and 4B). We used the mitochondrial potentiometric dye CMTMR to estimate  $\Delta\Psi_M$  (see (Grant et al., 1999; Jing et al., 1999; Sugrue et al., 1999; Wadia et al., 1998) for details of our use of CMTMR). We found a shift of  $\Delta\Psi_M$  distributions to lower values in cells expressing increased levels of GAPDH of greater than 250% (compare the CMTMR fluorescence distributions for cells maintained in tet (tet(+)) versus those in media without tet (tet(-)) in figure 4B). Although the mean  $\Delta\Psi_M$  levels were decreased by 20 to 30%, the most striking finding was a loss of mitochondria with high levels of  $\Delta\Psi_M$  (e.g. note the relative decrease in CMTMR fluorescence measures of 200 to 250 units in 4B for tet(-)). This is the first data to directly link GAPDH

apoptosis signaling to a decrease in  $\Delta\Psi_M$  and therefore an increase in mitochondrial membrane permeability. It directly suggests that GAPDH can be upstream to increased mitochondrial membrane permeability in some apoptosis signaling pathways.

The studies with the tet induction system also showed that about 25% of the PC12 cells died by apoptosis in the first 6 – 12 hours after GAPDH upregulation and that cells with increased levels of GAPDH showed increased vulnerability to apoptosis initiated by mitochondrial toxins, pro-oxidants and serum and NGF withdrawal (see figure 4C).

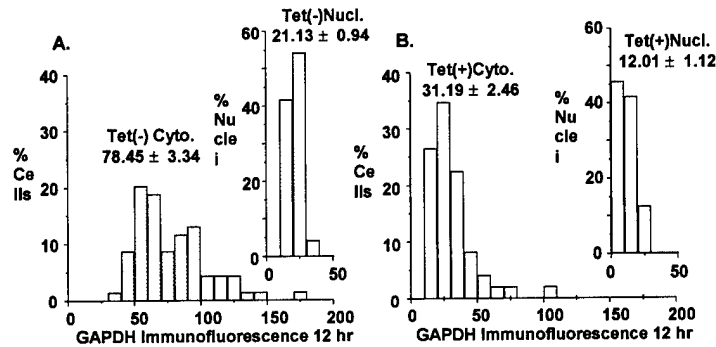


**Figure 5** – GAPDH overexpression using the tet(-) expression system in neuronally-differentiated PC12 cells. Abscissae show levels of GAPDH immunofluorescence in LCSM detector units while ordinates show percentages of cells. Values above distributions present mean  $\pm$  SEM for each distribution.

### Progress In Experimental Series 3.

We have delayed the mutation studies until year 3.

### Progress In Experimental Series 4

**Development of A Cell Free System Using Nuclei From Neuronally-Differentiated PC12 Cells And Hepatic Mitochondria.**

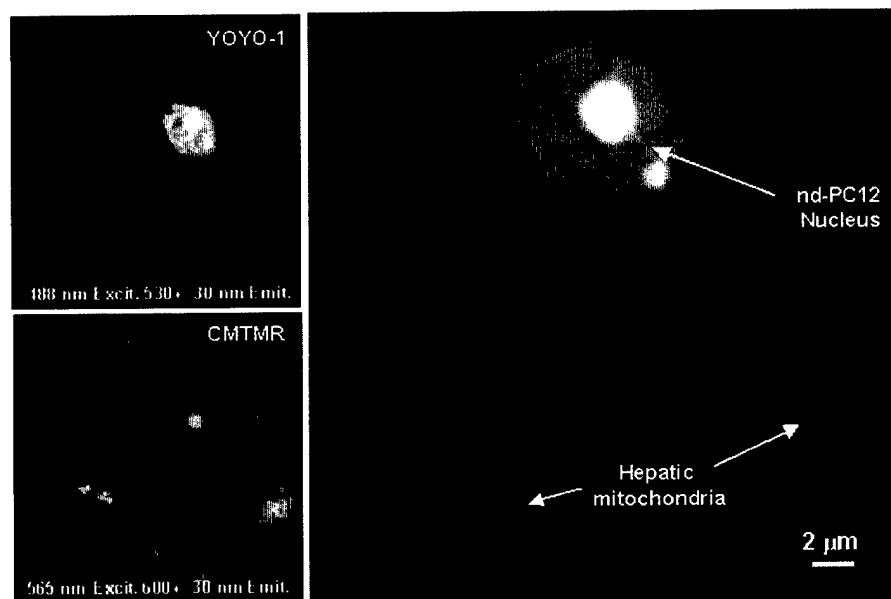


**Figure 6** – Example of hepatic mitochondria, stained with CMTMR, and PC12 nuclei, stained with YOYO-1, combined with PC12 cytosol into a cell free system. See details of preparation in section d2-VII below. The components are imbedded in low melting point agar. The two left-hand images are for identical image fields examined with different excitation and emission wavelengths. The YOYO fluorescence was recoloured red and the CMTMR fluorescence recoloured green and the recoloured images were digitally added to produce the right hand image. Similar procedures will be employed in the proposed studies using the cell free system.

We proposed to develop a cell free system that used xenopus oocytes in order to take advantage of the

large nuclei and mitochondria in those cells. On attempting to develop a working system we found that the oocytes resisted the dissociation of their subcellular components to an extent that would allow LCSM imaging and still maintain viability of the components. Therefore, instead we have created a cell free system that is comprised of PC12 nuclei together with the PC12 cytoplasmic fraction (the 16000xg fraction) and the mitochondrial fraction taken from rat liver cells. The living components, imbedded in low melting point agar can be LCSM imaged in an environmentally controlled chamber that controls temperature and ambient gas concentration while allowing for perfusion of the system (see for details of the chamber in (Wadia et al., 1998)). The low melting point agar provides for image stability during LCSM imaging (see figure 6).

The cell free system has been examined by initiating apoptosis using exposure to C2-ceramide. The nuclei in the system have shown evidence of chromatin condensation using the dye YOYO-1 (see above) and DNA gel electrophoresis has shown typical apoptotic DNA "laddering" (see (Chalmers-Redman et al., 1999; Tatton et al., 1994) for examples). We can now proceed to introduce varying concentrations of GAPDH, peptide fragments of GAPDH and  $\text{NAD}^+$  in order to determine their effect on apoptosis signaling mechanisms, particularly those signaling mechanisms which involve changes in mitochondrial membrane permeability.

### **Progress In Experimental Series 5.**

These studies will be carried out in year 3.

#### **(7) Key Research Accomplishments**

- Demonstration that glyceraldehyde-3-phosphate (GAPDH) contributes to apoptosis signaling and therefore nerve cell death initiated by a variety of insults, including exposure to a number of neurotoxins including glutamate excitotoxins, mitochondrial toxins, DNA and damaging agents.
- Evidence that GAPDH contributes to neuronal apoptosis in at least two human diseases – Parkinson's disease and glaucoma – by examining human postmortem brain and retinal tissue together with the examination of animal and culture models of the diseases.
- The finding that GAPDH upregulation results in a decrease in mitochondrial membrane potential and therefore an increase in mitochondrial membrane permeability which likely allows the release of mitochondrial signaling factors that activate a signaling cascade leading to neuronal apoptotic degradation.

#### **(8) Reportable Outcomes**

##### **a) Abstracts;**

Glyceraldehyde-3 Phosphate Dehydrogenase And Mitochondrial Membrane Potential In Apoptosis Signaling, W.G. Tatton and R.M.E. Chalmers-Redman, Proceedings XIV th International Congress Of Eye Research, page S180

##### **b) Presentations;**

Invited lecture, Glyceraldehyde-3-Phosphate Dehydrogenase in Neurodegeneration and Apoptosis Signaling, 8<sup>th</sup> International Winter Conference On Neurodegeneration, Tegernsee, Germany, 9-13 February 2000

Keynote Lecture, Glyceraldehyde-3 Phosphate Dehydrogenase And Mitochondrial Membrane Potential In Apoptosis Signaling, XIV th International Congress Of Eye Research October 2000, Santa Fe , New Mexico

##### **c) Degrees Obtained;**

None

##### **d) Development of Cell Lines, Tissue or Serum Repositories;**

Part of the research in year 3 will involve investigations of cutaneous fibroblasts cultured from patients with Parkinson's disease and from age matched controls. We have developed techniques for proliferating and passaging the fibroblasts and maintaining them in liquid nitrogen. To date, we have created a fibroblast bank for 14 Parkinson's disease patients and 11 age-matched controls.

We and others have shown that platelets and fibroblasts from about 70% of Parkinson's disease patients have decreases in mitochondrial respiratory complex I activity and decreases in mitochondrial membrane potential. The basis for the decreases in the two indexes of mitochondrial function are not known and their

understanding, particularly as it may relate to GAPDH, and mitochondrial toxins is an important aim of this research program.

We will make the fibroblasts available for the studies of others.

**e) Informatics:**

None

**f) Funding Applied For Based Upon This Work:**

None

**g) Experiences/ Training Supported By This Work**

A. Sud, MPharm exchange student from University College London is carrying out a project on the role of the lipid toxin, ceramide in signaling for GAPDH upregulation and nuclear accumulation. He is learning a variety of techniques including immunocytochemistry, protein co-immunoprecipitation and laser confocal scanning microscope imaging of living mitochondria.

**(9) Conclusions;**

In recent years, apoptosis has been found to contribute to a number of neurological diseases. The different signaling pathways that mediate the neurological disease related apoptosis are largely unknown. An understanding of the step by step apoptosis signaling in specific diseases, for example in Parkinson's disease or in brain damage induced by mitochondrial toxins, has the potential to lead to the development of agents that interrupt specific apoptosis signaling steps (e.g. by binding to a specific signaling protein in a manner similar to that which we have shown for propargylamine binding to GAPDH (Carlile et al., 2000, appended)) and thereby slowing or attenuating the disease.

In these investigations, we have investigated the role of GAPDH upregulation and nuclear accumulation in neuronal apoptosis signaling. During the first year, we have shown that GAPDH signaling contributes to a number of forms of neuronal apoptosis induced by toxin agents including glutaminergic excitotoxins, mitochondrial respiratory complex I toxins, DNA damaging agents, and lipid toxins like c2-ceramide. The mitochondrial toxins have been shown to induce a Parkinson's disease-like syndrome in animals and humans. We have provided evidence that GAPDH may contribute to neuronal apoptosis in Parkinson's disease by examining the mitochondrial toxin models and human postmortem brain tissue.

Our studies in cultured neural cells have begun to elucidate the role of GAPDH in apoptosis signaling. We have shown that GAPDH upregulation and nuclear accumulation precedes increases in mitochondrial membrane permeability as indicated by decreased mitochondrial membrane potential and the apoptotic degradation, which is consequent on the increased mitochondrial membrane permeability. We have used inducible gene transfection to directly show that GAPDH upregulation results in a decrease in mitochondrial membrane potential together with apoptosis in about 25% of neural cells and an increased vulnerability to apoptosis initiating insults in the remaining cells. These are the first findings to show that GAPDH functions upstream to mitochondrial signaling in some apoptosis signaling pathways.

**(10) References**

- Ankarcrona M, Dypbukt JM, Bonfoco E, Zhivotovsky B, Orrenius S, Lipton SA, Nicotera P. Glutamate-induced neuronal death: a succession of necrosis or apoptosis depending on mitochondrial function. *Neuron* 1995; 15: 961-73.
- Ankarcrona M, Dypbukt JM, Orrenius S, Nicotera P. Calcineurin and mitochondrial function in glutamate-induced neuronal cell death. *FEBS Lett* 1996; 394: 321-4.
- Beckman JS, Koppenol WH. Nitric oxide, superoxide, and peroxynitrite: The good, the bad, and the ugly. *American Journal of Physiology - Cell Physiology* 1996; 40: C1424-C1437.
- Bernardi P, Colonna R, Costantini P, Eriksson O, Fontaine E, Ichas F, Massari S, Nicolli A, Petronilli V, Scorrano L. The mitochondrial permeability transition. *Biofactors* 1998; 8: 273-81.
- Bernardi P, Scorrano L, Colonna R, Petronilli V, Di Lisa F. Mitochondria and cell death. Mechanistic aspects and methodological issues. *Eur J Biochem* 1999; 264: 687-701.
- Bloch DB, Chiche JD, Orth D, de la Monte SM, Rosenzweig A, Bloch KD. Structural and functional heterogeneity of nuclear bodies. *Mol Cell Biol* 1999; 19: 4423-30.
- Borden KL. Structure/function in neuroprotection and apoptosis. *Ann Neurol* 1998; 44: S65-71.
- Bradham CA, Qian T, Streetz K, Trautwein C, Brenner DA, Lemasters JJ. The mitochondrial permeability



transition is required for tumor necrosis factor alpha-mediated apoptosis and cytochrome c release. *Mol Cell Biol* 1998; 18: 6353-64.

Bratton SB, MacFarlane M, Cain K, Cohen GM. Protein complexes activate distinct caspase cascades in death receptor and stress-induced apoptosis. *Exp Cell Res* 2000; 256: 27-33.

Brune B, Lapetina EG. Glyceraldehyde-3-phosphate dehydrogenase: A target for nitric oxide signaling. In: Ignarro L and Murad F, editors. *Nitric Oxide*. 525 B Street/Suite 1900/San Diego/CA 92101-4495: Academic Press Inc, 1995: 351-360.

Brune B, Lapetina EG. Nitric oxide-induced covalent modification of glycolytic enzyme glyceraldehyde-3-phosphate dehydrogenase. In: Packer L, editor. *Nitric Oxide*, Pt B. 525 B Street/Suite 1900/San Diego/CA 92101-4495: Academic Press Inc, 1996: 400-407.

Carlile GW, Chalmers-Redman RM, Tatton NA, Pong A, Borden KE, Tatton WG. Reduced apoptosis after nerve growth factor and serum withdrawal: conversion of tetrameric glyceraldehyde-3-phosphate dehydrogenase to a dimer. *Mol Pharmacol* 2000; 57: 2-12.

Carlile GW, Tatton WG, Borden KL. Demonstration of a RNA-dependent nuclear interaction between the promyelocytic leukaemia protein and glyceraldehyde-3-phosphate dehydrogenase. *Biochem J* 1998; 335: 691-6.

Cassarino DS, Parks JK, Parker WD, Jr., Bennett JP, Jr. The parkinsonian neurotoxin MPP<sup>+</sup> opens the mitochondrial permeability transition pore and releases cytochrome c in isolated mitochondria via an oxidative mechanism. *Biochim Biophys Acta* 1999; 1453: 49-62.

Cassarino DS, Swerdlow RH, Parks JK, Parker WD, Jr., Bennett JP, Jr. Cyclosporin A increases resting mitochondrial membrane potential in SY5Y cells and reverses the depressed mitochondrial membrane potential of Alzheimer's disease cybrids. *Biochem Biophys Res Commun* 1998; 248: 168-73.

Chalmers-Redman RM, Fraser AD, Carlile GW, Pong A, Tatton WG. Glucose protection from MPP<sup>+</sup>-induced apoptosis depends on mitochondrial membrane potential and ATP synthase. *Biochem Biophys Res Commun* 1999; 257: 440-7.

Chalmers-Redman RME, Pong AW, Jagodzinski FB, Pong AW, Ju WYL, Mammen M, Tatton WG. Low level pro-oxidant exposure induces an anti-apoptotic program of new protein synthesis similar to deprenyl-related propargylamines. *J. Neurosci.* 2000; Submitted.

Chen RW, Saunders PA, Wei H, Li Z, Seth P, Chuang DM. Involvement of glyceraldehyde-3-phosphate dehydrogenase (GAPDH) and p53 in neuronal apoptosis: evidence that GAPDH is upregulated by p53. *J Neurosci* 1999; 19: 9654-62.

Chen Z, Wang ZY, Chen SJ. Acute promyelocytic leukemia: cellular and molecular basis of differentiation and apoptosis. *Pharmacol Ther* 1997; 76: 141-9.

Crompton M. The mitochondrial permeability transition pore and its role in cell death. *Biochemical Journal* 1999; 341: 233-249.

Fall CP, Bennett JP, Jr. Visualization of cyclosporin A and Ca<sup>2+</sup>-sensitive cyclical mitochondrial depolarizations in cell culture. *Biochim Biophys Acta* 1999; 1410: 77-84.

Finucane DM, Waterhouse NJ, AmaranteMendes GP, Cotter TG, Green DR. Collapse of the inner mitochondrial transmembrane potential is not required for apoptosis of HL60 cells. *Experimental Cell Research* 1999; 251: 166-174.

Gabellieri E, RahuelClermont S, Branlant G, Strambini GB. Effects of NAD(+) binding on the luminescence of tryptophans 84 and 310 of glyceraldehyde-3-phosphate dehydrogenase from *Bacillus stearothermophilus*. *Biochemistry* 1996; 35: 12549-12559.

Grant SM, Shankar SL, Chalmers-Redman RM, Tatton WG, Szyf M, Cuellar AC. Mitochondrial abnormalities in neuroectodermal cells stably expressing human amyloid precursor protein (hAPP751). *Neuroreport* 1999; 10: 41-6.

Gross A, Yin XM, Wang K, Wei MC, Jockel J, Milliman C, Erdjument-Bromage H, Tempst P, Korsmeyer SJ. Caspase cleaved BID targets mitochondria and is required for cytochrome c release, while BCL-XL prevents this release but not tumor necrosis factor-R1/Fas death. *J Biol Chem* 1999; 274: 1156-63.

Halestrap AP, Woodfield KY, Connern CP. Oxidative stress, thiol reagents, and membrane potential modulate the mitochondrial permeability transition by affecting nucleotide binding to the adenine nucleotide translocase. *Journal of Biological Chemistry* 1997; 272: 3346-3354.

Heiskanen KM, Bhat MB, Wang HW, Ma J, Nieminen AL. Mitochondrial depolarization accompanies cytochrome c release during apoptosis in PC6 cells. *J Biol Chem* 1999; 274: 5654-8.

- Huitorel P, Pantaloni D. Bundling of microtubules by glyceraldehyde-3-phosphate dehydrogenase and its modulation by ATP. *Eur J Biochem* 1985; 150: 265-9.
- Ishitani R, Chuang DM. Glyceraldehyde-3-phosphate dehydrogenase antisense oligodeoxynucleotides protect against cytosine arabinonucleoside-induced apoptosis in cultured cerebellar neurons. *Proceedings of the National Academy of Sciences of the United States of America* 1996; 93: 9937-9941.
- Ishitani R, Kimura M, Sunaga K, Katsube N, Tanaka M, Chuang DM. An antisense oligodeoxynucleotide to glyceraldehyde-3-phosphate dehydrogenase blocks age-induced apoptosis of mature cerebocortical neurons in culture. *Journal of Pharmacology and Experimental Therapeutics* 1996a; 278: 447-454.
- Ishitani R, Sunaga K, Hirano A, Saunders P, Katsube N, Chuang DM. Evidence that glyceraldehyde-3-phosphate dehydrogenase is involved in age-induced apoptosis in mature cerebellar neurons in culture. *Journal of Neurochemistry* 1996b; 66: 928-935.
- Ishitani R, Sunaga K, Tanaka M, Aishita H, Chuang DM. Overexpression of glyceraldehyde-3-phosphate dehydrogenase is involved in low K<sup>+</sup>-induced apoptosis but not necrosis of cultured cerebellar granule cells. *Molecular Pharmacology* 1997; 51: 542-550.
- Ishitani R, Tanaka M, Sunaga K, Katsube N, Chuang DM. Nuclear localization of overexpressed glyceraldehyde-3-phosphate dehydrogenase in cultured cerebellar neurons undergoing apoptosis. *Mol Pharmacol* 1998; 53: 701-7.
- Itoga M, Tsuchiya M, Ishino H, Shimoyama M. Nitric oxide-induced modification of glyceraldehyde-3-phosphate dehydrogenase with NAD(+) is not ADP-ribosylation. *Journal of Biochemistry* 1997; 121: 1041-1046.
- Jing Y, Dai J, Chalmers-Redman RM, Tatton WG, Waxman S. Arsenic trioxide selectively induces acute promyelocytic leukemia cell apoptosis via a peroxide-dependent pathway. *Blood*. Vol 94, 1999: 2102-11.
- Kaim G, Dimroth P. ATP synthesis by F-type ATP synthase is obligatorily dependent on the transmembrane voltage. *Embo J* 1999; 18: 4118-27.
- Kantrow SP, Piantadosi CA. Release of cytochrome c from liver mitochondria during permeability transition. *Biochemical and Biophysical Research Communications* 1997; 232: 669-671.
- Kelekar A, Chang BS, Harlan JE, Fesik SW, Thompson CB. Bad is a BH3 domain-containing protein that forms an inactivating dimer with Bcl-XL. *Mol Cell Biol* 1997; 17: 7040-6.
- Kluck RM, Bossy Wetzl E, Green DR, Newmeyer DD. The release of cytochrome c from mitochondria: a primary site for Bcl-2 regulation of apoptosis. *Science* 1997; 275: 1132-6.
- Korsmeyer SJ. BCL-2 gene family and the regulation of programmed cell death. *Cancer Res* 1999; 59: 1693s-1700s.
- Kroemer G, Petit P, Zamzami N, Vayssiere JL, Mignotte B. The biochemistry of programmed cell death. *Faseb J* 1995; 9: 1277-87.
- Kroemer G, Zamzami N, Susin SA. Mitochondrial control of apoptosis. *Immunol Today* 1997; 18: 44-51.
- Krohn AJ, Wahlbrink T, Prehn JH. Mitochondrial depolarization is not required for neuronal apoptosis. *J Neurosci* 1999; 19: 7394-404.
- Li P, Nijhawan D, Budihardjo I, Srinivasula SM, Ahmad M, Alnemri ES, Wang X. Cytochrome c and dATP-dependent formation of Apaf-1/caspase-9 complex initiates an apoptotic protease cascade. *Cell* 1997; 91: 479-89.
- Liu XS, Kim CN, Yang J, Jemmerson R, Wang XD. Induction of apoptotic program in cell-free extracts: Requirement for dATP and cytochrome c. *Cell* 1996; 86: 147-157.
- Liu XS, Zou H, Slaughter C, Wang XD. DFF, a heterodimeric protein that functions downstream of caspase-3 to trigger DNA fragmentation during apoptosis. *Cell* 1997; 89: 175-184.
- Loeffler M, Kroemer G. The mitochondrion in cell death control: certainties and incognita. *Exp Cell Res* 2000; 256: 19-26.
- Marzo I, Brenner C, Zamzami N, Jurgensmeier JM, Susin SA, Vieira HL, Prevost MC, Xie Z, Matsuyama S, Reed JC, Kroemer G. Bax and adenine nucleotide translocator cooperate in the mitochondrial control of apoptosis. *Science* 1998a; 281: 2027-31.
- Marzo I, Brenner C, Zamzami N, Susin SA, Beutner G, Brdiczka D, Remy R, Xie ZH, Reed JC, Kroemer G. The permeability transition pore complex: a target for apoptosis regulation by caspases and bcl-2-related proteins. *J Exp Med* 1998b; 187: 1261-71.
- Matera AG. Nuclear bodies: multifaceted subdomains of the interchromatin space. *Trends Cell Biol* 1999; 9: 302-9.

McDonald LJ, Moss J. Nitric oxide and NAD-dependent protein modification. *Molecular and Cellular Biochemistry* 1994; 138: 201-206.

Mittag TW, Danias J, Pohorenc G, Yuan HM, Burakgazi E, Chalmers-Redman R, Podos SM, Tatton WG. Retinal damage after 3 to 4 months of elevated intraocular pressure in a rat glaucoma model. *Invest Ophthalmol Vis Sci* 2000; 41: 3451-9.

Mohr S, Stamler JS, Brune B. Posttranslational modification of glyceraldehyde-3-phosphate dehydrogenase by S-nitrosylation and subsequent NADH attachment. *Journal of Biological Chemistry* 1996; 271: 4209-4214.

Montal M. Mitochondria, glutamate neurotoxicity and the death cascade. *Biochim Biophys Acta* 1998; 1366: 113-26.

Morgenegg G, Winkler GC, Hubscher U, Heizmann CW, Mous J, Kuenzle CC. Glyceraldehyde-3-phosphate dehydrogenase is a nonhistone protein and a possible activator of transcription in neurons. *J Neurochem* 1986; 47: 54-62.

Nagy E, Rigby WFC. Glyceraldehyde-3-phosphate dehydrogenase selectively binds AU-rich RNA in the NAD(+)-binding region (Rossmann fold). *Journal of Biological Chemistry* 1995; 270: 2755-2763.

Narita M, Shimizu S, Ito T, Chittenden T, Lutz RJ, Matsuda H, Tsujimoto Y. Bax interacts with the permeability transition pore to induce permeability transition and cytochrome c release in isolated mitochondria. *Proceedings of the National Academy of Sciences of the United States of America* 1998; 95: 14681-14686.

Nicholls DG, Budd SL. Mitochondria and neuronal survival. *Physiol Rev* 2000; 80: 315-60.

Nicolli A, Basso E, Petronilli V, Wenger RM, Bernardi P. Interactions of cyclophilin with the mitochondrial inner membrane and regulation of the permeability transition pore, and cyclosporin A- sensitive channel. *J Biol Chem* 1996; 271: 2185-92.

Pastorino JG, Chen ST, Tafani M, Snyder JW, Farber JL. The overexpression of Bax produces cell death upon induction of the mitochondrial permeability transition. *J Biol Chem* 1998; 273: 7770-5.

Pastorino JG, Tafani M, Rothman RJ, Marcineviciute A, Hoek JB, Farber JL. Functional consequences of the sustained or transient activation by Bax of the mitochondrial permeability transition pore. *J Biol Chem* 1999; 274: 31734-9.

Quignon F, De Bels F, Koken M, Feunteun J, Ameisen JC, de The H. PML induces a novel caspase-independent death process. *Nat Genet* 1998; 20: 259-65.

Rigobello MP, Scutari G, Friso A, Barzon E, Artusi S, Bindoli A. Mitochondrial permeability transition and release of cytochrome c induced by retinoic acids. *Biochemical Pharmacology* 1999; 58: 665-670.

Saunders PA, Chalecka-Franaszek E, Chuang DM. Subcellular distribution of glyceraldehyde-3-phosphate dehydrogenase in cerebellar granule cells undergoing cytosine arabinoside-induced apoptosis. *J. Neurochem.* 1997; 69: 1820-1828.

Saunders PA, Chen RW, Chuang DM. Nuclear translocation of glyceraldehyde-3-phosphate dehydrogenase isoforms during neuronal apoptosis. *J Neurochem* 1999; 72: 925-32.

Sawa A, Khan AA, Hester LD, Snyder SH. Glyceraldehyde-3-phosphate dehydrogenase: Nuclear translocation participates in neuronal and nonneuronal cell death. *Proceedings of the National Academy of Sciences of the United States of America* 1997; 94: 11669-11674.

Scorrano L, Nicolli A, Basso E, Petronilli V, Bernardi P. Two modes of activation of the permeability transition pore: The role of mitochondrial cyclophilin. *Molecular and Cellular Biochemistry* 1997a; 174: 181-184.

Scorrano L, Petronilli V, Bernardi P. On the voltage dependence of the mitochondrial permeability transition pore - A critical appraisal. *Journal of Biological Chemistry* 1997b; 272: 12295-12299.

Shashidharan P, Chalmers-Redman RM, Carlile GW, Rodic V, Gurvich N, Yuen T, Tatton WG, Sealfon SC. Nuclear translocation of GAPDH-GFP fusion protein during apoptosis. *Neuroreport* 1999; 10: 1149-53.

Sioud M, Jespersen L. Enhancement of hammerhead ribozyme catalysis by glyceraldehyde-3-phosphate dehydrogenase. *Journal of Molecular Biology* 1996; 257: 775-789.

Sirover MA. New insights into an old protein: the functional diversity of mammalian glyceraldehyde-3-phosphate dehydrogenase. *Biochim Biophys Acta* 1999; 1432: 159-84.

Sugrue MM, Shin DY, Lee SW, Aaronson SA. Wild-type p53 triggers a rapid senescence program in human tumor cells lacking functional p53. *Proc Natl Acad Sci U S A* 1997; 94: 9648-53.

Sugrue MM, Wang Y, Rideout HJ, Chalmers-Redman RM, Tatton WG. Reduced mitochondrial membrane potential and altered responsiveness of a mitochondrial membrane megachannel in p53-induced senescence.

Biochem Biophys Res Commun 1999; 261: 123-30.

Sunaga K, Takahashi H, Chuang DM, Ishitani R. Glyceraldehyde-3-phosphate dehydrogenase is over-expressed during apoptotic death of neuronal cultures and is recognized by a monoclonal antibody against amyloid plaques from Alzheimer's brain. *Neuroscience Letters* 1995; 200: 133-136.

Susin SA, Lorenzo HK, Zamzami N, Marzo I, Brenner C, Larochette N, Prevost MC, Alzari PM, Kroemer G. Mitochondrial release of caspase-2 and -9 during the apoptotic process. *J Exp Med* 1999a; 189: 381-94.

Susin SA, Lorenzo HK, Zamzami N, Marzo I, Snow BE, Brothers GM, Mangion J, Jacotot E, Costantini P, Loeffler M, Larochette N, Goodlett DR, Aebersold R, Siderovski DP, Penninger JM, Kroemer G. Molecular characterization of mitochondrial apoptosis-inducing factor. *Nature* 1999b; 397: 441-6.

Susin SA, Zamzami N, Kroemer G. Mitochondria as regulators of apoptosis: doubt no more. *Biochim Biophys Acta* 1998; 1366: 151-65.

Tatton NA. Increased Caspase 3 and Bax Immunoreactivity Accompany Nuclear GAPDH Translocation and Neuronal Apoptosis in Parkinson's Disease. *Exp Neurol* 2000; 166: 29-43.

Tatton NA, Kish SJ. In situ detection of apoptotic nuclei in the substantia nigra compacta of 1-methyl-4-phenyl-1,2,3,6-tetrahydropyridine-treated mice using terminal deoxynucleotidyl transferase labelling and acridine orange staining. *Neurosci* 1997; 77: 1037-1048.

Tatton NA, Maclean-Fraser A, Tatton WG, Perl DP, Olanow CW. A fluorescent double-labeling method to detect and confirm apoptotic nuclei in Parkinson's disease. *Ann Neurol* 1998; 44: S142-8.

Tatton NA, Rideout HJ. Confocal microscopy as a tool to examine DNA fragmentation, Chromatin condensation and other apoptotic changes in Parkinson's disease. *Parkinsonism and Rel. Disord.* 1999; 5: 179-186.

Tatton WG, Chalmers-Redman RME, Rideout HJ, Tatton NA. Mitochondrial permeability in neuronal death: possible relevance to pathogenesis of parkinson's disease. *Parkinsonism and Related Disord.* 1999; 5: 221-229.

Tatton WG, Ju WY, Holland DP, Tai C, Kwan M. (-)-Deprenyl reduces PC12 cell apoptosis by inducing new protein synthesis. *J Neurochem* 1994; 63: 1572-5.

Tenneti L, D'Emilia DM, Troy CM, Lipton SA. Role of caspases in N-methyl-D-aspartate-induced apoptosis in cerebrocortical neurons. *J Neurochem* 1998; 71: 946-59.

Volker KW, Knull HR. A glycolytic enzyme binding domain on tubulin. *Arch. Biochem. Biophys.* 1997; 338: 237-243.

Wadia JS, Chalmers-Redman RME, Ju WJH, Carlile GW, Phillips JL, Fraser AD, Tatton WG. Mitochondrial membrane potential and nuclear changes in apoptosis caused by serum and nerve growth factor withdrawal: time course and modification by (-)-deprenyl. *J Neurosci* 1998; 18: 932-47.

Wang ZG, Delva L, Gaboli M, Rivi R, Giorgio M, Cordon-Cardo C, Grosveld F, Pandolfi PP. Role of PML in cell growth and the retinoic acid pathway. *Science* 1998a; 279: 1547-51.

Wang ZG, Ruggero D, Ronchetti S, Zhong S, Gaboli M, Rivi R, Pandolfi PP. PML is essential for multiple apoptotic pathways [see comments]. *Nat Genet* 1998b; 20: 266-72.

Woodfield K, Ruck A, Brdziczka D, Halestrap AP. Direct demonstration of a specific interaction between cyclophilin-D and the adenine nucleotide translocase confirms their role in the mitochondrial permeability transition. *Biochem. J.* 1998; 336: 287-290.

Yang E, Zha J, Jockel J, Boise LH, Thompson CB, Korsmeyer SJ. Bad, a heterodimeric partner for Bcl-XL and Bcl-2, displaces Bax and promotes cell death. *Cell* 1995; 80: 285-91.

Yang J, Liu XS, Bhalla K, Kim CN, Ibrado AM, Cai JY, Peng TI, Jones DP, Wang XD. Prevention of apoptosis by Bcl-2: Release of cytochrome c from mitochondria blocked. *Science* 1997; 275: 1129-1132.

Zamzami N, Brenner C, Marzo I, Susin SA, Kroemer G. Subcellular and submitochondrial mode of action of Bcl-2-like oncoproteins. *Oncogene* 1998; 16: 2265-82.

Zamzami N, Marchetti P, Castedo M, Hirsch T, Susin SA, Masse B, Kroemer G. Inhibitors of permeability transition interfere with the disruption of the mitochondrial transmembrane potential during apoptosis. *FEBS Lett* 1996a; 384: 53-7.

Zamzami N, Susin SA, Marchetti P, Hirsch T, GomezMonterrey I, Castedo M, Kroemer G. Mitochondrial control of nuclear apoptosis. *Journal of Experimental Medicine* 1996b; 183: 1533-1544.

Zha J, Harada H, Osipov K, Jockel J, Waksman G, Korsmeyer SJ. BH3 domain of BAD is required for heterodimerization with BCL-XL and pro-apoptotic activity. *J Biol Chem* 1997; 272: 24101-4.

Zhong S, Salomoni P, Ronchetti S, Guo A, Ruggero D, Pandolfi PP. Promyelocytic leukemia protein (PML) and Daxx participate in a novel nuclear pathway for apoptosis. *J Exp Med* 2000; 191: 631-40.

Zou H, Henzel WJ, Liu XS, Lutschg A, Wang XD. Apaf-1, a human protein homologous to C-elegans CED-4, participates in cytochrome c-dependent activation of caspase-3. *Cell* 1997; 90: 405-413.

**(11) Appendices**

Carlile GW, Chalmers-Redman RM, Tatton NA, Pong A, Borden KE, Tatton WG. Reduced apoptosis after nerve growth factor and serum withdrawal: conversion of tetrameric glyceraldehyde-3-phosphate dehydrogenase to a dimer. *Mol Pharmacol* 2000; 57: 2-12.

Tatton NA. Increased Caspase 3 and Bax Immunoreactivity Accompany Nuclear GAPDH Translocation and Neuronal Apoptosis in Parkinson's Disease. *Exp Neurol* 2000; 166: 29-43.

**(12) Personnel Receiving Salary Support From The Research Effort**

William G. Tatton MD, PhD – Professor Principal Investigator  
R.M.E. Chalmers-Redman PhD – Assistant Professor  
Che. Juantu PhD – Molecular Biology/Protein Chemistry Technician  
M. Mammen MSc. – Tissue Culture Technician  
P. Jagodzinski BA – Laser Confocal Scanning Microscope Technician  
A. Sud – MPharm Graduate Trainee

# **Appendix**

## Reduced Apoptosis after Nerve Growth Factor and Serum Withdrawal: Conversion of Tetrameric Glyceraldehyde-3-Phosphate Dehydrogenase to a Dimer

GRAEME W. CARLILE, RUTH M. E. CHALMERS-REDMAN, NADINE A. TATTON, AMANDA PONG, KATHERINE E. BORDEN, and WILLIAM G. TATTON

*Departments of Neurology (G.W.C., R.M.E.C.-R., N.A.T., A.P., K.L.B.B., W.G.T.) and Physiology and Biophysics (K.L.B.B.), Mount Sinai School of Medicine, New York, New York*

Received August 5, 1999; accepted September 20, 1999

This paper is available online at <http://www.molpharm.org>

### ABSTRACT

Antisense oligonucleotides against the glycolytic enzyme glyceraldehyde-3-phosphate dehydrogenase (GAPDH) are able to reduce some forms of apoptosis. In those forms, overall GAPDH levels increase and the enzyme accumulates in the nucleus. The monoamine oxidase B (MAO-B) inhibitor, (–)-deprenyl (DEP), its metabolite (–)-desmethyldeprenyl, and a tricyclic DEP analog, CGP3466, can reduce apoptosis independently of MAO-B inhibition and have been found to bind to GAPDH. We used neuronally differentiated PC12 cells to show that DEP, DES, and CGP3466 reduce apoptosis caused by serum and nerve growth factor withdrawal over the concentration range of  $10^{-7}$  to  $10^{-13}$  M. We provide evidence that the DEP-like compounds bind to GAPDH in the PC12 cells and that they prevent both the apoptotic increases in GAPDH levels and nuclear accumulation of GAPDH. In vitro, the compounds en-

hanced the conversion of  $\text{NAD}^+$  to NADH by GAPDH in the presence of AUUUA-rich RNA and converted GAPDH from its usual tetrameric form to a dimeric form. Using cell lysates, we found a marked increase in rates of  $\text{NAD}^+$  to NADH conversion in early apoptosis, which was returned toward control values by the DEP-like compounds. Accordingly, the DEP-like compounds appear to decrease glycolysis by preventing the GAPDH increases in early apoptosis. GAPDH dimer may not have the capacity to contribute to apoptosis in a similar manner to the tetramer, which might account for the antiapoptotic capacity of the compounds. These actions on GAPDH, rather than MAO-B inhibition, may contribute to the improvements in Parkinson's and Huntington's diseases found with DEP treatment.

Studies with antisense oligonucleotides showed that glyceraldehyde-3-phosphate dehydrogenase (GAPDH) is necessary for apoptosis to proceed in cerebrocortical neurons and PC12 cells (Ishitani et al., 1996; Sawa et al., 1997). GAPDH levels increase during the early part of apoptosis (Sunaga et al., 1995; Ishitani et al., 1996, 1997, 1998; Saunders et al., 1997). In nonapoptotic cells, GAPDH is primarily found in the extra nuclear cytoplasm with only sparse localization to small punctate areas in the nucleus (Carlile et al., 1998). In apoptosis, GAPDH accumulates densely in the nucleus, and that accumulation has been proposed to underlie its role in apoptosis (Saunders et al., 1997; Sawa et al., 1997; Ishitani et al., 1998; Shashidharan et al., 1999).

GAPDH may participate in the pathogenesis of some neu-

rodegenerative diseases. GAPDH binds to the mutant proteins with polyglutamine repeats in Huntington's disease (HD) and related degenerative conditions (Burke et al., 1996). GAPDH is found in amyloid plaques in Alzheimer's disease (AD) brains (Sunaga et al., 1995), and GAPDH nuclear accumulation is present in association with apoptosis in nigral neuronal nuclei in postmortem Parkinson's disease (PD) brain (N. Tatton, unpublished observations). Although there is evidence for metabolic abnormalities in HD tissues, GAPDH glycolytic activity does not appear to be altered in HD brain tissue (Kish et al., 1998).

Neuronal loss, likely by apoptosis, is central to AD, HD, and PD (Cotman, 1998; Tatton et al., 1998; Petersen et al., 1999). The monoamine oxidase B (MAO-B) inhibitor (–)-deprenyl (DEP) slows the progression of PD clinical deficits (Parkinson's Study Group, 1993; Olanow et al., 1995) and

The work was supported by a Lowenstein Foundation Grant and Medical Research Council of Canada Grants (to W.G.T. and K.L.B.B.).

**ABBREVIATIONS:** GAPDH, glyceraldehyde-3-phosphate dehydrogenase; DEP, (–)-deprenyl; DES, (–)-desmethyldeprenyl; PML, promyelocytic leukemia; BL, BODIPY-labeled; PND, partially neuronally differentiated; LCSM, laser confocal scanning microscopy; M/S+N, minimum essential medium with serum and nerve growth factor; BCA, bicinchoninic acid; NGF, nerve growth factor; M/O, minimum essential medium only; CGP3466, *N*-methyl-*N*-propargyl-10<sup>+</sup>-aminomethyl-dibenzo[*b,f*]oxepin; HD, Huntington's disease; AD, Alzheimer's disease; PD, Parkinson's disease; MAO-B, monoamine oxidase B.

may also reduce clinical deficits in HD (Patel et al., 1996). The basis for clinical improvements with DEP are uncertain because the clinical trial data do not allow for the differentiation of a slowed rate of neuronal loss from a symptomatic effect like that caused by increased dopamine availability (see Fahn, 1996). DEP and its metabolite, (-)-desmethyldesprenyl (DES), reduce apoptosis in a variety of cells (Tatton et al., 1994; Le et al., 1997; Paterson et al., 1997, 1998; Kragten et al., 1998; Magyar et al., 1998; Maruyama et al., 1998; Wadia et al., 1998) via mechanisms that are independent of MAO-B inhibition (Tatton and Chalmers-Redman, 1996) and require new protein synthesis (Tatton et al., 1994). CGP3466, a tricyclic DEP analog (*N*-methyl-*N*-propargyl-10-amino-methyl-dibenzo[*b,f*]oxepin), which does not have the capacity to inhibit MAO-B, reduces apoptosis and binds specifically to GAPDH (Kragten et al., 1998). The GAPDH binding has been proposed to account for the antiapoptotic capacities of DEP-like compounds.

We have carried out experiments *in vivo* and *in vitro* to determine whether DES and CGP3466 reduce apoptosis caused by serum and NGF withdrawal in a similar manner to DEP (Tatton et al., 1994; Wadia et al., 1998) and whether any

reduction in apoptosis by DES and CGP3466 can be linked to actions on GAPDH.

## Materials and Methods

PC12 cells were propagated in minimum essential medium (MEM) containing 10% horse serum and 5% fetal bovine serum. The cells were transferred to 24-well plates and partially neuronally differentiated (PND) for 6 days in the same media supplemented with 100 ng/ml 7S nerve growth factor (NGF; MEM with serum and NGF (M/S+N); see Wadia et al. (1998) for details of culture, treatment, preparation, staining, and counting). On day 6, the cells were washed repeatedly to remove NGF and serum-borne trophic agents and replaced in M/S+N as controls, in MEM only (M/O) for trophic withdrawal, or in MEM with DEP, DES, or CGP3466 at concentrations varying from  $10^{-5}$  to  $10^{-13}$  M. At 24 h after washing, cells were harvested and lysed, and intact nuclei were counted as an estimate of cell survival (Fig. 1A, filled circles).

The cells were also grown and treated as above on poly(L-lysine)-treated coverglass and were stained with YOYO-1 (Molecular Probes, Eugene, OR) at various times after washing to reveal chromatin condensation as a marker of apoptotic nuclear degradation (see Wadia et al., 1998, for references). Cells on coverglass were washed three times in PBS and then put in 100% methanol at  $-20^{\circ}\text{C}$

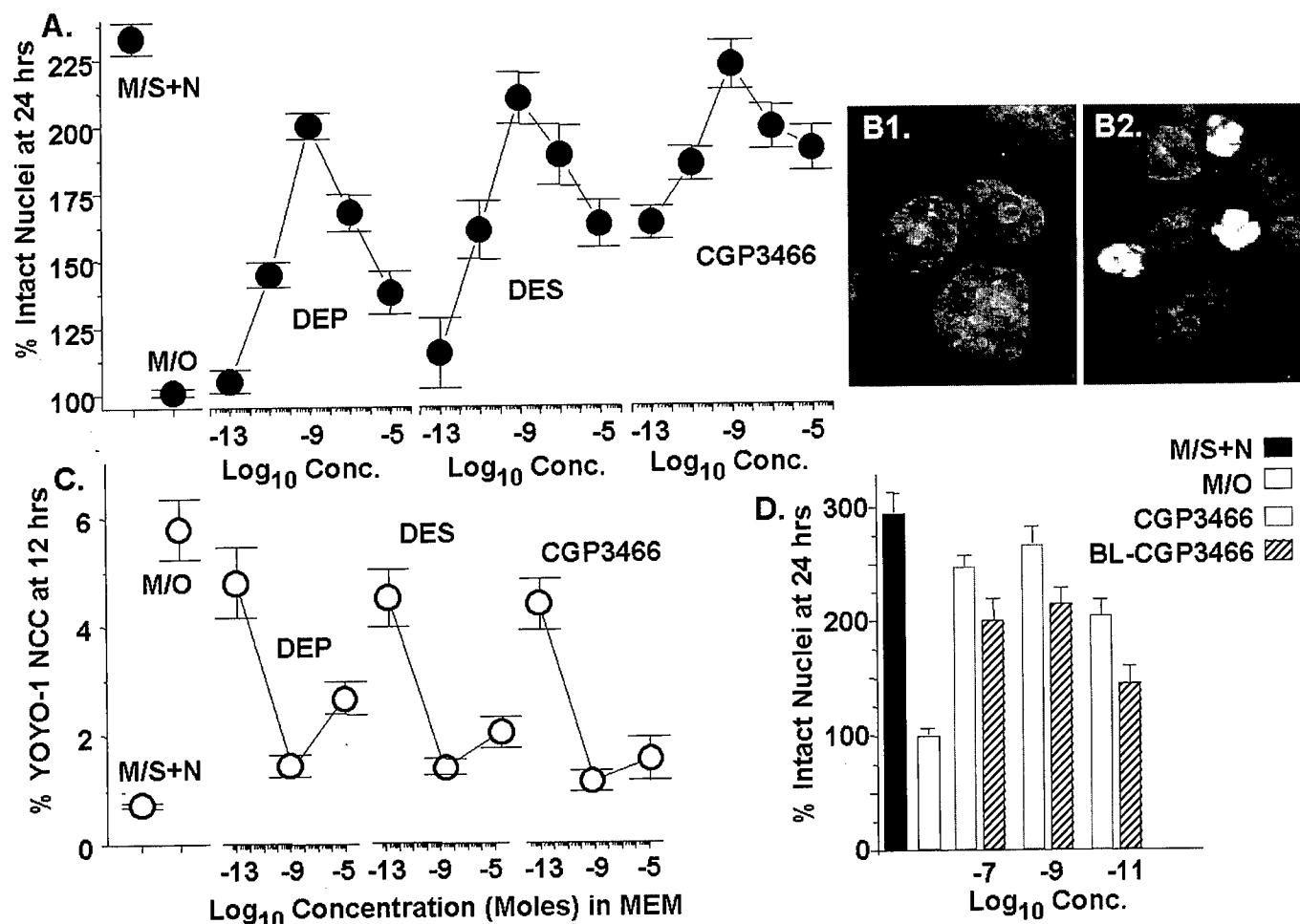


**Fig. 1.** DEP-related compounds reduce apoptosis. DEP, DES, and CGP3466 at concentrations ranging between  $10^{-13}$  and  $10^{-5}$  M increase the survival of PND-PC12 cells as estimated by numbers of intact nuclei (A) and decrease the number of nuclei with apoptotic nuclear degradation as shown by nuclear chromatin condensation revealed by YOYO-1 DNA staining at the same concentrations (C). M/S+N indicates cells that were washed repeatedly to remove trophic support and then replaced in MEM with serum and NGF. M/O indicates cells that were washed and then placed in MEM only. B1 and B2, typical examples of YOYO-1 stained normal nuclei and nuclei with chromatin condensation, respectively. D, comparison of the numbers of intact nuclei for cells treated with CGP3466 and those treated with BL-CGP3466 showing that the BL compound retains most of the capacity of the unlabeled compound to reduce cell death.



for 30 s. The cells on coverglass were then incubated in 1.5  $\mu$ M YOYO-1 in PBS at room temperature for 30 min. The cells were then washed three times in PBS and mounted in Aquamount (Gurr, England). The total number of YOYO-1 stained nuclei were counted on 25 fields for each coverslip, each field was chosen by the use of pairs of randomly generated *x-y* coordinates, and the number of nuclei with chromatin condensation were expressed as a percentage. The values were pooled for three coverslips for each treatment and time point.

Laser confocal scanning microscopic (LCSM) images were collected using a Leica TCS4D confocal microscope equipped with a tunable excitation filter. Images were collected with a 100 $\times$  1.4 NA objective at a pinhole setting of 20 to minimize focal depth. Images were collected in a 512  $\times$  512  $\times$  8 bit format and saved as TIFF files. Images of live cells exposed to BODIPY-labeled (BL)-CGP3466 or DES were similarly acquired using an environmentally controlled chamber (Medical Systems Corp.) that houses a 25-mm coverglass on which PC12 cells were plated and treated as above. YOYO-1 was imaged using excitation/emission values of 488 nm/515 to 545 nm, whereas BODIPY-FL images and GAPDH immunoreaction fluorescence were taken at 568/585 to 615 and 647/660 long pass, respectively.

To identify the proteins that bind CGP3466 in the PND PC12 cells, cells were incubated with  $^{125}$ I photoaffinity-labeled CGP3466 at varying times after serum and NGF withdrawal. After exposure to ultraviolet light, total protein was extracted, run on gels, and transferred to a membrane. PC-12 cells were grown in MEM with serum and NGF for 6 days, and then serum and NGF were withdrawn. One hour before harvesting, 6  $\mu$ Ci of the photoaffinity-labeled CGP3466 was added. Thirty minutes later, the dishes were put in a UV transilluminator for 20 min to activate the azido group. After removal of the medium and one wash with balanced salt solution, the cells were harvested using trypsin-EDTA and then centrifuged at 1000g for 5 min. The supernatant was removed and the cells were washed twice in PBS. The cells were lysed in lysis buffer (25 mM Tris  $\cdot$  HCl, pH 7.5, 150 mM NaCl, 1 mM EDTA, and 1% Triton X-100), and the samples were stored frozen at  $-20^{\circ}\text{C}$ . Samples were run on an SDS-polyacrylamide gel and transferred to a nitrocellulose membrane. The membrane was dried and exposed on x-ray film. After completion of the autoradiographic exposure, the same membranes were probed for GAPDH immunoreactivity using a mouse monoclonal antibody (Chemicon International, Temecula, CA) at a dilution of 1:400.

For determinations of the time course of changes in GAPDH levels, cells were grown on 10-cm Petri dishes for 6 days and treated as above. At 0.5 to 12 h after washing, cells were harvested, and a lysate was produced. The medium was removed and placed in a separate tube on ice, and 2 ml of PBS was added to each dish. The cells were removed with a cell scraper and centrifuged for 5 min at 1500g at  $4^{\circ}\text{C}$ , followed by cold PBS washes. The cells were then centrifuged at 2000g and lysed in lysis buffer (25 mM Tris  $\cdot$  HCl, pH 7.5, 150 mM NaCl, 1 mM EDTA, 1% Triton X-100, and 5  $\mu$ g/ml leupeptin, chymostatin, pepstatin A, and aprotinin, plus 1 mM benzamide). The lysate was stored at  $-30^{\circ}\text{C}$ . Protein was assayed by the bicinchoninic acid (BCA) method.

To obtain protein from various subcellular fractions, the cells were treated as above and harvested by centrifugation at 1000g for 5 min at  $4^{\circ}\text{C}$ . The pellets were washed twice in cold PBS and resuspended in buffer containing 25 mM HEPES-KOH, pH 7.5, 10 mM KCl, 1.5 mM  $\text{MgCl}_2$ , 1 mM NaEDTA, 1 mM NaEGTA, 1 mM dithiothreitol, and 5  $\mu$ g/ml leupeptin, chymostatin, pepstatin A, and aprotinin, plus 1 mM benzamide and 250 mM sucrose. The cells were homogenized by 12 to 15 strokes of a glass Dounce homogenizer. The homogenates were then centrifuged at 700g for 10 min at  $4^{\circ}\text{C}$ . This pellet is the nuclear fraction, and the supernatants were further centrifuged at 10,000g for 15 min at  $4^{\circ}\text{C}$ . The resulting pellet represents the mitochondrially enriched fraction, and the supernatant represents the cytoplasmic fraction. Both nuclear and mitochondrially enriched fractions were resuspended in 50  $\mu$ l of the above buffer. Samples were then frozen

at  $-30^{\circ}\text{C}$ . Before use, the samples were protein assayed by the BCA method. Equal amounts of whole-cell or subcellular fraction lysates were run on a SDS-polyacrylamide gel, Western blotted, and probed for GAPDH as above.

To demonstrate the enrichment of cellular subfractions, equal amounts of protein from each fraction were Western blotted and probed with antibodies for nucleolin (1:500; Santa Cruz Biochemicals, Santa Cruz, CA), 14-3-3  $\beta$  protein (1:400; Santa Cruz Biochemicals), and cytochrome oxidase (0.1  $\mu$ g/ml; Molecular Probes, Eugene, OR), which are markers for the nuclear, cytoplasmic, and mitochondrial fractions, respectively.

For immunocytochemistry and the examination of the kinetics of cellular entry and accumulation of fluorescently labeled DES and CGP3466, PC-12 cells were grown on a coverglass and partially neuronally differentiated as described (for details, see Tatton et al., 1994; Wadia et al., 1998). Cells were fixed in 4% paraformaldehyde and then washed once in PBS and placed in 5% normal goat serum and 0.01% Tween-20 in PBS for 1 h at room temperature. The cell on coverglass were again washed with PBS; placed in a solution containing 0.5% normal serum, 0.01% Tween-20, and mouse monoclonal GAPDH antibody at a 1:300 dilution; and incubated overnight at  $4^{\circ}\text{C}$ . The cells on a coverglass were washed four times with PBS and exposed to a Cy5-labeled goat anti-mouse secondary antibody (Jackson Immunoresearch, West Grove, PA) at a dilution of 1:500 in PBS containing 0.5% normal serum and 0.01% Tween-20 for 1 h at room temperature. The cells on coverglass were washed five times in PBS and mounted in Aquamount.

Three-dimensional protein structural models of rat GAPDH were produced as in Borden (1998) and are described here briefly. The structure of rat GAPDH has not been reported. GAPDH structures were obtained from the Brookhaven protein database. GAPDH is highly conserved in terms of its amino acid sequence and three-dimensional structure (Kim et al., 1995). After inspection of structures of GAPDH from several species, we decided to use a GAPDH from *Leishmania mexicana*, in which the structure had been determined under physiological salt conditions, although this structure did not look significantly different from any other GAPDH structures in the database (Kim et al., 1995). Using the program Insight (Biosym, San Diego, CA), we modeled the rat GAPDH sequence onto the *L. mexicana* structure. The subsequent structure was subjected to molecular dynamics at 1000 K, followed by cooling to 300 K, and then underwent 1000 steps of conjugate gradient minimization using Discover (Biosym).

The glycolytic activity of GAPDH, measured by the increase in absorption at 340 nm, resulting from the reduction of  $\text{NAD}^+$  to NADH according to the reaction glyceraldehyde-3-phosphate +  $\text{NAD}^+$  +  $\text{P}_i$  = 1,3-diphosphoglycerate + NADH. The enzyme assay was carried out in the presence of 0.015 M sodium pyrophosphate, pH 8.5, 7.5 mM  $\text{NAD}^+$ , 0.1 M dithiothreitol, and 0.015 M GAPDH. Immediately before its use, the enzyme was diluted in the pyrophosphate buffer to a concentration of 30  $\mu$ g/ml. A synthetic RNA oligonucleotide of 15 residues consisting of three repeating AUUUA sequences (Genosys, Ltd., Cambridge, UK) was used in the glycolytic studies. The glycolytic activity of cell lysates produced from a 6-h exposure to MS+N, M/O, and MO+DES was similarly determined. Cells were collected in 0.015 M sodium pyrophosphate buffer, pH 8.5, and homogenized with a Dounce homogenizer; protein was assayed by the BCA method (Pierce Chemical, Rockford, IL) and stored at  $-20^{\circ}\text{C}$ . Equal amounts of total protein were incubated in 0.015 M sodium pyrophosphate, pH 8.5, with  $\text{NAD}^+$  and dithiothreitol, and the conversion of  $\text{NAD}^+$  to NADH was determined as above.

To examine the oligomeric states of GAPDH, Sephacryl H-300 was poured into a glass column to a height of 12 cm and diameter of 1 cm. The column was washed using a buffer containing 20 mM HEPES, pH 7.5, 25 mM KCl, and 10% glycerol. Samples were loaded onto the column in volumes of less than 100  $\mu$ l. Samples including more than one component were coinubated briefly before addition to the column. GAPDH, CGP3466, and RNA were used in nanomolar concen-

trations in a strict ratio of 1 molecule of GAPDH to 2 of RNA and/or 2 of CGP3466. All samples were dissolved in this buffer. Where indicated, 0.1% of SDS was used. To calibrate the column, the fractions for the following proteins were determined: cytochrome *c* (12.4 kDa) fraction 23, lysozyme (14.4 kDa) fraction 23, carbonic anhydrase (20 kDa) fraction 20, BSA (67 kDa) fraction 18,  $\beta$ -galactosidase (116 kDa) fraction 16, aldolase (158 kDa) fraction 13, and macroglobulin (170 kDa) fraction 10 (see calibration bar below Fig. 7B3). Protein was detected by monitoring the absorbance of individual fractions at 280 nm and confirmed at 293 nm. Nucleic acid was detected similarly by monitoring absorbance at 260 nm.

## Results

We previously showed that apoptosis initiated by serum and NGF withdrawal from PND-PC12 cells can be reduced by DEP (Tatton et al., 1994; Wadia et al., 1998). In this study, we used the same model to compare the antiapoptotic capacities of DEP, DES, and CGP3466. Reductions in apoptosis were estimated by two complementary measures: 1) counts of intact nuclei as an indicator of cell survival and 2) counts of cells with nuclear chromatin condensation using a fluorescent DNA binding dye, YOYO-1, as a measure of apoptotic nuclear degradation (examples in Fig. 1, B1 and B2). DES and CGP3466 showed similar or superior capacities to DEP

to increase survival (Fig. 1A) and to reduce the proportion of nuclei with chromatin condensation (Fig. 1C) over concentration ranges of  $10^{-5}$  to  $10^{-13}$  M. At  $10^{-9}$  M, all three agents at least doubled the proportion of cells that survived for 24 h after NGF and serum withdrawal. In a similar manner, the same concentration reduced the proportion of cells with nuclear chromatin condensation to less than 25% of that found at 12 h after NGF and serum withdrawal.

We also compared the capacity of a BL-CGP3466 (Zimmermann et al., 1998) for details of the fluorescently labeled DES and CGP3466) with that of CGP3466 in reducing apoptosis in the PND-PC12 model (Fig. 1D). Over the concentration range of  $10^{-7}$  to  $10^{-11}$  M, the BL-CGP3466 retained 75 to 80% of the capacity of CGP3466 to increase cell survival.

We then used the BL-CGP3466 with LCSM to follow the entry and localization of BL-CGP3466 in living PND-PC12 cells maintained in an environmentally controlled chamber. The BL-CGP3466 fluorescence revealed reproducible rates of entry and subcellular localization in the cells and displayed classic competition curves for preadded unlabeled CGP3466. Figure 2 provides an example of the competition in which the addition of  $10^{-9}$  M BL-CGP3466 to the chamber resulted in a gradual accumulation of subcellular fluorescence over about 30 min (Fig. 2, top). The subcellular distribution of the BL-CGP3466

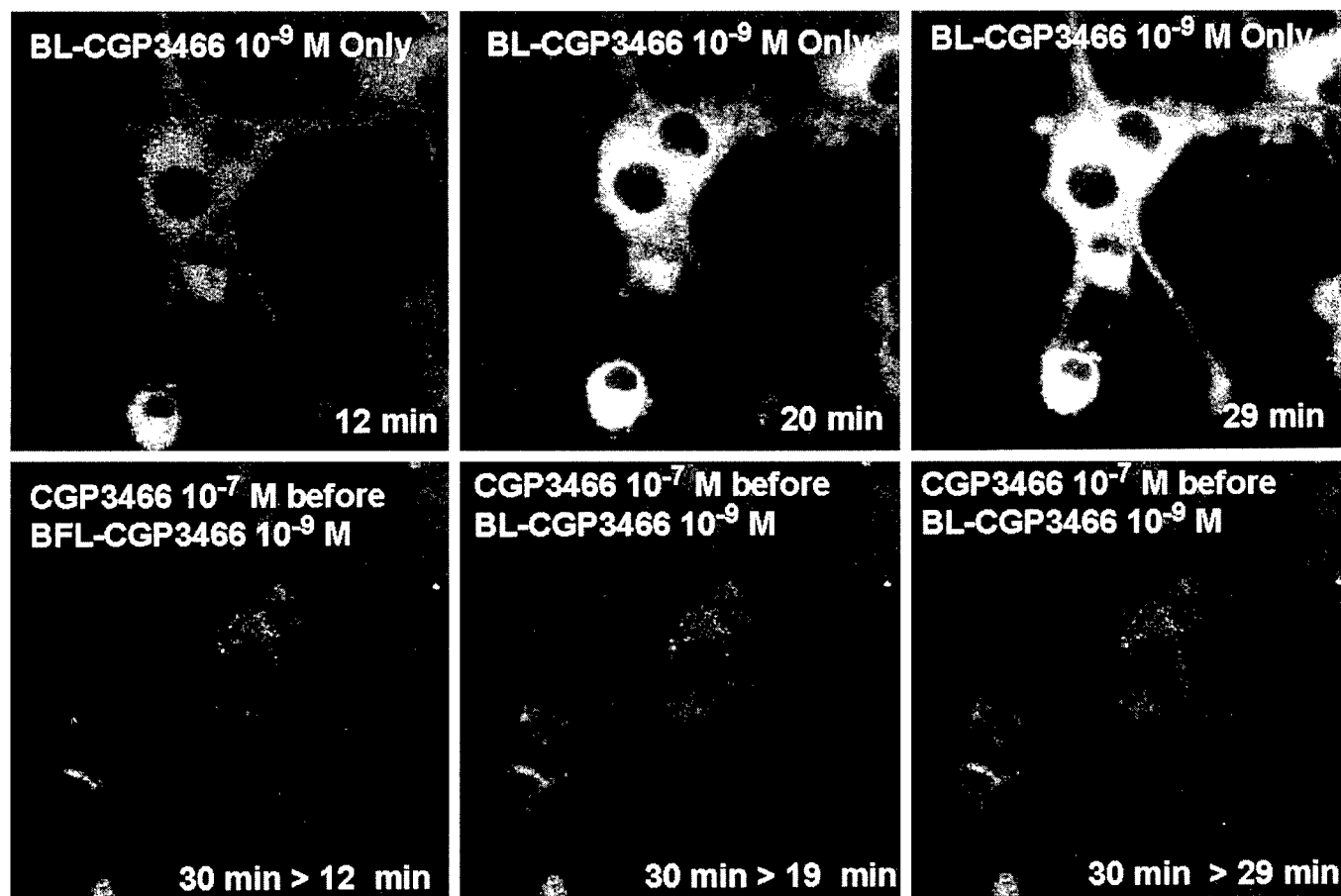


**Fig. 2.** BL-CGP3466 fluorescence seen with LCSM is gradually retained in the extranuclear cytosol, and preincubation with higher concentrations of unlabeled CGP3466 markedly reduces the retention. Top three panels, LCSM images of the retention of BL-CGP3466 fluorescence in living PND-PC12 cells maintained in an environmental chamber containing MEM with serum and NGF at 12, 20, and 29 min after the addition of  $10^{-9}$  M BL-CGP3466. Note the gradual increase in extranuclear cytosolic fluorescence. Bottom three panels, LCSM images of another group of cells that were preincubated with  $10^{-7}$  M of unlabeled CGP3466 for 30 min before the addition of  $10^{-9}$  M BL-CGP3466 and then imaged at 12, 19, and 29 min. Note that the preincubation with the unlabeled CGP3466 reduced the appearance of the BL-CGP3466 fluorescence at all time points, showing that the BL-CGP3466 retention was specific for CGP3466 binding sites.

fluorescence was very similar to that found for antibodies against GAPDH in the cells (see examples in Fig. 5, A1–A4). That is, the BL-CGP3466 fluorescence gradually accumulated in the extra nuclear cytosol with relatively light and scattered accumulation in the nucleus. Thirty minutes of preincubation of the cells with  $10^{-7}$  M unlabeled CGP3466 followed by the addition of  $10^{-9}$  M BL-CGP3466 markedly reduced the accumulation of BL-CGP3466 fluorescence (Fig. 2, bottom). Similarly, incubation of BL-CGP3466 with paraformaldehyde-fixed PC12 cells on a coverglass showed subcellular distributions of BL-CGP3466 (Fig. 3A1) that were similar, if not identical, to those found in living cells using the environmentally controlled chamber (Fig. 2) and those found for a mouse monoclonal antibody against GAPDH (see Fig. 5A3). Similar results were obtained with BL-DES (not shown).

We used photoaffinity-labeled CGP3466 (Zimmermann et

al., 1998) to determine whether the DEP analog binds to GAPDH in the serum and NGF-withdrawn PND-PC12 cells in a similar manner as that reported for rat hippocampal homogenates (Kragten et al., 1998). Autoradiographs revealed major bands at about 37, 43, 50, and possibly 200 kDa, which appeared similar to those found for rat hippocampal tissue. Figure 3B shows a typical autoradiograph for protein extracted from cells at 3, 6, and 9 h after washing and placement in M/O. Figure 3C1 shows a higher power example of the 37-kDa band. The same membranes used for autoradiography were immunoreacted with a monoclonal antibody against GAPDH, and an immunodense band corresponding in position to the 37-kDa autoradiographic band was found (Fig. 3C2 was immunoreacted for the same membrane examined autoradiographically in Fig. 3C1). The similarity of the subcellular distribution of BL-CGP3466 fluorescence and

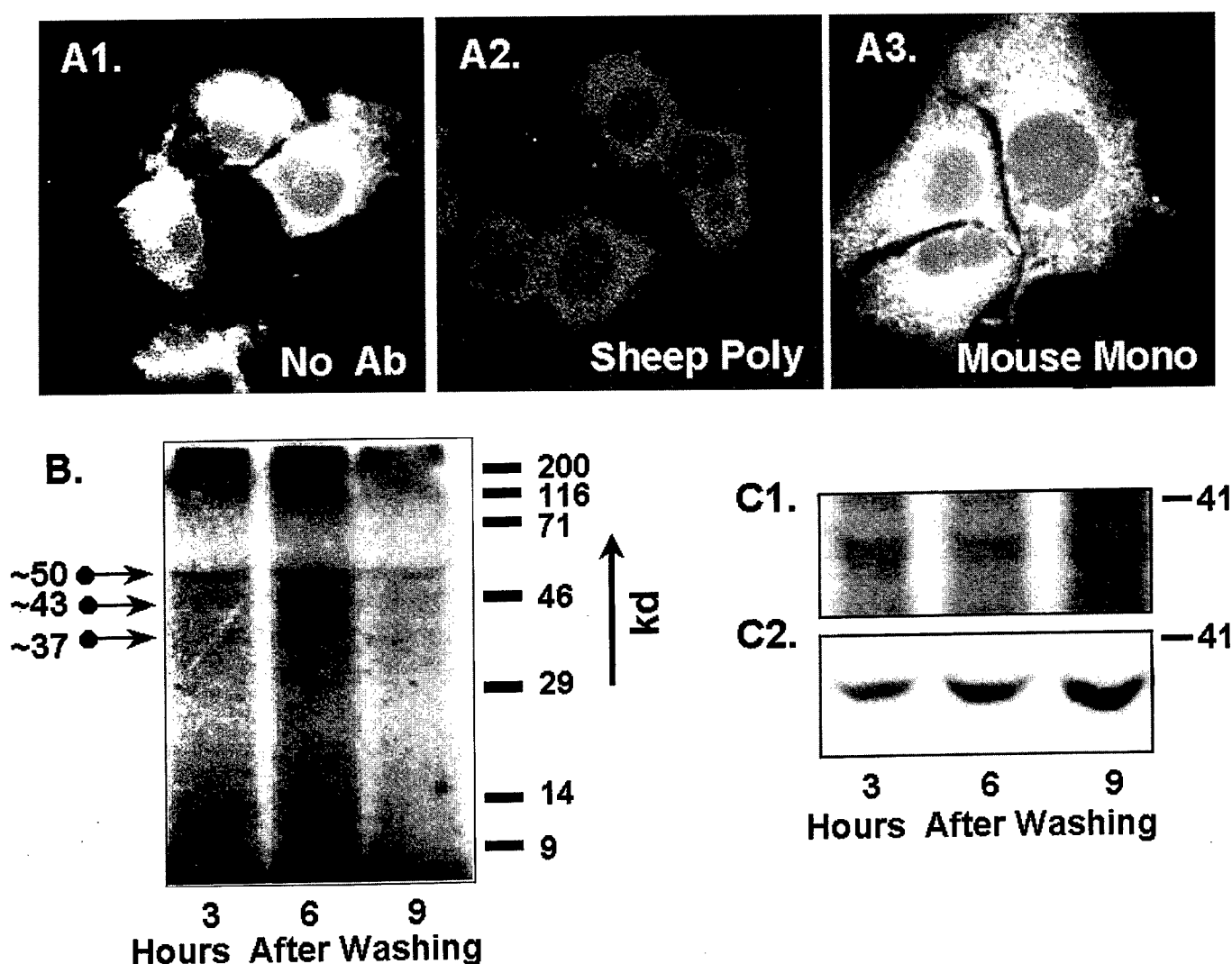


**Fig. 3.** CGP3466 photoaffinity labeling and BL-CGP3466 labeling of cells imaged with LCSM. A1–A3, paraformaldehyde-fixed cells on coverglass that were incubated with BL-CGP3466 for 30 min and then imaged using LCSM. A2 and A3, cells were preincubated with a sheep polyclonal (1:250) and a mouse monoclonal antibody (1:400) for 30 min before the addition of BL-CGP3466. Note that the BL-CGP3466 fluorescence is scattered throughout the extranuclear cytosol and that the sheep antibody, but not the mouse antibody, blocked the retention of the BL-3466 in the cells. B, autoradiograph for total protein extracted from PND-PC12 cells at 3, 6, and 9 h after serum and NGF withdrawal. Before withdrawal, the cells were incubated with a photoaffinity-labeled,  $^{125}$ I-tagged CGP3466 and then exposed to ultraviolet light to activate the azido group of the photoaffinity label. The autoradiographs revealed at least three bands, as shown, at 37, 43, and 47 kDa. C1, section of a photoaffinity-labeled,  $^{125}$ I-tagged CGP3466 autoradiograph for total protein extracted from PND-PC12 cells at 3, 6, and 9 h after serum and NGF withdrawal showing the distinct band at 37 kDa, which increased in intensity from 3 to 9 h. C2, probing the same membrane with an antibody against GAPDH showed an immunodense band that was located at the identical position to the 37-kDa autoradiography band and also increased in intensity from 3 to 9 h.

GAPDH immunofluorescence and the subcellular colocalization of a portion of photoaffinity-labeled CGP3466 autoradiographic activity with GAPDH immunoreaction seem in accord previous findings showing that one of the proteins binding CGP3466 is GAPDH (Kragten et al., 1998).

In solution, GAPDH can take a monomeric, dimeric, or tetrameric form but greatly favors the tetramer (Minton and Wilf, 1981). Molecular modeling of the GAPDH tetramer revealed a central channel at the interface between the four monomers (see Fig. 7, A1 and A2; also see Fig. 7 in Borden, 1998). Examination of the GAPDH tetramer model suggested that CGP3466 and DES were most likely to bind in this central channel. (See Figure 7B1 for a model of CGP3466 in the channel.) A sheep polyclonal antibody (Biogenesis, Poole, Dorset, UK), which was raised against residues located in a position that would likely block entry to the channel (see location of the residues in Fig. 7C), was applied to fixed cells on a coverglass that were subsequently treated with BL-CGP3466. Cells that were preincubated with the sheep antibody showed markedly reduced BL-CGP3466 cellular fluorescence, even after prolonged incubation with BL-CGP3466 (compare Fig. 3, A1 and A2). In contrast, preincubation with

a mouse antibody against GAPDH (Chemicon), which reacted against residues near to the N terminus, placing the residues in or near to the Rossman fold region of the tetramer (see Fig. 7A1, RF), did not alter the BL-CGP3466 fluorescence (compare Fig. 3, A1 and A3).

To determine whether the PND-PC12 cell apoptosis was typical of GAPDH-associated apoptosis found in other cellular models, WESTERN blots were prepared for total protein extracted from cells at multiple time points after washing and placement in medium without serum and NGF. The blots showed that GAPDH levels began to increase at about 2 h after washing and placement in serum and NGF-free medium (Fig. 4A). GAPDH levels did not appear to increase in serum and NGF-withdrawn cells that were treated with  $10^{-9}$  M CGP3466 or  $10^{-9}$  M DES (Fig. 4B).

In parallel experiments, Western blots for protein extracted from the nuclear, mitochondrial, and cytosolic cellular subfractions at 3, 6, 9, and 12 h after serum and NGF withdrawal were examined for GAPDH protein levels. Control blots were prepared for the subfractions using antibodies against nucleolin, cytochrome oxidase, and 14-3-3  $\beta$  protein that are known to react with proteins in the nuclear, mito-

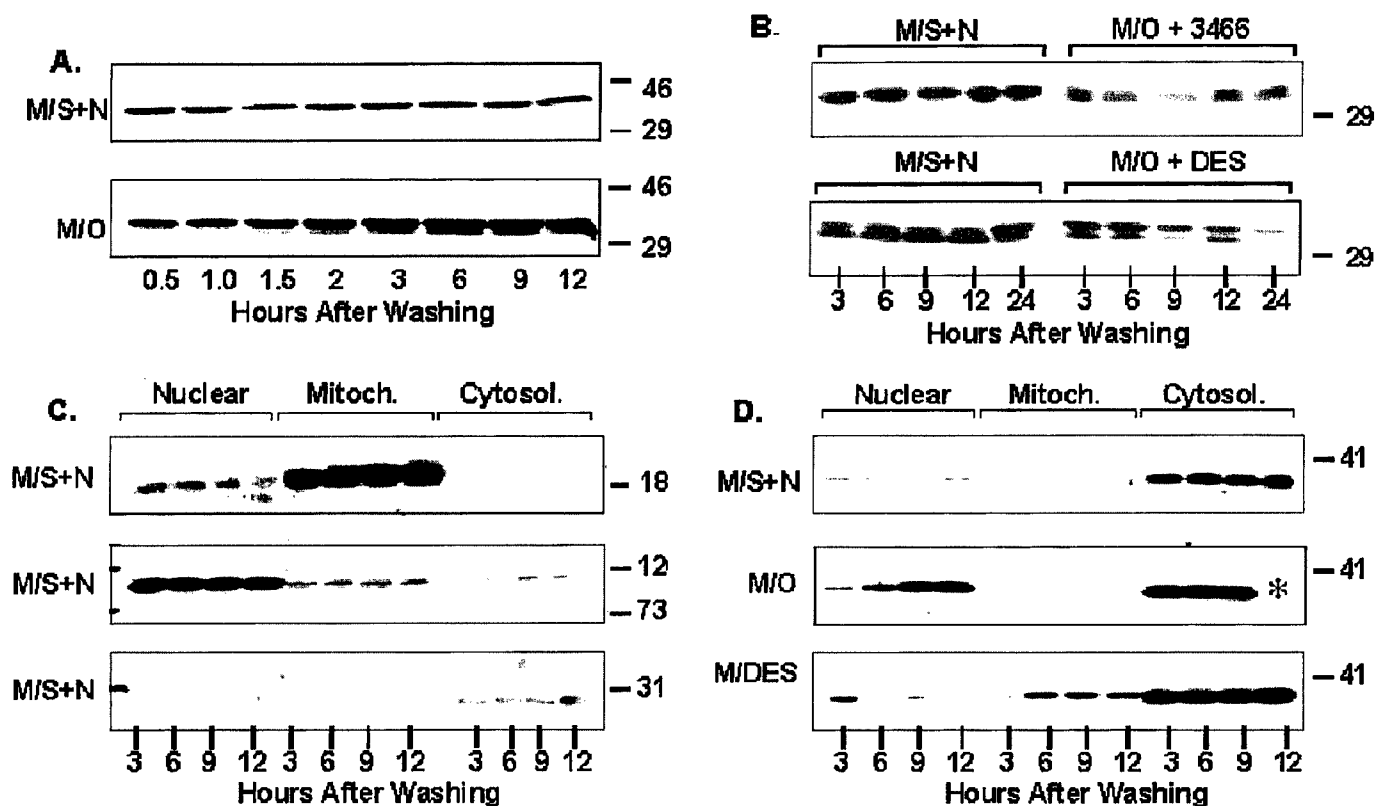


**Fig. 4.** GAPDH levels increase in PND-PC12 cells after serum and NGF withdrawal, and DES and CGP3466 prevent the increase. **A**, Western blot labeled M/S+N for an experiment in which cells were washed and replaced in MEM with serum and NGF (top) as a control together with a blot for an experiment in which cells were washed and placed in MEM only (bottom) to induce apoptosis by trophic withdrawal. Note the relative increase in GAPDH immunoreactivity beginning at the 2-h band after washing for the trophically withdrawn cells but not the control cells. **B**, similar experiments to those in **A** but CGP3466 (top) or DES (bottom) at  $10^{-9}$  M was added to the MEM only. Note that the additions prevented increases in GAPDH levels. **C**, each panel from top to bottom shows immunodensity for the nuclear (Nuclear), mitochondrial (Mitoch.), and cytosolic (Cytosol.) subcellular fractions at 3, 6, 9, and 12 h after washing for nucleolin, cytochrome oxidase, and 14-3-3  $\beta$  protein, respectively. Note that each of the protein immunoreactions is concentrated in a different subfraction. **D**, each panel shows Western blots for protein taken from the subcellular fractions at 3, 6, 9, and 12 h after washing and replacement into MEM with serum and NGF as a control (top) or placement into MEM only to induce apoptosis (middle). Note the progressive increase in nuclear GAPDH beginning between 3 and 6 h after washing and serum and NGF withdrawal together with the maintained increase in cytosolic GAPDH that was present at 3 to 9 h. Similar panels for experiments in which the cells were placed in MEM with  $10^{-9}$  M DES (bottom) after washing. Note that the DES prevents the progressive increase in GAPDH immunoreactivity in the nuclear subfraction. On all blots, identical amounts of total protein were loaded into each lane. \*In the 12 h Cytosol. lane for the M/O panel, indicates that protein was not loaded onto that lane.

chondrial, and cytosolic fractions, respectively (see Fig. 4C for examples of the use of the three antibodies with protein subfractions taken from cells in M/S+N). The blots indicated that GAPDH was largely concentrated in the cytosolic subfraction in control cells that were washed and then replaced into M/S+N. GAPDH levels appeared to increase in the cytosolic subfraction after serum and NGF withdrawal and also progressively increased in the nuclear subfraction at each of the 3-, 6-, 9-, and 12-h time points. Treatment with  $10^{-9}$  M DES or CGP3466 largely prevented the increase in GAPDH immunoreaction for the nuclear fraction.

Recognizing that subcellular fractionation enriches the proportions of proteins localized in particular organelles but may not exclusively contain proteins from those organelles (see Fig. 4C), we also examined the subcellular distribution of GAPDH immunoreactivity using LCSM. The GAPDH immunocytochemistry combined with YOYO-1 staining for DNA showed that GAPDH was concentrated in the cytosol with only light punctate immunoreaction in the nuclei in control cells that were washed and then replaced in M/S+N (see examples in Fig. 5, A1–A4). Serum and NGF withdrawal induced a dense increase in nuclear GAPDH immunoreaction, excluding the nucleolus (see examples in Fig. 5, B1–B4). The nuclear increase and subnuclear distribution were similar to those we demonstrated using a GAPDH-green fluorescent fusion protein in several other models of apoptosis (Shashidharan et al., 1999).

During the first 24 h after washing and replacement into medium with serum and NGF, about 2 to 3% of control cells showed baseline dense nuclear GAPDH immunoreactivity at all time points (Fig. 6C2), contrasting with those that were NGF and serum withdrawn, in which about 6% showed dense nuclear GAPDH immunoreactivity by 3 h, followed by a progressive increase to about 25% by 12 h. On average, the increase in nuclei with dense nuclear GAPDH immunoreaction preceded the increase in nuclei with chromatin condensation, as demonstrated by YOYO-1 staining by at least 3 h (compare Fig. 6, C1 and C2). Treatment with  $10^{-9}$  M DES or CGP3466 markedly reduced both the percentage of nuclei with chromatin condensation and those with dense GAPDH immunoreaction at all time points (Fig. 6, B1 and B2). Accordingly, Western blotting and LCSM immunocytochemistry indicated that both DES and CGP3466 reduce the increased levels of GAPDH and the nuclear accumulation of GAPDH that occurs early in apoptosis induced in PND-PC12 cells by serum and NGF withdrawal.

In an attempt to understand the basis for DES and CGP3466 prevention of increases in GAPDH levels and GAPDH nuclear accumulation, we first examined the effect of CGP3466 and DES on the glycolytic activity of GAPDH *in vitro*. The addition of  $10^{-9}$  M CGP3466 to GAPDH in solution by itself did not alter the extent or rate of  $\text{NAD}^+$  conversion to NADH (Fig. 6A1). The Rossman fold region of GAPDH binds tRNA and AU-rich RNA, particularly AUUUA base sequences (Nagy and Rigby, 1995; also see a computer model of RNA binding in the Rossman fold in Fig. 6 of Borden, 1998). We therefore added a synthetic RNA with repeated AUUUA sequences to the solution and found that the addition reduced the extent of NADH production by about 25% (Fig. 6A1). The addition of CGP3466 to the solution containing both GAPDH and the synthetic RNA resulted in almost

complete recovery of the NADH production. Similar results were obtained with DES (not shown).

We then examined the conversion of  $\text{NAD}^+$  to NADH in cell lysates after washing (Fig. 6A2). We chose a 6-h time point because GAPDH levels were markedly increased (Fig. 4A) but relatively few cells had entered the phase of nuclear degradation at that time (Fig. 5C1). Lysates from cells that had undergone serum and NGF withdrawal showed marked increases in both the extent and rate of  $\text{NAD}^+$  to NADH conversion compared with control cells in M/S+N. The addition of  $10^{-9}$  M DES to the withdrawn cells induced a partial reduction in the extent of  $\text{NAD}^+$  to NADH conversion. Accordingly, these data suggest that the addition of DEP-like compounds can alter GAPDH glycolytic activity, possibly by altering the configuration of GAPDH or its interaction with AU-rich RNA.

Because binding of CGP3466 in the channel of tetrameric GAPDH might alter the interface between the substituent GAPDH monomers (Fig. 7A2), we used size exclusion chromatography to determine whether CGP3466 or DES affected the oligomeric form of the enzyme. The addition of  $10^{-9}$  M CGP3466 (or DES) to GAPDH in solution altered a major proportion of the protein from a size equivalence of 148 kDa to 74 kDa (Fig. 6B1, see size exclusion calibration scale below Fig. 6B3), consistent with a change from a tetrameric form to a dimeric form. Similarly, the addition of poly(U) RNA to GAPDH in solution shifted the peak to a size equivalence of more than 200 kDa, and the addition of CGP3466 (or DES) induced size equivalence changes indicative of the freeing of tetrameric GAPDH from the RNA and its conversion to a dimeric form (Fig. 6B2). GAPDH was placed in SDS to convert it to a monomer. The addition of CGP3466 or DES to the solution containing SDS induced a shift in the size equivalence of the major peak, suggesting a change in the configuration of the monomeric form, and converted a small proportion of the protein to a size equivalence consistent with a dimer (Fig. 6B3).

## Discussion

The serum and NGF-withdrawn PND-PC12 cells showed increases in GAPDH levels and nuclear GAPDH accumulation that were similar to those reported for other apoptosis models (Sunaga et al., 1995; Ishitani et al., 1996, 1997, 1998; Saunders et al., 1997; Sawa et al., 1997; Shashidharan et al., 1999). Most importantly, CGP3466 and DES prevented both the increases in GAPDH and the nuclear accumulation. Transcriptional or translational inhibitors can reduce the increase in GAPDH levels in early apoptosis (Ishitani et al., 1997), suggesting that newly synthesized GAPDH contributes to the protein's role in apoptosis. The signaling pathways that lead to increased GAPDH levels in early apoptosis are not known. p53 overexpression induces apoptosis that is associated with downstream increases in expression of a large number of genes, including GAPDH (Polyak et al., 1997). Accordingly, a p53-dependent signaling pathway may contribute to GAPDH-associated apoptosis. Our recent studies using the expression of GAPDH/green fluorescent fusion protein have shown accumulation of the fusion protein in the nuclei of a variety of cell types in early apoptosis (Shashidharan et al., 1999). The accumulation of the fusion protein was similar to that shown in the serum and NGF-withdrawn PND-PC12 cells in the present study and pro-

vided evidence that at least part of the GAPDH that accumulates in the nucleus was previously resident in the cytoplasm and was not newly synthesized.

This study, similar to our previous studies (Tatton et al., 1994; Wadia et al., 1998), showed that apoptotic nuclear degradation begins in the PND-PC12 cells at about 6 h after serum and NGF withdrawal and is maximal at 12 to 18 h. Therefore, the increases in GAPDH levels and GAPDH nu-

clear accumulation are early events in this form of apoptosis and precedes the onset of nuclear degradation by 3 or more hours. Hence, the participation of GAPDH in the apoptotic cascade seems to be well upstream from the events that mediate apoptotic degradation.

DES is a relatively poor MAO-B inhibitor compared with DEP (Heinonen et al., 1997), and CGP3466 does not inhibit MAO-B (Kragten et al., 1998). Decreases in apoptosis with

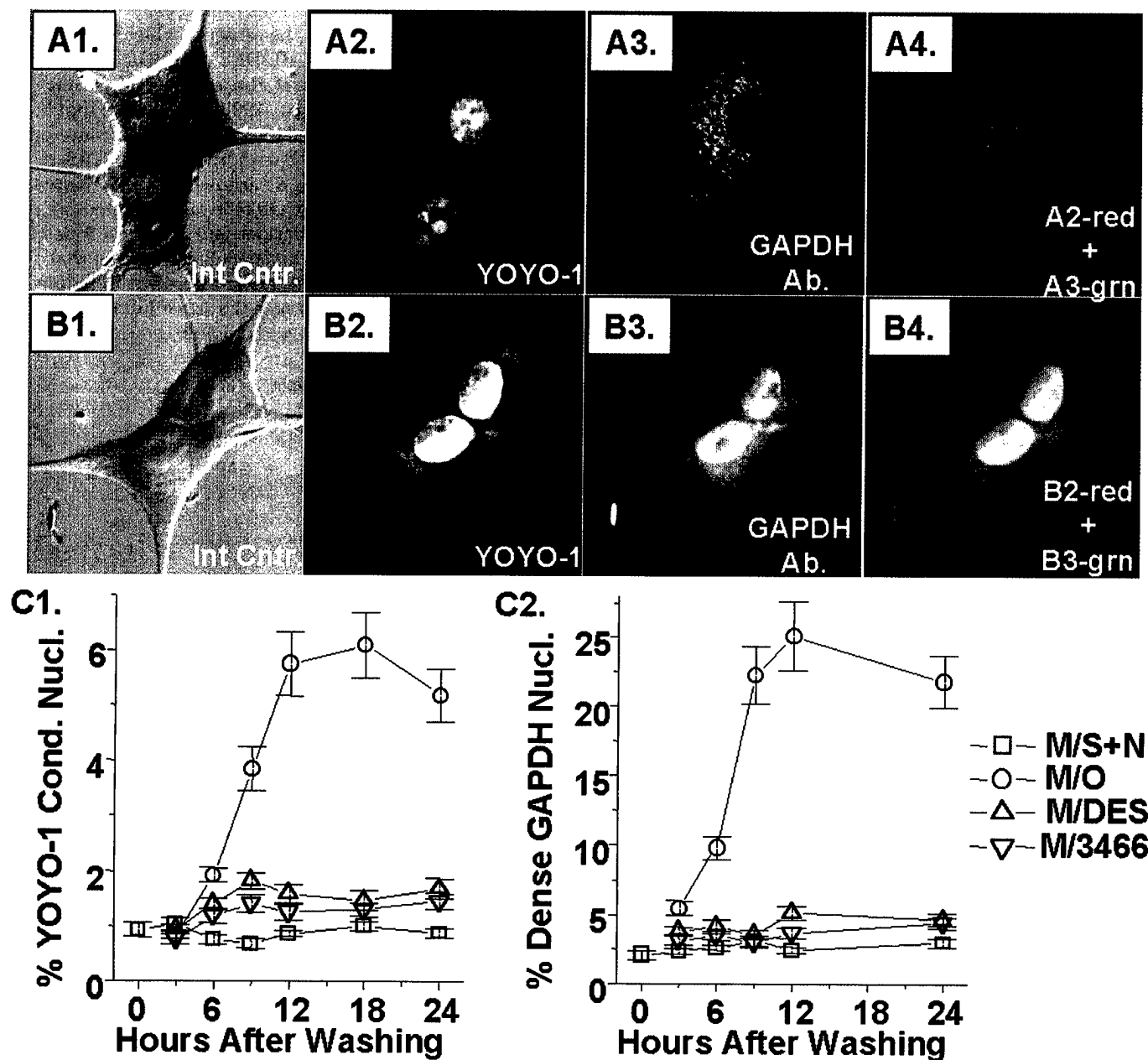


**Fig. 5.** GAPDH immunoreactivity in PND-PC12 cells after serum and NGF withdrawal visualized with LCSM. A1–A4, LCSM micrographs from identical image fields consist of an interference contrast micrograph, fluorescence micrograph for YOYO-1 DNA binding, immunocytochemistry for GAPDH, and a combined image in which A2 (recolored red) and A3 (recolored green) were digitally added. The cells were washed and then replaced in MS+N as a control (example at 6 h after washing). The maintained separation of the red and green color in A4 shows that GAPDH is largely extranuclear in location. B1–B4, an identical series of LCSM micrographs for cells that were washed and placed in MO to induce apoptosis by serum and NGF withdrawal showed dense GAPDH immunoreaction in the nucleus that spared the nucleolus (example at 6 h after washing). The orange-yellow color in B4 shows the colocalization of DNA YOYO-1 binding and GAPDH immunoreaction and illustrates typical dense nuclear GAPDH accumulation. C1 and C2, counts of cells with nuclei showing YOYO-1-stained chromatin condensation, and those with dense GAPDH nuclear immunoreaction, respectively, show that the percentages of nuclei with GAPDH nuclear accumulation was significantly increased by 3 h after washing, whereas the percentages with apoptotic chromatin condensation did not begin to increase until 6 h after washing and placement in MEM only. DES (plots labeled M/DES) and CGP3466 (plots labeled M/3466) at  $10^{-9}$  M markedly decreased the percentage of nuclei with chromatin condensation and those with dense GAPDH nuclear immunoreaction.

DEP or DES can be obtained at concentrations or dosages that do not inhibit MAO-A or MAO-B (Ansari et al., 1993; Tatton and Chalmers-Redman, 1996; Le et al., 1997). In this study, concentrations of DEP and DES ranging from  $10^{-5}$  to  $10^{-13}$  M showed similar capacities to increase survival, whereas CGP3466 induced greater levels of survival, particularly at concentrations of less than  $10^{-9}$  M. Cytochrome P-450 inhibitors block the capacity of DEP, but not DES, to reduce apoptosis in a variety of apoptosis models (W. G. Tatton and R. M. Chalmers-Redman, unpublished observations). Accordingly, the antiapoptotic capacity of DEP appears to depend on its metabolism to DES.

Based on our results with photoaffinity CGP3466 and the BL-labeled compounds, it is likely that CGP3466 and DES bind to GAPDH in the PND-PC12 cells in a similar manner to that shown for rat hippocampus (Kragten et al., 1998). Our antibody studies suggest that the binding may occur in or near to the channel of GAPDH tetramer. Size exclusion data indicate that a portion of GAPDH converts to a dimer in the presence of CGP3466 or DES. There are three possible dimers that could be produced (Fig. 7, D1–D3): 1) the channel could be bisected lengthwise, resulting in a loss of the channel but retaining the RNA binding site in the Rossman fold;

2) the channel is bisected across its width, resulting in a dimer with a channel but no RNA binding site; and 3) the channel is cut across its width so that two diagonally associated monomers form the dimer. At this time, we do not have data to predict which of these dimer forms predominate. DEP that has not been metabolized to DES may not bind to GAPDH. Studies using photoaffinity-labeled DEP in the presence of cytochrome P-450 inhibitors will be required to determine whether DEP itself can bind to GAPDH.

CGP3466 differs from DES in the replacement of the single phenol ring with three rings, the center of which includes an oxygen. In BL-CGP3466 and BL-DES, the BODIPY was attached to the ring portions of the compounds through a flexible link (Zimmermann et al., 1998). We showed that both BL compounds retain most of their capacity to reduce apoptosis in the serum and NGF-withdrawn PND PC12 cells. Furthermore, even with the attachment of the relatively bulky BODIPY moiety, BL-CGP3466 accumulated in the cells with a subcellular distribution similar to those found for GAPDH immunoreactivity. Our modeling suggests that the bulky BODIPY moiety should not interfere with binding in the channel. BL-CGP3466 entry to the subcellular sites could be blocked by preincubation with higher concentrations of

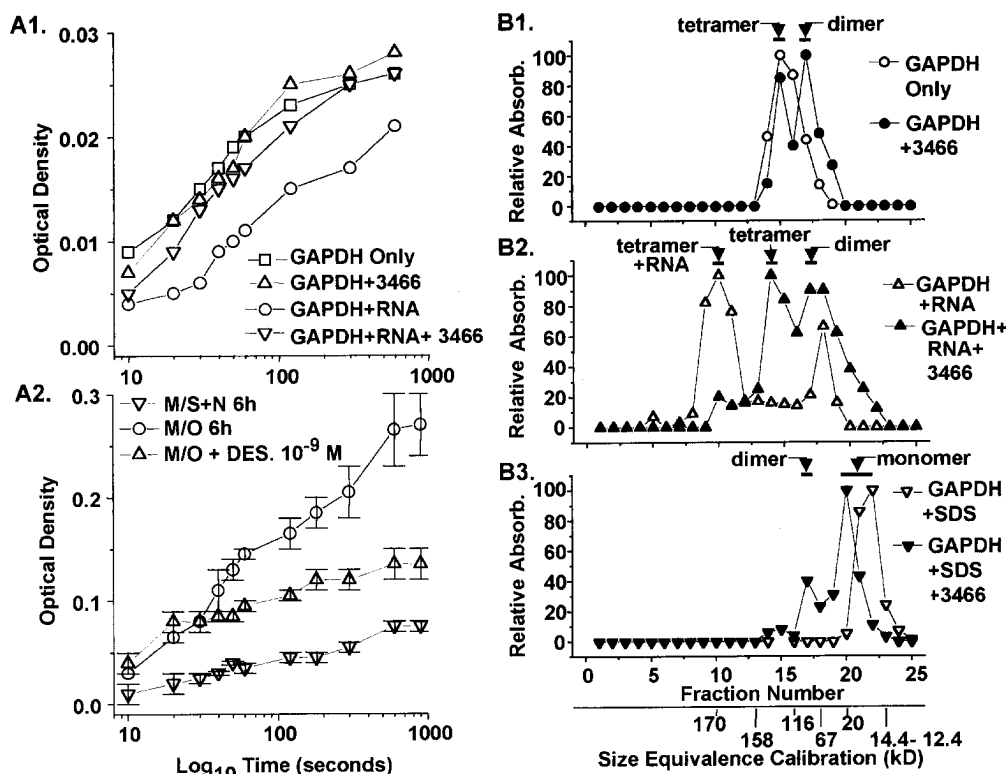


**Fig. 6.** Effects of CGP3466 on the glycolytic capacity of GAPDH in vitro and in vivo and evidence for the conversion of GAPDH to a dimer by CGP3466. A1, NADH production from NAD<sup>+</sup> over time was measured in an in vitro system. The addition of CGP3466 does not significantly alter enzymatic activity of GAPDH, whereas the addition of AUUUA synthetic RNA sequences had little effect on the rate but reduced extent of the glycolytic activity of GAPDH. The addition of  $10^{-9}$  M CGP3466 induced a recovery of glycolytic activity, suggesting that the compound altered the relationship between GAPDH and RNA. A2, measurement of NAD<sup>+</sup> to NADH conversion in lysates taken at 6 h after washing from control cells (M/S+N 6 h), cells after NGF and serum withdrawal (M/O 6 h), and cells after serum and NGF withdrawal treated with  $10^{-9}$  M DES (M/O+DES 6 h). B1–B3, size exclusion chromatography for GAPDH in solution alone, with poly(U) RNA, or with detergent. B1, GAPDH alone in solution forms a tetramer with a size equivalence of 148 kDa in fraction 14. In the presence of  $10^{-9}$  M CGP3466, more than half of GAPDH appears as a dimer in fraction 17 with a size equivalence of 74 kDa. B2, GAPDH binds to poly(U) RNA. The peak at fraction 10, which indicates a size equivalence of more than 170 kDa, indicates an amalgam of RNA and GAPDH. Fraction 10 was also shown to include RNA by the finding of a peak at 260 nm on the spectrophotometer. In the presence of  $10^{-9}$  M CGP3466, the shifts in the equivalence values of the peaks indicate that GAPDH has separated from RNA and that there is a large increase in GAPDH dimer. B3, in the presence of 0.1% SDS, GAPDH alone is found in fraction 23 with a size equivalence consistent with a monomer. After the addition of  $10^{-9}$  M CGP3466, a small proportion of GAPDH shows a size equivalence consistent with a dimer, even in the presence of the detergent.



unlabeled CGP3466, which indicated the specificity of the BL compounds for CGP3466 binding sites. This is the first report of the use of a fluorescently labeled compound with LCSM to examine the subcellular localization and the binding specificity of a compound in living or fixed cells.

GAPDH largely exists as a tetramer with minor populations of dimers and monomers. Our data indicate that CGP3466 and DES increase the stability of GAPDH as a dimer. We therefore propose that agents that stabilize GAPDH as a dimer, rather than a tetramer, prevent the early apoptotic GAPDH increase and nuclear accumulation and thereby induces a decrease in apoptosis. If GAPDH dimer cannot accumulate in the nucleus, it would explain part of our results. It is more difficult to understand how the presence of GAPDH dimer would prevent GAPDH up-regulation. The increased expression may depend on nuclear accumulation of constitutive protein. Our findings indicating a tetrameric/dimeric conversion were obtained *in vitro*, and it is therefore possible that GAPDH dimerization does not occur *in vivo* in response to DES or CGP3466 binding. *In vivo*, the binding of the DEP-related compounds to GAPDH might result in a more subtle change in GAPDH structure. If, as we have hypothesized, the conversion of GAPDH to a dimer robs the protein of its capacity to participate in apoptosis, the DEP-related compounds will be the first compounds shown to reduce cell death by altering oligomerization.

*In vitro*, the DEP-like compound binding results in stabi-

lization of the dimer, increases the catalysis of glycolytic activity by GAPDH, and decreases GAPDH affinity for RNA. These effects are likely interrelated. The glycolytic action and RNA binding of GAPDH occur in the same region of the protein. Conversion of GAPDH from a tetramer to a dimer is known to increase its glycolytic capacity (Minton and Wilf, 1981). Dimerization of GAPDH, together with a freeing of GAPDH from AUUUA RNA, could explain the facilitation of glycolysis by CGP3466 and DES *in vitro*.

This is the first study to show increased glycolytic activity in cells entering apoptosis. The increase may result from the increase in GAPDH levels associated with apoptosis in the PND-PC12 cells. It also could result, in part, from freeing of the Rossman fold region of the protein from AUUUA-rich RNA binding with consequent increased availability of the fold for  $\text{NAD}^+$  to NADH conversion. The relative decrease in glycolysis induced by the DEP-like compounds likely reflects their capacity to reduce or prevent the increase in GAPDH levels that we found in early apoptosis.

The DEP-related compounds appear to reduce the apoptotic function of GAPDH while at the same time facilitating or maintaining the glycolytic function of protein at levels that exceed those in control cells but are reduced compared with those in apoptotic cells. GAPDH is a multifunction protein and participates in functions like tubulin polymerization, endocytosis, translational control of gene expression, nuclear tRNA export, DNA replication, and DNA repair (see Sirover,

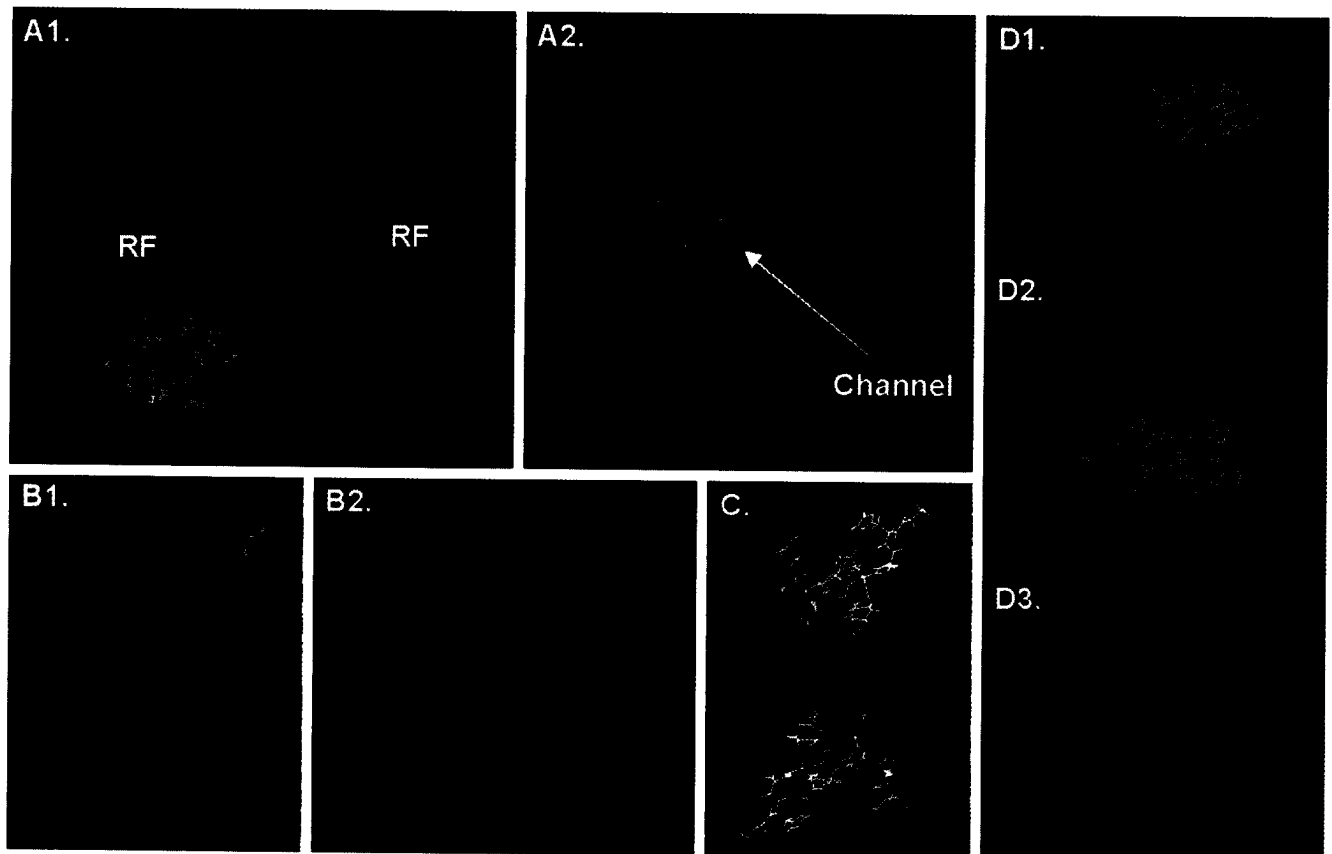


**Fig. 7.** Models of the rat GAPDH tetramer showing the putative DEP-like compound binding channel. A1, the four identical monomers which make up the GAPDH tetramer are shown in different colors. The  $\text{NAD}^+$  binding site, the Rossman fold, is indicated by RF. A2, a 90-degree rotation of the image in A1. The putative DEP-like compound binding channel is indicated where the four monomers join. B1, CGP3466 (blue) is shown in the channel. B2, a view of CGP3466-BODIPY (yellow) located in the channel. C, residues in white indicate the epitope site for the sheep polyclonal antibody, which reduced the cellular accumulation of BL-CGP3466. D1–D3, the three possible dimers of GAPDH that might be formed by the binding of DEP-like compounds. All images were produced in Insight (Biosym).



1997). It will be interesting to determine which of those functions are maintained and which are altered by the binding of DEP-related compounds.

In normal nuclei, GAPDH binds to promyelocytic leukemia (PML) protein in an RNA-dependent fashion (Carlile et al., 1998). PML localizes to PML nuclear bodies, which have been implicated in apoptosis, suppression of oncogenic transformation and growth suppression (Melnick and Licht, 1999). PML and the other protein components of PML nuclear bodies appear to function in regulation of both transcription and translation (Borden et al., 1998). Nuclear GAPDH could therefore contribute to apoptosis by modifying either transcription (Ronai, 1993) or translation (Sioud and Jespersen, 1996), perhaps mediated through an interaction with PML.

Finally, DEP-related compounds have been shown to reduce neuronal and non-neuronal death in a wide variety of models, many of which are independent of MAO-B inhibition (Tatton and Chalmers-Redman, 1996). The basis for clinical slowing of the progression of PD (Parkinson's Study Group, 1993; Olanow et al., 1995) and the preliminary indications of improvement in HD with DEP treatment (Patel et al., 1996) are unknown and have been variously suggested to result from slowed neuronal death (Olanow et al., 1995), improved dopaminergic transmission or increased dopamine levels (Schulzer et al., 1992), and the actions of the DEP metabolites (-)-amphetamine and (-)-methamphetamine (Karoum et al., 1982). If GAPDH contributes to a reduction in neuronal death in PD, the clinical benefits of DEP treatment may result, in part, from the action of DES on GAPDH rather than on MAO-B.

## Acknowledgments

CGP3466, photoaffinity-labeled CGP3466, BL-CGP3466, and BL-DES were provided by Novartis (Basel, Switzerland). Dr. J. Casals contributed to the preparation of the manuscript.

## References

- Ansari KS, Yu PH, Kruck TP and Tatton WG. (1993) Rescue of axotomized immature rat facial motoneurons by R(-)-deprenyl: Stereospecificity and independence from monoamine oxidase inhibition. *J Neurosci* **13**:4042–4053.
- Borden KL (1998) Structure/function in neuroprotection and apoptosis. *Ann Neurol* **44**:S65–S71.
- Borden KL, Campbell Dwyer EJ, Carlile GW, Djavani M and Salvato MS (1998) Two ring finger proteins, the ocoprotein PMB and the arenavirus protein Z associate with the ribosomal P-proteins. *J Virol* **72**:3819–3826.
- Burke JR, Engchild JJ, Martin ME, Jou YS, Myers RM, Roses AD, Vance JM and Strittmatter WJ (1996) Huntington and DRPLA proteins selectively interact with the enzyme GAPDH. *Nat Med* **2**:347–350.
- Carlile GW, Tatton WG and Borden KLB (1998) Demonstration of a RNA-dependent nuclear interaction between the promyelocytic leukaemia protein and glyceraldehyde-3-phosphate dehydrogenase. *Biochem J* **335**:691–696.
- Cotman CW (1998) Apoptosis decision cascades and neuronal degeneration in Alzheimer's disease. *Neurobiol Aging* **19**:S29–S32.
- Fahn S (1996) Controversies in the therapy of Parkinson's disease. *Adv Neurol* **69**:477–486.
- Heinonen EH, Anttila MI, Karnani HL, Nyman LM, Vuorinen JA, Pyykko KA and Lammintausta RA (1997) Desmethylselegiline, a metabolite of selegiline, is an irreversible inhibitor of monoamine oxidase type B in humans. *J Clin Pharmacol* **37**:602–609.
- Ishitani R, Sunaga K, Hirano A, Saunders P, Katsube N and Chuang DM (1996) Evidence that glyceraldehyde-3-phosphate dehydrogenase is involved in age-induced apoptosis in mature cerebellar neurons in culture. *J Neurochem* **66**:928–935.
- Ishitani R, Sunaga K, Tanaka M, Aishita H and Chuang DM (1997) Overexpression of glyceraldehyde-3-phosphate dehydrogenase is involved in low K<sup>+</sup>-induced apoptosis but not necrosis of cultured cerebellar granule cells. *Mol Pharmacol* **51**:542–550.
- Ishitani R, Tanaka M, Sunaga K, Katsube N and Chuang DM (1998) Nuclear localization of overexpressed glyceraldehyde-3-phosphate dehydrogenase in cultured cerebellar neurons undergoing apoptosis. *Mol Pharmacol* **53**:701–707.
- Karoum F, Chuang LW, Eisler T, Calne DB, Liebowitz MR, Quitkin FM, Klein DF and Wyatt RJ (1982) Metabolism of (-) deprenyl to amphetamine and methamphetamine may be responsible for deprenyl's therapeutic benefit: A biochemical assessment. *Neurology* **32**:503–509.
- Kim H, Feil IK, Verlinde CL, Petra PH and Hol WG (1995) Crystal structure of glycosomal glyceraldehyde-3-phosphate dehydrogenase from *Leishmania mexicana*: Implications for structure-based drug design and a new position for the inorganic phosphate binding site. *Biochemistry* **34**:14975–14986.
- Kish SJ, Lopes-Cendes I, Guttman M, Furukawa Y, Pandolfo M, Rouleau GA, Ross BM, Nance M, Schut L, Ang L and DiStefano L (1998) Brain glyceraldehyde-3-phosphate dehydrogenase activity in human trinucleotide repeat disorders. *Arch Neurol* **55**:1299–1304.
- Kragten E, Lalande I, Zimmermann K, Roggo S, Schindler P, Muller D, van Oostrum J, Waldmeier P and Furst P (1998) Glyceraldehyde-3-phosphate dehydrogenase, the putative target of the antiapoptotic compounds CGP 3466 and R(-)-deprenyl. *J Biol Chem* **273**:5821–5828.
- Le W, Jankovic J, Xie W, Kong R and Appel SH (1997) (-)-Deprenyl protection of 1-methyl-4-phenylpyridinium ion (MPP<sup>+</sup>)-induced apoptosis independent of MAO-B inhibition. *Neurosci Lett* **224**:197–200.
- Magyar K, Szende B, Lengyel J, Tarczali J and Szatmary I (1998) The neuroprotective and neuronal rescue effects of (-)-deprenyl. *J Neural Transm Suppl* **52**:109–123.
- Maruyama W, Takahashi T and Naoi M (1998) (-)-Deprenyl protects human dopaminergic neuroblastoma SH-SY5Y cells from apoptosis induced by peroxynitrite and nitric oxide. *J Neurochem* **70**:2510–2515.
- Melnick A and Licht JD (1999) Deconstructing a disease: RARalpha, its fusion partners, and their roles in the pathogenesis of acute promyelocytic leukemia. *Blood* **93**:3167–3215.
- Minton AP and Wilf J (1981) Effect of macromolecular crowding upon the structure and function of an enzyme: Glyceraldehyde-3-phosphate dehydrogenase. *Biochemistry* **20**:4821–4826.
- Nagy E and Rigby WF (1995) Glyceraldehyde-3-phosphate dehydrogenase selectively binds AU-rich RNA in the NAD(+) binding region (Rossmann fold). *J Biol Chem* **270**:2755–2763.
- Olanow CW, Hauser RA, Gauger L, Malapira T, Koller W, Hubble J, Bushenbark K, Lilienfeld D and Esterlitz J (1995) The effect of deprenyl and levodopa on the progression of Parkinson's disease. *Ann Neurol* **38**:771–777.
- Parkinson's Study Group (1993) Effects of tocopherol and deprenyl on the progression of disability in early Parkinson's disease. *N Engl J Med* **328**:176–183.
- Patel SV, Tariot PN and Asnis J (1996) 1-Deprenyl augmentation of fluoxetine in a patient with Huntington's disease. *Ann Clin Psychiatry* **8**:23–26.
- Paterson IA, Barber AJ, Gelowitz DL and Voll C (1997) (-)-Deprenyl reduces delayed neuronal death of hippocampal pyramidal cells. *Neurosci Biobehav Rev* **21**:181–186.
- Paterson IA, Zhang D, Warrington RC and Boulton AA (1998) R-Deprenyl and R-2-heptyl-N-methylpropargylamine prevent apoptosis in cerebellar granule neurons induced by cytosine arabinoside but not low extracellular potassium. *J Neurochem* **70**:515–523.
- Petersen A, Mani K and Brundin P (1999) Recent advances on the pathogenesis of Huntington's disease. *Exp Neurol* **157**:1–18.
- Polyak K, Xia Y, Zweier JL, Kinzler KW and Vogelstein B (1997) A model for p53-induced apoptosis [see comments]. *Nature (Lond)* **389**:300–305.
- Ronai Z (1993) Glycolytic enzymes as DNA binding proteins. *Int J Biochem* **25**:1073–1076.
- Saunders PA, Chalecka-Franaszek E and Chuang DM (1997) Subcellular distribution of glyceraldehyde-3-phosphate dehydrogenase in cerebellar granule cells undergoing cytosine arabinoside-induced apoptosis. *J Neurochem* **69**:1820–1828.
- Sawa A, Khan AA, Hester LD and Snyder SH (1997) Glyceraldehyde-3-phosphate dehydrogenase: Nuclear translocation participates in neuronal and nonneuronal cell death. *Proc Natl Acad Sci USA* **94**:11669–11674.
- Schulzer M, Mak E and Calne DB (1992) The antiparkinson efficacy of deprenyl derives from transient improvement that is likely to be symptomatic [see comments]. *Ann Neurol* **32**:795–798.
- Shashidharan P, Chalmers-Redman RM, Carlile GW, Rodic V, Gurchich N, Yuen T, Tatton WG and Sealfon SC (1999) Nuclear translocation of GAPDH-GFP fusion protein during apoptosis. *Neuroreport* **10**:1149–1153.
- Sioud M and Jespersen L (1996) Enhancement of hammerhead ribozyme catalysis by glyceraldehyde-3-phosphate dehydrogenase. *J Mol Biol* **257**:775–789.
- Sirover MA (1997) Role of the glycolytic protein, glyceraldehyde-3-phosphate dehydrogenase, in normal cell function and in cell pathology. *J Cell Biochem* **66**:133–140.
- Sunaga K, Takahashi H, Chuang DM and Ishitani R (1995) Glyceraldehyde-3-phosphate dehydrogenase is over-expressed during apoptotic death of neuronal cultures and is recognized by a monoclonal antibody against amyloid plaques from Alzheimer's brain. *Neurosci Lett* **200**:133–136.
- Tatton NA, Maclean-Fraser A, Tatton WG, Perl DP and Olanow CW (1998) A fluorescent double-labeling method to detect and confirm apoptotic nuclei in Parkinson's disease. *Ann Neurol* **44**:S142–S148.
- Tatton WG and Chalmers-Redman RM (1996) Modulation of gene expression rather than monoamine oxidase inhibition: (-)-Deprenyl-related compounds in controlling neurodegeneration. *Neurology* **47**:S171–S183.
- Tatton WG, Ju WY, Holland DP, Tai C and Kwan M (1994) (-)-Deprenyl reduces PC12 cell apoptosis by inducing new protein synthesis. *J Neurochem* **63**:1572–1575.
- Wadia JS, Chalmers-Redman RME, Ju WJH, Carlile GW, Phillips JL, Fraser AD and Tatton WG (1998) Mitochondrial membrane potential and nuclear changes in apoptosis caused by serum and nerve growth factor withdrawal: Time course and modification by (-)-deprenyl. *J Neurosci* **18**:932–947.
- Zimmermann K, Roggo S, Kragten E, Furst P and Waldmeier P (1998) Synthesis of tools for target identification of the anti-apoptotic compound CGP 3466: Part I. *Bioorg Med Chem Lett* **8**:1195–1200.

**Send reprint requests to:** Dr. William G. Tatton, Department of Neurology, Annenberg 14-70, Mount Sinai Medical Center, One Gustave L. Levy Place, New York, NY 10029. E-mail: william\_tatton@msmplink.mssm.edu

## Increased Caspase 3 and Bax Immunoreactivity Accompany Nuclear GAPDH Translocation and Neuronal Apoptosis in Parkinson's Disease

Nadine A. Tatton

Department of Neurology, Mt. Sinai School of Medicine/NYU, New York, New York 10029

Received January 31, 2000; accepted May 10, 2000

***In situ* end labeling combined with YOYO staining was used to mark apoptotic DNA fragmentation and chromatin condensation respectively in human post-mortem brain sections. Increased numbers of apoptotic neuronal nuclei were identified in the Parkinson's disease (PD) nigra compared with age-matched controls. Caspase 3 and Bax showed increased immunoreactivity in melanized neurons of the PD nigra compared with controls. Importantly, GAPDH nuclear accumulation was also observed in the PD nigra, suggesting apoptotic rather than necrotic cell death. Interestingly, both Lewy bodies and the intranuclear Marinesco's bodies were GAPDH immunoreactive in the PD brain.** © 2000 Academic Press

**Key Words:** Parkinson's disease; apoptosis; caspase 3; Bax; mitochondria; GAPDH; TUNEL; nuclear.

### INTRODUCTION

At present, there is no consensus as to whether apoptosis is the predominant mode of neuronal death in Parkinson's disease (PD). Several laboratories have used *in situ* end labeling (ISEL), commonly called the TUNEL method (23), to detect double-strand DNA fragmentation, a feature considered pathognomic for apoptosis. Some laboratories have reported ISEL-positive neuronal nuclei in the PD nigra (30, 41, 63) while others found no evidence of end-labeled neuronal nuclei (19, 32, 68) or only ISEL-positive glia (5).

Unfortunately, ISEL, when used alone, cannot provide unequivocal identification of an apoptotic nucleus. Endonucleases which digest DNA can create single- and/or double-strand breaks (see 61 for review) resulting initially in high-molecular-weight (50–300 kb) DNA fragments (66). Often, but not always, DNA digestion continues, with the ultimate production of low-molecular-weight oligonucleosomal-sized fragments (12, 46). It is thought that single-strand DNA breaks accumulate in the linker regions between oligonucleosomes prior to the double-strand DNA breaks which create a "ladder" pattern when observed by gel electrophoresis (47, 65). The ISEL method was considered to

be selective in detecting the double-stranded 3'-OH, protruding ends of endonuclease-digested DNA between oligonucleosomes. However, the terminal transferase enzyme (TdT), commonly used for ISEL, is generally supplied with a protocol that requires increased cobalt chloride (2.5 mM) in the reaction mix, which allows TdT to label double-strand breaks (protruding, blunt, and recessed ends) as well as single-strand DNA breaks (16, 58). Importantly, cells dying by necrosis have also been reported to contain single- and/or double-strand breaks, and thus the ISEL method may not always distinguish between the two modes of cell death (18, 21, 22, 34). A second, independent method is therefore required to confirm apoptosis where there is demonstrable DNA fragmentation.

Chromatin condensation is considered to be an independent event from DNA fragmentation and requires the presence of ATP (28) and specific proteins, such as the caspase 3-activated acinus, which can initiate chromatin condensation (51). Apoptotic chromatin condensation, similar to the pattern first described by Kerr *et al.* (29) has been observed in the PD nigra with electron microscopy (3, 4, 63) but this method is impractical for routine screening of cases. We have previously used confocal microscopy to demonstrate apoptotic chromatin condensation in the MPTP-treated mouse nigra and the PD nigra using fluorescent nucleic acid-binding dyes such as acridine orange and YOYO-1 (59, 60). We now present data from 10 clinically and neuropathologically identified cases of PD, combining ISEL/YOYO with confocal microscopy, to provide unequivocal evidence of increased neuronal apoptosis in the PD brain compared to age-matched controls.

The use of *in situ* markers to identify this final, degradative phase of apoptosis unfortunately cannot determine the signaling pathway involved in the death process. Identification of effector molecules participating in the apoptotic signaling cascade could lead to the development of new therapies that would selectively block or slow cell death in PD. Increases in the signaling proteins, p53 and Fas ligand, have been reported in the PD brain, but it is not clear whether these changes

are related to neuronal apoptosis (24, 43). We present immunocytochemical evidence for nuclear accumulation of the proapoptotic protein glyceraldehyde-3-phosphate dehydrogenase (GAPDH) and increased somal immunoreactivity for the apoptotic effector proteins caspase 3 and Bax in the PD nigra. Taken together, these data support the hypothesis that PD nigral dopaminergic neurons die by apoptosis, possibly via a mitochondrially dependent pathway.

### MATERIALS AND METHODS

Five-micrometer-thick serial sections (for a maximum of 20 sections) through the nigra were obtained from archival paraffin blocks of clinically and neuropathologically confirmed cases of PD ( $n = 8$ , age range 75–94 years). The presence of Lewy bodies in nigral neurons was confirmed in all cases. Control sections were obtained from archival blocks of cases without gross or microscopic neuropathological changes ( $n = 4$ , age range 53–78 years). All nigral tissue blocks were uniformly dissected from the lower midbrain at the emergence of the third cranial nerve. This portion of the nigra provides a high cell density and increases the opportunity of finding Lewy bodies to support the PD diagnosis. Blocks from neonate brains ( $n = 4$ , age range 17–28 weeks) were used to provide positive control tissue for developmentally programmed cell death. The postmortem interval ranged between 2.75 and 7 h for all PD cases; the postmortem interval for aged normal controls ranged between 8 and 11 h. In addition, ISEL/YOYO staining was performed on 10- $\mu$ m-thick, frozen serial sections through two PD cases (81 and 87 years) and two neuropathologically normal controls (61 and 77 years) (see 60 for methods). Of the 10 PD cases available, 5 had been treated with levodopa and 5 had not.

#### *Microwave Pretreatment of Paraffin Sections*

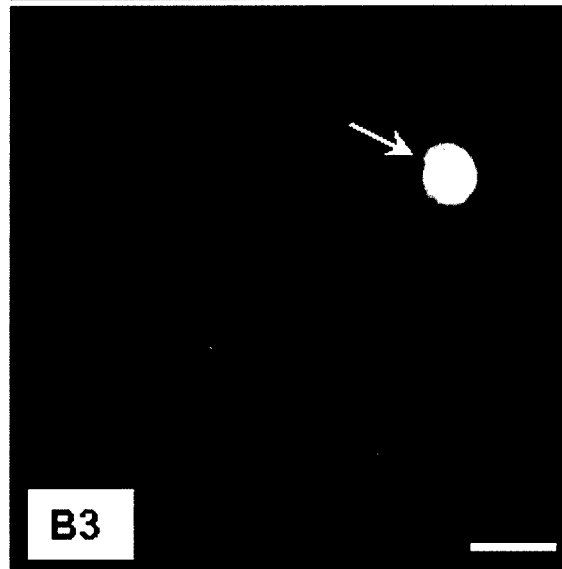
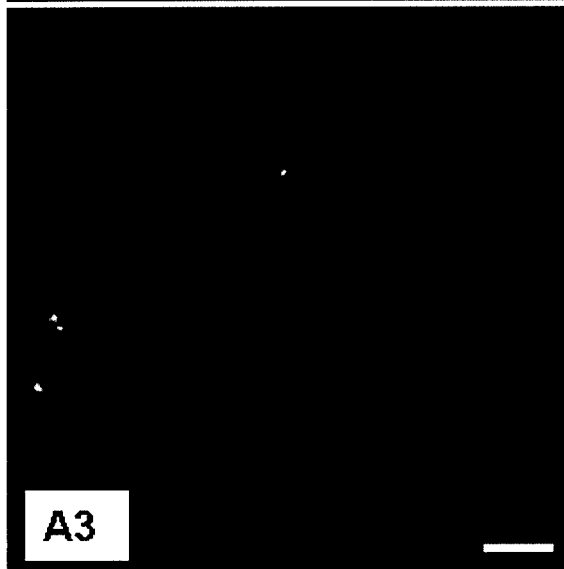
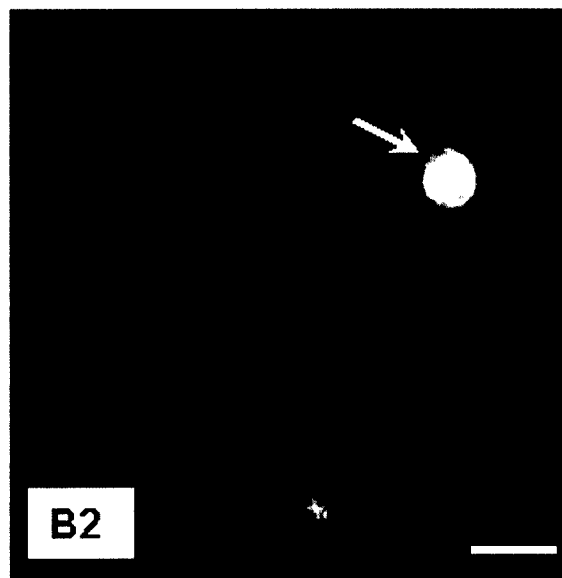
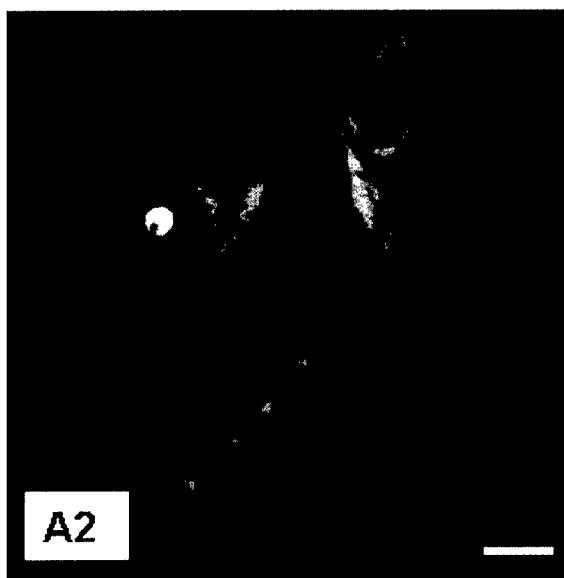
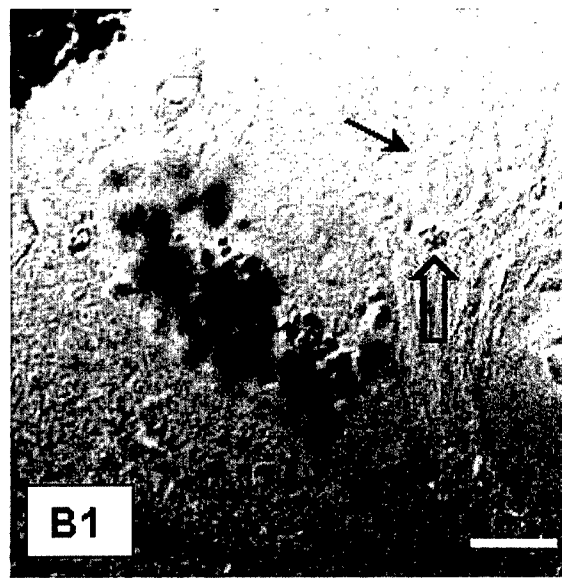
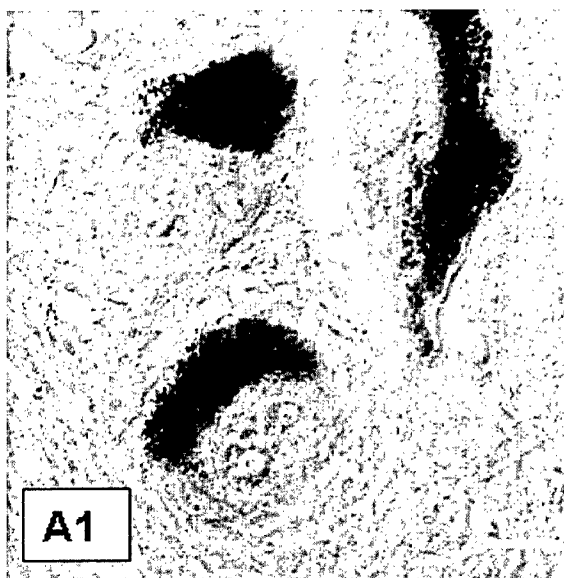
All sections were dewaxed and brought to water prior to microwave pretreatment. No more than 8–10 slides were placed in a plastic rack submerged under 400 ml of antigen unmasking solution (Vector Labs), sufficient to cover the slides. For ISEL/YOYO staining, the container plus slides were heated at a medium

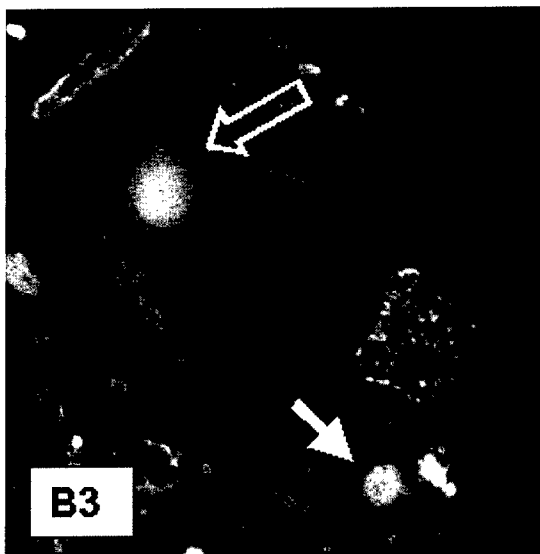
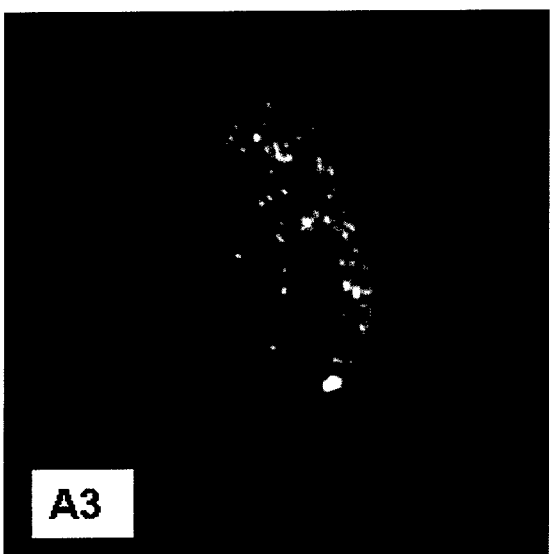
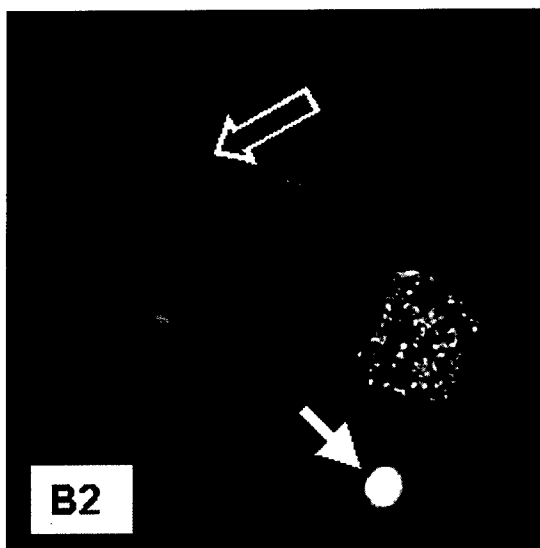
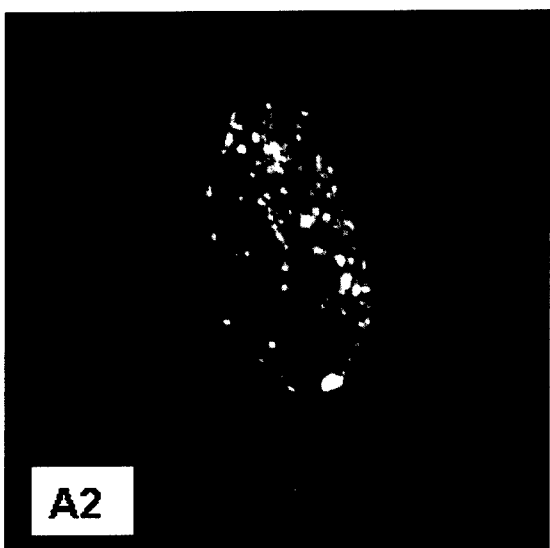
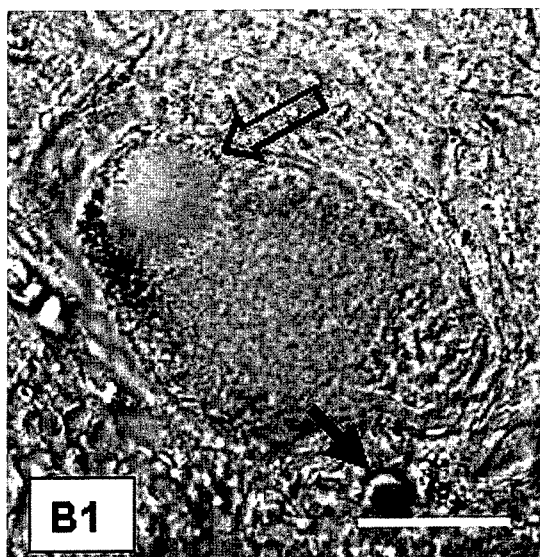
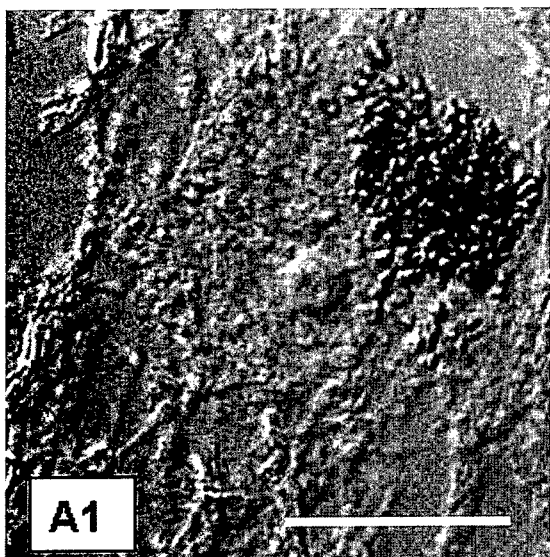
power setting for 4 min to reach a final temperature between 60 and 62°C. Slides remained submerged in buffer for 30 min. Processing a small number of slides was critical to achieving uniform heating and reproducible labeling. The remaining sections were processed for immunocytochemistry. Slides processed for immunocytochemistry were placed in antigen unmasking solution previously brought to boil by microwaving at high power for 5 min. A rack of 8–10 slides was added immediately thereafter and the solution was heated at medium-high power and allowed to boil for 1 min only. Slides remained submerged in buffer for 40 min before further processing.

#### *ISEL/YOYO Staining to Detect Apoptotic Nuclei*

Every fourth section from a series of 20 nigral sections from each PD and aged control case (providing 5–6 sections per sample) was taken for ISEL/YOYO staining. After cooling, slides were rinsed in 0.1 M phosphate-buffered saline (PBS, 9 g NaCl, 3.2 g sodium phosphate monobasic, 10.9 g sodium phosphate dibasic/liter) and then treated for 10 min in 3% hydrogen peroxide/methanol at room temperature. Slides were rinsed in PBS and then treated with RNase A (100  $\mu$ g/ml) in  $2\times$  SSC (8.82 g sodium citrate, 17.53 g NaCl/liter) for 25 min, at 37°C. Following a  $2\times$  SSC rinse, the sections were digested with proteinase K (20  $\mu$ g/ml) for 3 min, 37°C, and then placed into ice-cold 0.1 M glycine/0.1 M Tris (pH 7.2) for 15 min. Sections were incubated with an equilibration buffer (Intergen, S7106) for 10 min at room temperature. Excess buffer was blotted off and the sections were exposed to the TdT reaction mix (Boehringer Mannheim, 220–582) for 1 h at 37°C. The reaction mix contained 2.5 mM  $\text{CoCl}_2$ , 35 units TdT (1.4  $\mu$ l/100  $\mu$ l) and 0.7 mM (1.4  $\mu$ l/100  $\mu$ l) Bodipy-TR-14-dUTP (Molecular Probes, C7618). Slides were washed in an excess volume of  $2\times$  SSC, at 37°C,  $3 \times 10$  min, followed by a 5-min PBS rinse. All sections were then incubated with YOYO-1 (1:500 in PBS) (Molecular Probes, Y-3601) for 30 min at room temperature. Slides were washed  $3\times$  in PBS and coverslipped with Gelmount (Biomed). When dry, slides were examined by epifluorescence microscopy (Olympus AX-70, U-MFI/TRITC filter) to determine the number of apoptotic nuclei per section. Slides were then

**FIG. 1.** Confocal digital images of joint ISEL/YOYO-stained sections reveal condensed apoptotic nuclei in the PD nigra. (A) A control nigral section; (B) a PD nigral section. The top panels (1) depict interference contrast images to demonstrate neuromelanin in nigral neurons, the middle panels (2) present YOYO-1 staining of the same section, and the bottom panels (3) present ISEL of the same sections. All panels represent laser confocal scans of the same plane of focus. Control nigral neurons (A2) demonstrate little nuclear YOYO staining, although the nucleolus and cytoplasmic RNA are brightly labeled. In contrast, the small, round apoptotic nucleus in the top half (closed arrow, B2) is brightly labeled and reveals a heterogeneous condensation pattern. Note that there is a small amount of neuromelanin still associated with this nucleus, just visible by interference contrast (open arrow, B1). This same nucleus demonstrates a heterogeneous pattern of intense ISEL signal (closed arrow, B3) denoting the presence of DNA fragmentation. Note that the nonapoptotic neuron, partially out of the plane of focus in B, is ISEL negative and does not show bright YOYO condensation. Nuclei of control nigral neurons are also ISEL negative (A3). Note the low background in both ISEL-reacted PD and control sections. Bar, 10  $\mu$ m.





examined by laser confocal scanning microscopy to obtain high-resolution digital images of individual nuclei. PD brain sections were always run with age-matched controls and neonate brain apoptosis-positive controls. Control sections run with reaction mix but no TdT were blank (data not shown). The numbers of surviving melanized neurons (containing a nucleolus) per section were counted using Nomarski optics. We found that the number of apoptotic nuclei ranged between 0 and 12 per section, with the total number of labeled nuclei varying randomly throughout the sampled sections. The number of melanized neurons with nucleolus was sometimes fewer than 10 per section in the PD cases. Therefore, stereological sampling methods were considered impractical for estimating cell counts in this study.

#### *Immunocytochemical Detection of Bax, Caspase 3, and GAPDH*

The remaining sections were immunoreacted with antisera against Bax (N-20, Santa Cruz, sc-493), pro- and activated caspase 3 (PharMingen, 65906E), cleaved caspase 3 product (New England BioLabs, 9661S), or GAPDH (Chemicon, MAB374). Caspase 3 (pro- and activated forms) and Bax sections were processed using the Autoprobe III kit which utilizes 3-amino-9-ethylcarbazole (AEC) to form a bright red reaction product (Biomed, 08-083). Following dewaxing and rehydration, sections were given a pepsin digest (Biomed, M77) for 12 min at 37°C and then rinsed in buffer. Slides were microwaved as described above and processed according to Autoprobe kit instructions, except that all primary antisera incubations were performed overnight at 4°C (Bax, 1:200; caspase 3, 1:500). A second group of sections (three PD cases, three age-matched controls) were processed for immunofluorescence using an antisera specific for the activated form of caspase 3, recognizing the 17- to 21-kb active fragment of caspase 3 (New England BioLabs). Following dewaxing and rehydration, sections were exposed to methanol for 10 min, -20°C, and then rinsed in PBS after the microwave pretreatment. Slides were blocked with 10% normal goat serum/0.2% Tween 20 in PBS for 30 min. Excess serum was blotted away and sections were incubated with active caspase 3 antisera (1:100 in 1% NGS/0.2% Tween 20/PBS) overnight at 4°C. Slides

were then rinsed in PBS and incubated for 1 h with Alexa 594- or 488-conjugated (Molecular Probes, A-11012, A-11001) goat anti-rabbit IgG (1:200 in 1% normal goat serum/0.2% Tween 20/PBS). Sections exposed to Alexa 594-IgG were rinsed with PBS and further incubated with YOYO-1 (1:500 in PBS) for 30 min in the dark. All sections were rinsed again and mounted with Gelmount and examined by epifluorescent and confocal microscopy.

Sections incubated with GAPDH antibodies were treated with methanol for 10 min, -20°C, and then rinsed in PBS after the microwave pretreatment. Sections were given a brief RNase A digest (100 µg/ml 2× SSC) for 3 min and then placed in ice-cold 0.1 M glycine/0.1 M Tris (pH 7.2) for 5 min. After a PBS rinse, slides were blocked with 10% normal goat serum/0.2% Tween 20 in PBS for 15 min. Excess serum was blotted away and sections were incubated with GAPDH antisera (1:200 in 1% normal goat serum/0.2% Tween 20/PBS) overnight at 4°C. Slides were then rinsed in PBS, incubated for 1 h with Alexa 594-conjugated (Molecular Probes, A-11005) goat anti-mouse IgG (1:200 in 1% normal goat serum/0.2% Tween 20/PBS). Slides were rinsed with PBS and coverslipped with Gelmount. A portion of slides was counterstained with YOYO-1 following the application of the secondary antibody.

#### *Laser Confocal Microscopy*

All ISEL/YOYO-stained sections were examined by confocal microscopy (Leica TCS 4D) using two independent channels to detect specific ISEL (Bodipy-TR-14-dUTP emission maximum 625 nm) and YOYO (emission maximum 509 nm) fluorescence. Alexa 594 (emission maximum 617 nm) or Alexa 488 (emission maximum 519 nm) was used to set the detection limits for GAPDH and the activated caspase 3 fragment immunofluorescence. In order to distinguish autofluorescent signal contribution, cells of interest were also scanned in the far-red range (comparable to Cy5, emission peak 670 nm) to eliminate contribution from Bodipy, YOYO, or Alexa 594 or 488. Consecutive, digital images were subjected to 32-line averaging to eliminate out-of-focus fluorescent haze and then stored on a Maxoptix optical data storage system.

**FIG. 2.** Confocal imaging reveals a second unique ISEL/YOYO staining pattern in PD nigral nuclei. Interference contrast images in the top panel demonstrate the presence of dark neuromelanin granules in both neurons (A, B) as well as a Lewy body in the upper right-hand panel (open arrow, B1). Note a small extracellular body with neuromelanin in the neuropil immediately below (filled arrow, B1). The middle panel depicts a bright, granular pattern of YOYO nuclear staining in both PD neurons (A2, B2), with a bright nuclear perimeter of YOYO staining. In some PD neurons, these nuclei displayed an identical granular ISEL pattern (A3, B3). This pattern was not observed in neurons outside of the PD nigra and was not found in control nigral sections. Note that Lewy bodies can demonstrate a nonspecific ISEL signal (B3) but it is not due to the presence of any nucleic acid, since they do not stain with YOYO (B2). Note that extracellular neuromelanin can demonstrate a broad autofluorescent spectrum (B2, B3). Bar, 5 µm (A) and 10 µm (B).

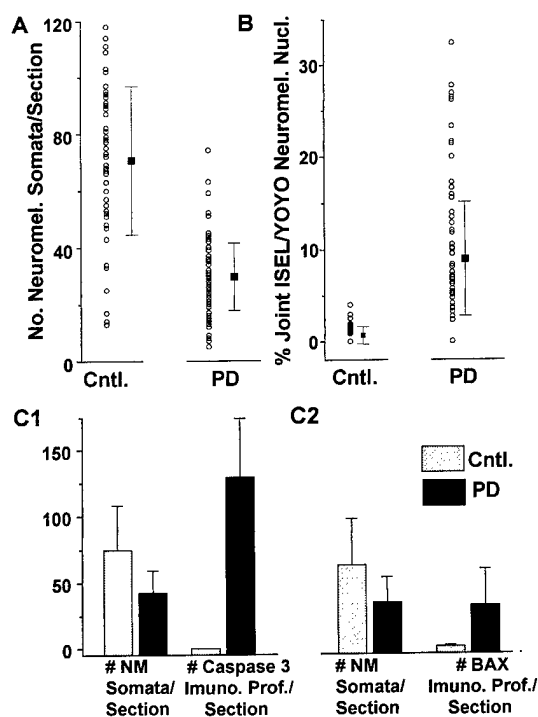


**FIG. 3.** Counts of joint ISEL/YOYO-stained apoptotic nuclei, neuromelanin-containing neurons, and caspase 3- and Bax-immunoreactive profiles are increased in the PD nigra compared to controls. Counts of condensed apoptotic nuclei were taken from every fourth section through PD and control nigral sections. The number of apoptotic nuclei per number of neuromelanin neurons (with a nucleolus) per section was obtained and presented as a scatterplot with accompanying standard deviation. The number of neuromelanin somata/section from the ISEL/YOYO-treated sections is plotted in (A) demonstrating a frank loss of melanized neurons in the PD cases compared to controls. Joint ISEL/YOYO-positive (apoptotic) nuclei per neuromelanin somata for individual sections are presented in (B). Note that apoptotic nuclei are present in age-matched controls but a significantly greater number are found in PD sections. Mann-Whitney U tests demonstrated a significant difference between all counts in PD sections compared with age-matched controls ( $P$  value 0.0005). Histograms shown in (C1 and C2) present the number of immunoreactive profiles (somata with nucleolus and portions of cell somata) of caspase 3 (C1) or Bax (C2) compared with the number of neuromelanin somata (with a nucleolus) per section. Note the frank loss of melanized neurons per section in the PD nigra compared to controls and the increased numbers of caspase 3- and Bax-immunoreactive profiles per section. No caspase 3-immunoreactive profiles were detected in simultaneously reacted control sections, while only a small number of Bax profiles were found in the control group. Note that more caspase 3-immunoreactive profiles were observed in the PD sections than Bax profiles. NM, neuromelanin. Mann-Whitney U tests revealed a significant difference between the number of caspase 3- and Bax-immunoreactive profiles in the PD nigra compared to age-matched control nigra ( $P$  value 0.0005).

## RESULTS

### *Two Patterns of ISEL/YOYO-Positive Staining in PD Nigral Nuclei*

The ISEL/YOYO method can be applied to frozen (see 60 for method) or paraffin sections; however, par-

affin sections provided superior morphological detail compared with cryosections. When observed with epifluorescence microscopy, normal neurons in age-matched control nigral sections exhibited bright green YOYO-1 fluorescence associated with RNA in the nucleolus and cytoplasm, with no obvious nuclear DNA staining. Similarly, the red ISEL fluorescent signal in control nuclei did not rise above cytoplasmic background levels. In contrast, apoptotic, ISEL-positive nuclei displayed a bright red fluorescence with a concomitant bright green fluorescent YOYO signal which reflected condensed chromatin. Colocalization of these fluorochromes gave the condensed, apoptotic nuclei a yellow-orange appearance when viewed with a dual excitation filter cube. The majority (>90%) of these small, oval-round nuclei were usually associated with a few remaining neuromelanin granules and thus confirmed that these were dopaminergic, neuronal nuclei and not glial nuclei. Such yellow-orange condensed nuclei were clearly visible in cryosections; however, it was difficult to visualize neuromelanin granules in the frozen sections.

Figure 1A1 presents interference contrast, confocal images of typical neuromelanin-containing neurons from an aged control nigra. Figure 1B1 presents a condensed apoptotic nucleus (filled arrow) with associated neuromelanin (open arrow) near a larger, partially out of focus melanized neuron. Confocal microscopy revealed that the condensed, YOYO-bright nuclei viewed with epifluorescence microscopy did indeed have an apoptotic chromatin condensation pattern while normal, control nuclei showed no such condensation pattern (Figs. 1A and B2). Note that an intense ISEL signal, reflecting DNA fragmentation, occurred concomitantly with chromatin condensation in the condensed apoptotic nucleus (Fig. 1B3) while nonapoptotic nuclei demonstrated only a low background signal with Bodipy-ISEL (Fig. 1A3).

A second, unique pattern of ISEL/YOYO staining was observed only in the PD nigra (Fig. 2). A limited number of melanized neurons, with or without Lewy bodies (Figs. 2A1 and 2B1), contained nuclei with small, YOYO-bright granules, often accompanied by an increased density of YOYO staining at the nuclear perimeter (Figs. 2A2 and 2B2). The Lewy body is indicated by the open arrow in Fig. 2B and is immediately bordered by small, dark intracellular neuromelanin granules. A round clump of extracellular neuromelanin granules is indicated by the filled arrow immediately below the Lewy body-containing neuron in Fig. 2B. Note that extracellular neuromelanin can be strongly autofluorescent. The plasma membrane of these dopaminergic neurons appeared to be intact and there was no obvious swelling (or condensation) of the cell. The YOYO granularities were accompanied by similar-sized bright concentrations of ISEL that appeared to colocalize with the YOYO granularities (Figs. 2A3 and 2B3).



It is not clear if this represents an early stage of apoptotic nuclear degeneration since no other markers were used on these sections to detect proapoptotic proteins. It is possible that the concentrations of ISEL could reflect increased DNA vulnerability to strand breakage in the PD brain compared to aged control brain, but this would not explain the corresponding condensation of chromatin which is an energy-dependent event (28). It does not seem likely that this pattern is the result of nonspecific DNA degradation due to perimortem events or tissue processing, since only a small number of melanized neurons were affected and only in the nigra of the PD cases. Importantly, a granular ISEL pattern was never observed without an accompanying granular YOYO pattern, although granular YOYO staining on its own could be observed. This could be interpreted to suggest that chromatin condensation may precede detectable DNA fragmentation.

#### *Increased Incidence of Apoptotic Nuclei Correlates with Decreased Number of Neuromelanin Neurons in PD Nigra*

There was no obvious difference in the sensitivity of the ISEL/YOYO method to detect apoptotic nuclei in frozen or paraffin sections; therefore, data from both frozen (corrected for section thickness) and paraffin sections were combined. The number of neuromelanin-containing neurons (with a nucleolus) was counted under Nomarski optics on all PD and control sections treated with ISEL/YOYO and are presented in Fig. 3A as a scatterplot with accompanying standard deviation. There is a clear decrease in the number of intact neuromelanin-containing neurons in the randomly chosen PD nigral sections compared to the aged control nigral sections. Only small, condensed apoptotic nuclei (joint positive ISEL/YOYO staining) were counted and expressed as a percentage of the number of neuromelanin cells on each section (Fig. 3B). This was done in order to facilitate comparisons between the number of apoptotic nuclei in PD and control tissue. When expressed this way, it was apparent that a significantly smaller percentage of apoptotic nuclei were found in aged control nigral sections compared to PD sections. The percentage value is not to be considered as equivalent to the rate of cell death, but rather represents the frequency of detectable apoptotic nuclei that are present in the selected tissue for the time window sampled. Further, the marking system (ISEL/YOYO) detects a specific stage of the apoptotic process and the duration of this stage in the human brain is unknown. In this study, the postmortem interval ranged between 2.75 and 7 h in PD cases and 8 and 11 h in control cases. The duration of the postmortem interval can have direct consequences on the specificity of the ISEL method. Others have found that a prolonged postmortem interval (>24 h) can produce increased numbers of

ISEL-positive, but not necessarily apoptotic, nuclei in control sections (30) (see Discussion). Nonparametric Mann-Whitney U tests revealed that there was a significant difference between age-matched controls and PD cases for both the number of remaining melanized somata/section and the number of ISEL/YOYO-positive nuclei/melanized somata at a *P* value of 0.0005.

#### *Increased Caspase 3 and Bax Immunoreactivity in PD*

Collapse of the mitochondrial membrane potential is an early event in apoptosis (64) compared to nuclear degradative events. Normally, the permeability transition pore is held closed, but opening of the pore during apoptosis can lead to a decline in the mitochondrial membrane potential and uncoupling of the respiratory chain. *In vitro* studies have shown that Bax moves from the cytosol to the mitochondria during apoptosis and binds to the adenine nucleotide translocator, a component of the pore complex, and holds the pore open during apoptosis (37, 67). Alternately, Bax may destabilize the outer mitochondrial membrane (7) or associate with the voltage-dependent anion channel (55) and permit the release of cytochrome *c* into the cytosol. Once in the cytosol, cytochrome *c* promotes the activation of procaspase 9, which then activates caspase 3 (31, 57). Activated caspase 3 can in turn activate other caspases as well as induce nuclear apoptotic degeneration via DNA fragmentation factor or acinus (35, 51).

Bax and caspase 3 immunoreactivity was visualized with a red, aminoethylcarbazole reaction product, in order to readily distinguish it from the brown-black neuromelanin granules found in the soma. Both Bax and (pro- and activated) caspase 3 immunoreactivity occurred in clusters of melanized cells or was associated with membrane-enclosed neuromelanin debris in the neuropil of the PD nigra (Figs. 4A1 and 4B1). The extent of detectable caspase 3 or Bax immunoreactivity varied among cells. In some cells, Bax immunoreactivity appeared as a fine, punctate staining pattern while in other cells Bax appeared to occupy a significant proportion of the cytosol in the immediate vicinity of the neuromelanin granules (indicated by arrows in Fig. 4B2). Cytosolic caspase 3 immunoreactivity was found in close association with neuromelanin granules occupying a varying proportion of the cytosol (indicated by arrows in Fig. 4A2). Only a very few Bax-positive cells were observed among all of the control sections reacted simultaneously with PD sections, but no caspase 3-immunopositive cells were observed. This may be related to the low number of apoptotic nuclei found in the control brain sections. Caspase 3- and Bax-immunoreactive profiles were counted and expressed per number of neuromelanin somata (with a nucleolus) per section (Figs. 3C1 and 3C2). The number of neuromelanin



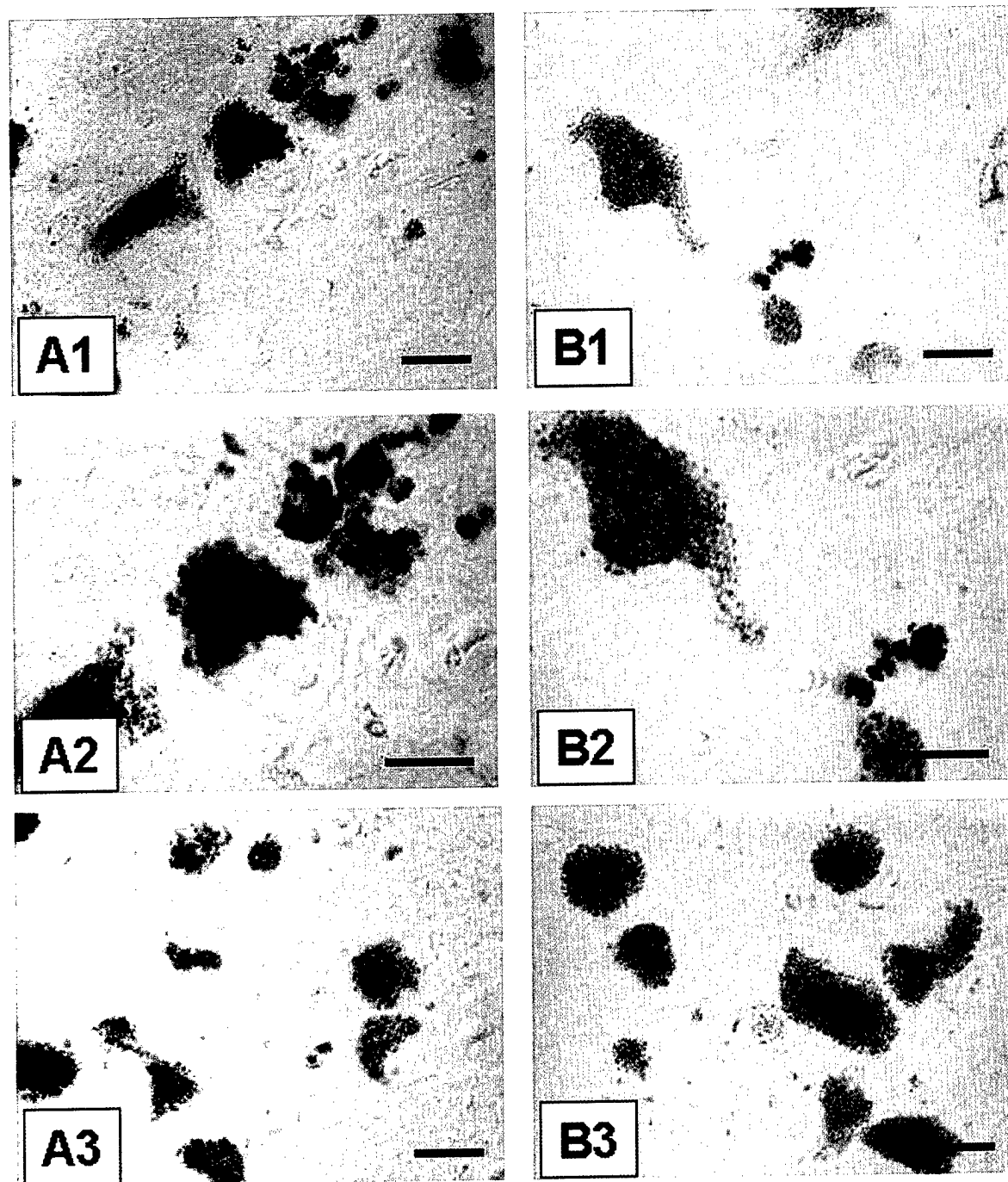


**FIG. 4.** Increased caspase 3 and Bax immunoreactivity in the PD nigra compared to control sections. The left-hand panel represents a low (A1) and a higher power (A2) view of the same (pro- and activated) caspase 3-immunoreacted PD nigral section. (B) A low (B1) and a higher power view (B2) of a Bax-immunoreacted PD nigral section. Black arrows in the middle panel indicate red immunoreaction product. Note that both proapoptotic proteins seem to appear in clusters of neuromelanin-containing neurons or with membrane-enclosed remnants of neuromelanin-containing somata in the neuropil. Immunoreactivity for both proteins appeared to concentrate in the cytosol surrounding neuromelanin granules, surrounding a few or the majority of neuromelanin granules in the cell profile. The bottom panels (A, B) represent simultaneously reacted control sections for caspase 3 and Bax, respectively. Bar, 10  $\mu$ m.

somata in control and PD sections is compared on the left half of each pair of histograms, while on the right are the number of immunoreactive profiles per neuromelanin somata per section. A greater number of

Bax- and caspase 3-immunoreactive profiles were observed in PD nigral sections compared to aged, control nigral sections. Further, more caspase 3-immunoreactive profiles were observed in the PD nigra compared to

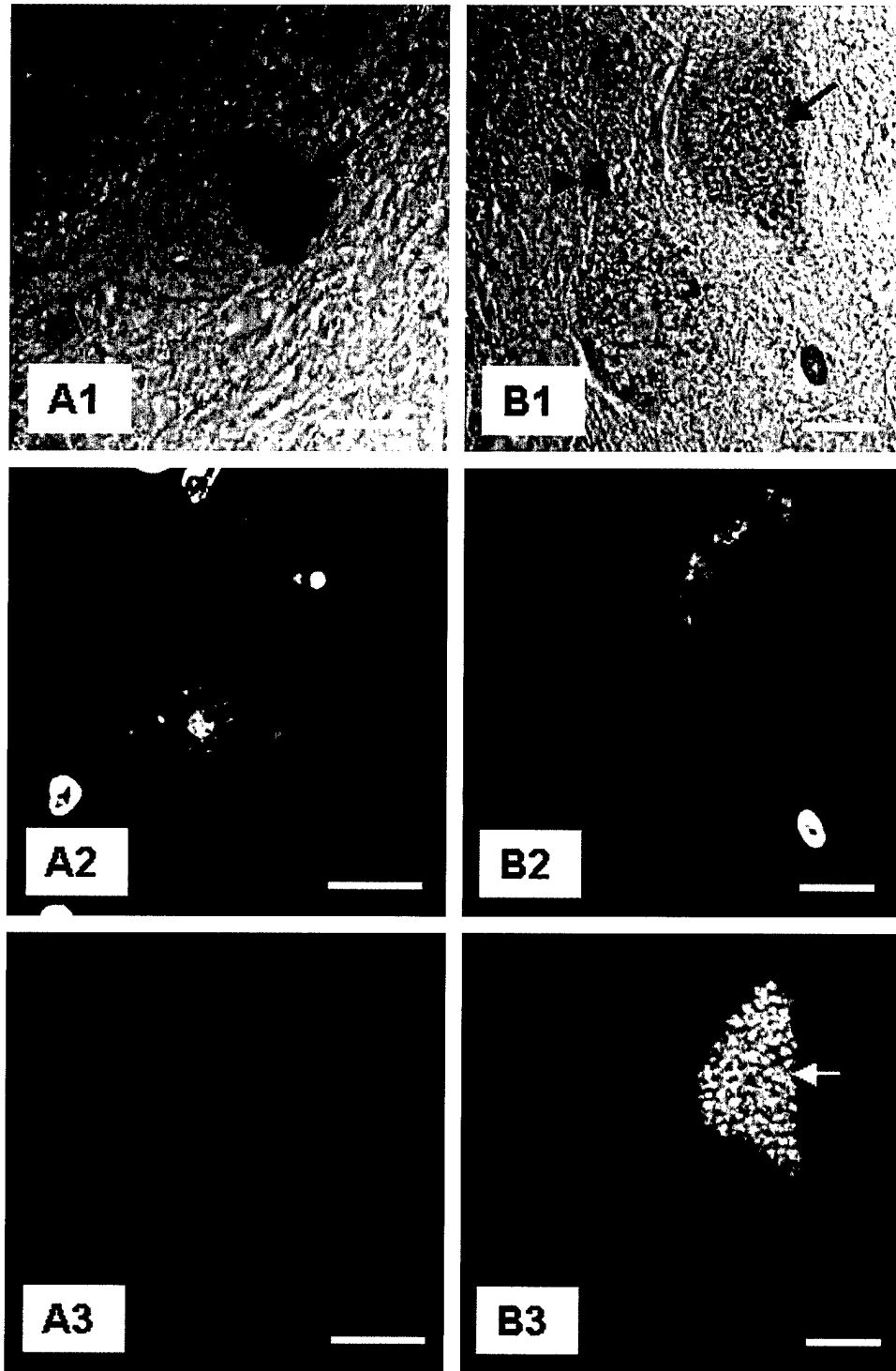


**FIG. 5.** Antiserum specific for activated caspase 3 shows an identical distribution pattern in PD nigral neurons. The left panel (A) depicts a melanized neuron from an age-matched control nigra while the right panel (B) depicts two melanized neuron profiles from a PD nigra. The top panel depicts digital interference contrast images; note the overall pallor of the melanized neurons in the PD nigra (arrow, B1) with a small amount of neuromelanin retaining the intense brown-black (arrowhead, B1) observed in the age-matched control (large arrowhead, A1). The middle panel represents the YOYO-1 staining pattern of the same sections with bright cytoplasmic fluorescence reflecting the presence of RNA. The bottom panel presents activated caspase 3 immunofluorescence (594 nm emission). Note the absence of immunofluorescence in the control nigral neuron (A3) while the uppermost neuron in the PD nigra (B3) shows bright caspase 3 immunofluorescence (white arrow) while the adjacent neuron shows limited immunoreactivity. A scan of the section in the far-red range (670 nm) revealed the signal contribution is due to specific immunoreactivity and not autofluorescence (data not shown). Bar, 10  $\mu$ m.

Bax-immunoreactive profiles. This would suggest either that caspase 3 is more accessible to antibody recognition or that the expression time window of these effector molecules during apoptosis is markedly different. Mann-Whitney U tests revealed that the number of caspase 3- or Bax-immunoreactive profiles was significantly different in PD cases compared to age-matched controls ( $P$  value of 0.0005).

The antiserum initially employed to detect caspase 3 immunoreactivity could not discriminate between procaspase 3 and activated caspase 3, although there was no detectable immunoreaction product observed in the age-matched controls run simultaneously with the PD sections. More recently, another antiserum became available which on immunoblotting was specific for the 17- to 20-kDa, activated caspase 3 fragment (45) and was accordingly tested on a limited number of PD and control nigral sections. An identical distribution was observed for the activated- caspase 3 immunoreactivity (Figs. 5A and 5B). A nigral neuron from an age-matched control is shown in Fig. 5A, while two neurons from a PD nigral section are shown in Fig. 5B. The arrows in the top panel (Fig. 5A1 and 5B1) identify neuromelanin granules in the interference contrast images. Note the overall pallor of the nigral neurons in the PD section compared with the age-matched control neuron. A small portion of one PD nigral neuron still retains intense brown-black neuromelanin pigmentation (arrowhead, Fig. 5B1). The middle panel depicts the identical section scanned for YOYO-1 fluorescence. In the bottom panel, activated caspase 3 immunofluorescence is demonstrated in the same section. Note the low background in the age-matched control nigral section (Fig. 5A3). Strong immunofluorescence for the active caspase 3 fragment was observed in the uppermost PD neuron profile in Fig. 5B3 (white arrow) but little or no immunoreactivity in the adjacent PD neuron. The overall staining pattern in the PD sections with antiserum to the active fragment appeared identical to that observed with the other caspase 3 antiserum shown in Fig. 4. Only one, immunopositive nigral neuron was observed among three sections selected from three dif-

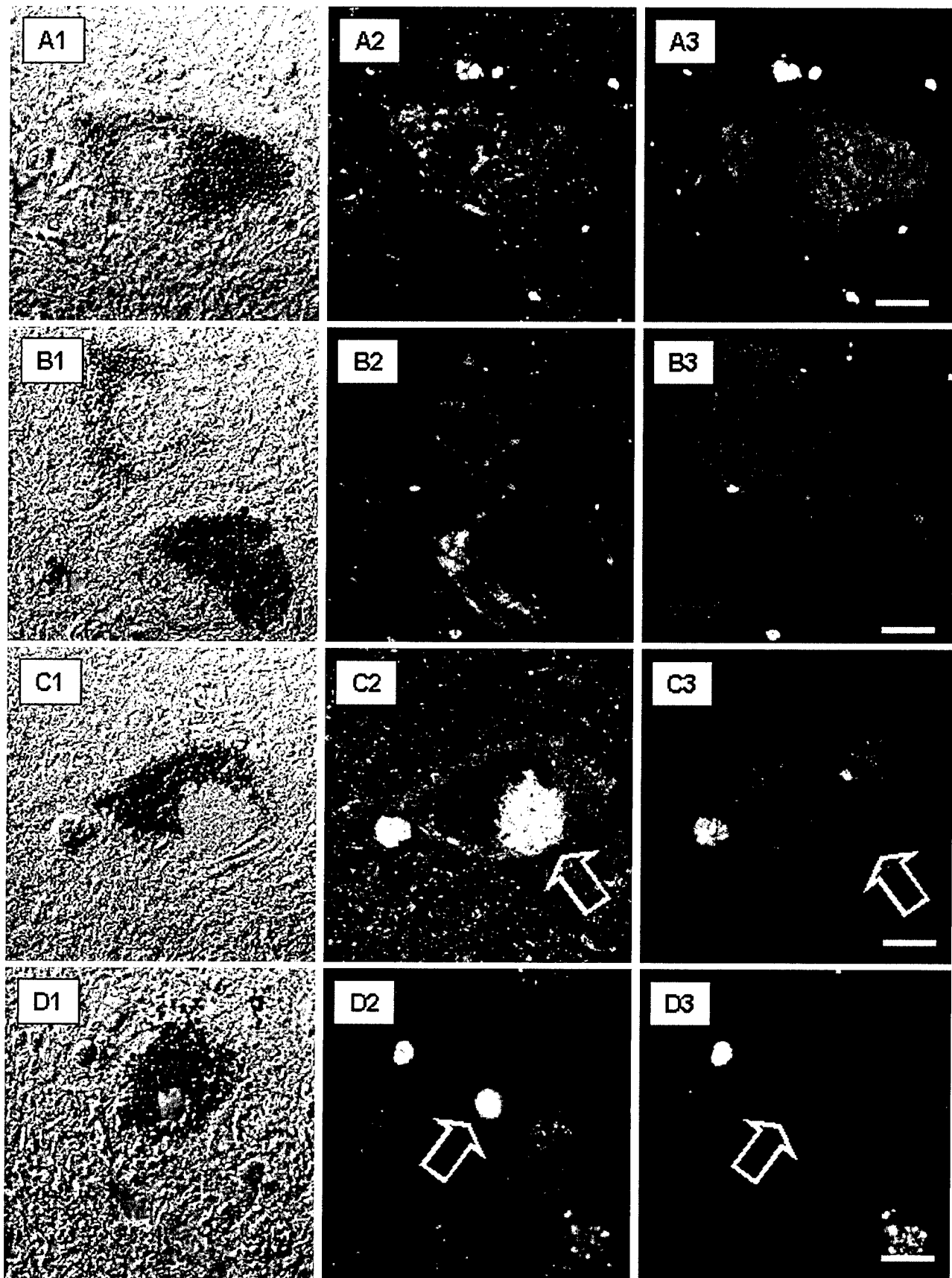
ferent age-matched control cases using antiserum to the active caspase 3 fragment.

#### *Nuclear Translocation of GAPDH in the PD Nigra*

GAPDH is a key enzyme in the glycolytic pathway but it also plays a role in endocytosis, mRNA regulation, and nuclear tRNA transport (56). Recently, *in vitro* studies have shown that overexpressed GAPDH translocates to the neuronal nucleus during apoptosis, but not in necrosis (26, 27) for both immature (1 day *in vitro*) and mature (7 days *in vitro*) cerebellar granule cells. GAPDH nuclear accumulation has also been observed in postmitotic cortical neurons undergoing apoptosis in serum-free media as well as nonneuronal cells *in vitro* (52). Antisense oligonucleotides for GAPDH block apoptosis (25) suggesting that this protein may play a direct role in apoptosis. Translocation of GAPDH occurs prior to nuclear degeneration and thus the addition of deprenyl-like compounds which block the nuclear translocation of GAPDH also reduce the number of apoptotic nuclei (9).

In aged control nigral sections, confocal microscopy revealed GAPDH in the cytosol of melanized neurons (Fig. 6A2), but that it tended to aggregate in areas of reduced neuromelanin presence, such as the somal periphery in some PD neurons (Fig. 6B2). YOYO-1 counterstaining of a few sections demonstrated that cytosolic RNA tended to concentrate along the perimeter of neurons with abundant neuromelanin (see Fig. 1). Nuclear accumulation of GAPDH was observed in a small number of melanized neurons in all PD sections reacted (two to three sections per case) although not all immunopositive nuclei demonstrated complete filling with GAPDH as shown in Fig. 6C2. Note that the nuclear staining pattern is not homogeneous, suggesting that GAPDH may have a specific nuclear protein or DNA association. GAPDH nuclear accumulation was not observed in control nigral sections. Many Lewy bodies in the PD nigra were found to be strongly immunofluorescent for GAPDH (Fig. 6D2) although it is not known whether all Lewy bodies are GAPDH im-

**FIG. 6.** Confocal microscopy reveals nuclear translocation of GAPDH in melanized neurons of the PD nigra and GAPDH immunoreactivity in the Lewy body. The left panel represents digital interference contrast images of all cells, the middle panel presents GAPDH immunofluorescence (594 nm emission), and the right panel presents signal contribution from tissue autofluorescence. The top horizontal panel depicts a normal neuromelanin-containing neuron (A1) from a control nigra while the second panel shows a nonapoptotic melanized neuron (B1) from a PD nigral section. Note that GAPDH distribution in the normal control neuron (A2) appears as punctate staining in areas of cytosol with little neuromelanin while GAPDH in the nonapoptotic PD neuron tends to be localized in the cell periphery, also away from neuromelanin granules (B2). When the same sections are viewed with filters to detect fluorescent contribution from far red wavelengths (670 nm emission) which excludes specific GAPDH immunofluorescence only the autofluorescent signal contribution is evident (A3, B3). The third horizontal pattern shows a neuromelanin-containing neuron from a PD nigral section (C1) with nuclear translocation of GAPDH (open arrow, C2). Note the heterogeneous pattern of nuclear immunoreactivity suggesting that GAPDH may associate with specific nuclear components. Importantly, the nuclear immunofluorescence is entirely due to GAPDH and not autofluorescence since no nuclear signal is apparent when scanned in the far-red range (open arrow, C3). Note that a small clump of extracellular neuromelanin in the neuropil immediately left of the neuron retains its autofluorescence in the far-red range (C3). The bottom panel shows a melanized neuron from a PD nigral section (D1) with a Lewy body, which is strongly immunofluorescent for GAPDH (open arrow, D2). Note that there was no autofluorescent component to the Lewy body fluorescence (open arrow, D3). Bar, 10  $\mu$ m.



munopositive. In order to demonstrate that cellular GAPDH staining was not due to autofluorescence, each cell was also imaged under excitation/emission filters to detect fluorescent signal contribution in the far-red range (690 nm) which would include autofluorescence but exclude GAPDH signal (Figs. 6A1–6D3). Note that the somal and nuclear GAPDH patterns demonstrated in the center panels were therefore due exclusively to GAPDH immunoreactivity.

Nuclear inclusion bodies, known as Marinesco's bodies, can occur in melanized neurons in the aged brain. These bodies may be as large as the nucleolus, are eosinophilic (Figs. 7A1 and 7B1), and have been found to contain 12- to 14-nm-thick filaments when observed by electron microscopy (20). In the aged control nigra, Marinesco's bodies were GAPDH immunonegative (data not shown). In contrast, these bodies were GAPDH immunopositive in nonapoptotic PD nigral neurons while the nucleolus remained GAPDH immunonegative (Fig. 7B2). The purpose of these nuclear inclusion bodies remains unknown as well as the nature of the association with GAPDH.

## DISCUSSION

### *Critical Considerations in the Application of ISEL to Human Postmortem Tissue*

The enhanced spatial resolution of confocal laser microscopy can provide subnuclear detail of ISEL/YOYO-labeled nuclei to confirm that neuronal apoptosis in PD presents a classic pattern of chromatin condensation (60) accompanied by apoptosis-specific DNA fragmentation. Critical to the success of the ISEL method is a brief postmortem interval (preferably less than 12 h) which decreases the probability of nonapoptotic DNA strand breaks being available for labeling (2, 30, 48). Forensic DNA studies report a steady increase in DNA degradation, as observed by electrophoresis, following several hours or days of postmortem interval delay (6). Proteinase K digestion, often used to improve ISEL signal strength, can also increase the probability of nonspecific ISEL in the nucleus and cytoplasm following excessive digestion (38, 59). Choice of enzyme can also influence ISEL outcome. DNA polymerase has been reported to produce a weaker ISEL signal, possibly by preferential single-strand labeling and more nonspecific labeling under certain conditions (36). Variations in the incubation time allowed for the TdT labeling reaction also affect the strength of the ISEL signal (38). A 60-min TdT incubation produces a clear nuclear signal in the PD nigra (30, 41, 60) while a 30-min TdT incubation does not appear to produce a convincing signal (68). Similarly, a low concentration (0.1 mM) of cobalt chloride in the reaction mix appears insufficient to drive the enzyme (32). On the other hand, a 1.0–2.5 mM cobalt chloride concentration

would encourage the labeling of single- and double-strand DNA breaks and potentially improve signal strength (41, 60).

### *Number of Apoptotic Nuclei and the Rate of Cell Death*

It is generally considered that apoptotic cells survive only for a few hours *in vivo*, but there is no evidence to support this assumption in the human brain. In fact, some have argued that apoptotic neurons may survive for several months *in situ* in the human cortex (8). In animal models, neurons enter the apoptotic pathway at different times following the initial stimulus, demonstrating that apoptosis is an asynchronous event which may be influenced by the nature of the initiating insult (34, 50, 59). In PD, the nature and delivery of the initiating insult remains unknown and therefore it is difficult to determine not only the "survival" time of an apoptotic neuron, but also whether apoptosis follows a linear, logarithmic, or even sinusoidal progression. Different drug regimens, stage of the disease, and overall health must be considered as contributing factors to cell survival and may thus be capable of affecting the number of apoptotic cells observed (see (15) for details). The "lifetime" of an apoptotic cell will thus influence the number of dying cells observed per section.

Further, the probability of detecting an apoptotic cell will vary depending on the marker chosen. The duration of events that typify different phases of apoptosis such as GAPDH nuclear accumulation, Bax upregulation, or DNA fragmentation remains unknown. Thus the percentage of apoptotic cells detected per section will vary according to the "expression time" of the specific biological marker chosen. Based on this assumption, our data would suggest that detectable caspase 3 upregulation may have a longer expression time compared to upregulated Bax expression time. Thus, a different percentage of apoptotic cells per section (or per surviving neuron) is calculated, depending on the selected marker. Therefore, the percentage of ISEL/YOYO-positive apoptotic nuclei cannot be considered as equivalent to the rate of cell death.

### *Increased Caspase 3, Bax, and GAPDH Immunoreactivity*

The finding of GAPDH nuclear accumulation is preliminary, since the limited number of sections did not allow for a representative quantitative assessment of the number of GAPDH-immunoreactive nuclei in PD nigra. However, taken together with the ISEL/YOYO data and the increased immunoreactivity for caspase 3 and Bax, it would suggest that nuclear accumulation of GAPDH might be considered as an indicator of apoptosis in the PD nigra. It is not yet clear whether all  $\alpha$ -synuclein-immunopositive Lewy bodies are also

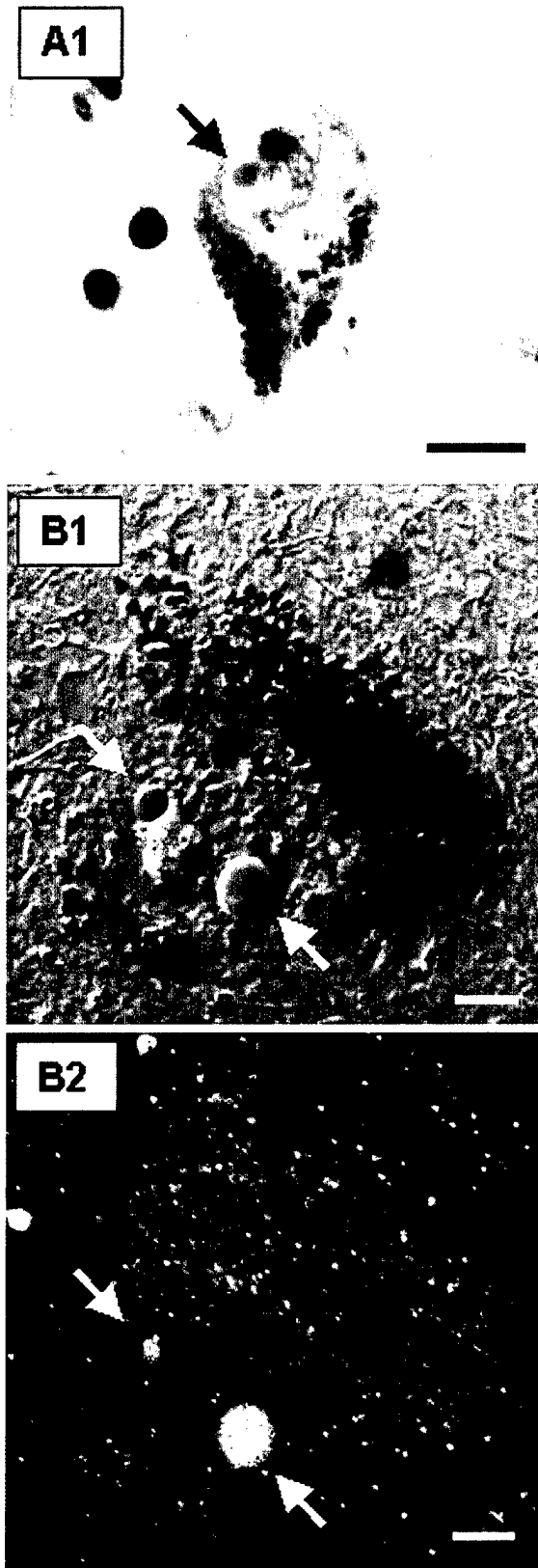


**FIG. 7.** Marinesco's bodies are GAPDH immunoreactive in melanized neurons in the PD nigra. The top panel (A1) depicts a hematoxylin and eosin-stained paraffin section of a PD nigral neuron

GAPDH immunopositive. If this is the case, then this observation may foreshadow other roles for GAPDH protein-protein interactions in neurodegeneration (9). Our finding of increased caspase 3 immunoreactivity in PD neurons using antiserum against pro- and activated caspase 3 was supported by examination of sections with antiserum specific to the activated form of caspase 3 which is now commercially available.

#### *Apoptosis and Mitochondrial Dysfunction in PD*

Other studies have reported defects in mitochondrial complex I activity in the PD nigra (13, 53, 54) and in the activity of other mitochondrial respiratory enzymes (10, 39, 40). Mutations in mitochondrial DNA may underlie some of the defects in mitochondrial energy metabolism and thus contribute to the pathogenesis of the disease (17, 33). Our findings of increased Bax and caspase 3 immunoreactivity might be interpreted as mitochondrially dependent pathways. But, a recent report notes that following stimulation by the Fas ligand, a cell can follow a Bid-dependent mitochondrial route for caspase 3 activation or bypass the mitochondria and trigger caspase 3 activation directly via caspase 8 activation (44). The finding of increased soluble Fas ligand and CD95 immunoreactivity in the PD brain makes the determination of which apoptotic signaling cascade is followed by PD neurons an intriguing question (24, 42)

GAPDH nuclear translocation has been observed to precede the decline in mitochondrial membrane potential *in vitro* (9, 62, 64) and its nuclear accumulation in PD nigral neurons would argue for a mitochondrially dependent apoptotic pathway. GAPDH was previously identified as a PIG (p53-induced gene) (49) by gene screening and more recently its upregulation *in vitro* has been shown to be modulated by p53 (11). Both caspase 3 and Bax have been reported to participate in a p53-dependent apoptotic signaling cascade (1, 14, 69). Studies are now in progress in order to determine whether nigral neurons can invoke p53 or Fas apoptotic signaling pathways in idiopathic PD. Knowledge of the signaling cascade(s) could lead to the development of drugs which would selectively block neuronal apoptotic pathways and thus halt the progress of the disease.

containing an eosinophilic Marinesco body in the nucleus (arrow). Bar, 25  $\mu$ m. (B1) A digital confocal image of a PD-melanized nigral neuron with two Marinesco's bodies (arrows) on either side of the nucleolus. (B2) Depicts a confocal image of the neuron in the same plane of focus demonstrating punctate GAPDH immunofluorescence in the cytosol and in the Marinesco's bodies (arrows). Note that the nucleolus is GAPDH immunonegative. Marinesco's bodies in control nigral sections were notably GAPDH immunonegative (not shown). Bar, 5  $\mu$ m (B1, B2).

## ACKNOWLEDGMENTS

The author thanks W. G. Tatton for assistance with GAPDH confocal imaging and Dr. Dan Perl and Dr. Dushyant Purohit for neuropathological assessment of all cases. This study was supported by a grant from the Bachmann-Strauss Dystonia & Parkinson Foundation, Inc.

## REFERENCES

1. Aloyz, R. S., S. X. Bamji, C. D. Pozniak, J. G. Toma, J. Atwal, D. R. Kaplan, and F. D. Miller. 1998. P53 is essential for developmental neuron death as regulated by the TrkA and p75 neurotrophin receptors. *J. Cell Biol.* **143**: 1691–1703.
2. Anderson, A. J., J. H. Su, and C. W. Cotman. 1996. DNA damage and apoptosis in Alzheimer's disease: Colocalization with c-Jun immunoreactivity, relationship to brain area, and effect of postmortem delay. *J. Neurosci.* **16**: 1710–1719.
3. Anglade, P., S. Vyas, E. C. Hirsch, and Y. Agid. 1997. Apoptosis in dopaminergic neurons of the human substantia nigra during normal aging. *Histol. Histopathol.* **12**: 603–610.
4. Anglade, P., S. Vyas, F. Javoy-Agid, M. T. Herrero, P. P. Michel, J. Marquez, A. Mouatt-Prigent, M. Ruberg, E. C. Hirsch, and Y. Agid. 1997. Apoptosis and autophagy in nigral neurons of patients with Parkinson's disease. *Histol. Histopathol.* **12**: 25–31.
5. Banati, R. B., S. E. Daniel, and S. B. Blunt. 1998. Glial pathology but absence of apoptotic nigral neurons in long-standing Parkinson's disease. *Mov. Disord.* **13**: 221–227.
6. Bar, W., A., Kratzer, M. Machler, and W. Schmid. 1988. Post-mortem stability of DNA. *Forensic Sci. Int.* **39**: 59–70.
7. Basanez, G., A. Nechushtan, O. Drozhinin, A. Chanturiya, E. Choe, S. Tutt, K. A. Wood, Y. Hsu, J. Zimmerberg, and R. J. Youle. 1999. Bax, but not Bcl-xL, decreases the lifetime of planar phospholipid bilayer membranes at subnanomolar concentrations. *Proc. Natl. Acad. Sci. USA* **96**: 5492–5497.
8. Busser, J., D. S., Geldmacher, and K. Herrup. 1998. Ectopic cell cycle proteins predict the sites of neuronal cell death in Alzheimer's disease brain. *J. Neurosci.* **18**: 2801–2807.
9. Carlile, G. W., R. M. E. Chalmers-Redman, N. A. Tatton, K. L. B. Borden, and W. G. Tatton. 2000. Reduced apoptosis after NGF and serum withdrawal: Conversion of tetrameric glyceraldehyde-3-phosphate dehydrogenase. *Mol. Pharm.* **571**: 2–12.
10. Cassarino, D. S., and J. Bennett. 1999. An evaluation of the role of mitochondria in neurodegenerative diseases: Mitochondrial mutations and oxidative pathology, protective nuclear responses, and cell death in neurodegeneration. *Brain Res. Rev.* **29**: 1–25.
11. Chen, R.-W., P. A. Saunders, H. Wei, L. Zhuangwu, P. Seth, and D.-M. Chuang. 1999. Involvement of glyceraldehyde-3-phosphate dehydrogenase (GAPDH) and p53 in neuronal apoptosis: Evidence that GAPDH is upregulated by p53. *J. Neurosci.* **19**: 9654–9662.
12. Cohen, G. M., X. M. Sun, R. T. Snowden, D. Dinsdale, and D. N. Skilleter. 1992. Key morphological features of apoptosis may occur in the absence of internucleosomal DNA fragmentation. *Biochem. J.* **286**: 331–334.
13. Cooper, J. M., V. M. Mann, D. Krige, and A. H. Schapira. 1992. Human mitochondrial complex I dysfunction. *Biochim. Biophys. Acta* **1101**: 198–203.
14. Cregan, S. P., J. G. MacLaurin, C. G. Craig, C. G. Robertson, G. S. Robertson, D. W. Nicholson, D. S. Park, and R. S. Slack. 1999. Bax-dependent caspase-3 activation is a key determinant in p53-induced apoptosis in neurons. *J. Neurosci.* **19**: 7860–7869.
15. Darzynkiewicz, Z., and F. Traganos. 1998. Measurement of apoptosis. *Adv. Biochem. Eng./Biotechnol.* **62**: 34–73.
16. Deibel, M., and M. S. Coleman. 1980. Biochemical properties of purified human terminal deoxynucleotidyltransferase. *J. Biol. Chem.* **255**: 4206–4212.
17. Di Monte, D. A. 1991. Mitochondrial DNA and Parkinson's disease. *Neurology* **41**(Suppl. 2): 38–42.
18. Didenko, V. V., and P. J. Hornsby. 1996. Presence of double-strand breaks with single-base 3' overhangs in cells undergoing apoptosis but not necrosis. *J. Cell Biol.* **135**: 1369–1376.
19. Dragunow, M., R. L. Faull, P. Lawlor, E. J. Beilharz, K. Singleton, E. B. Walker, and E. Mee. 1995. In situ evidence for DNA fragmentation in Huntington's disease striatum and Alzheimer's disease temporal lobes. *NeuroReport* **6**: 1053–1057.
20. Duchen, L. W. 1992. General pathology of neurons and neuroglia. In *Greenfield's Neuropathology* (J. H. Adams and L. W. Duchen, Eds.), pp. 1–68. Oxford Univ. Press, New York.
21. Dypbukt, J. M., M. Ankarcrona, M. Burkitt, A. Sjöholm, K. Stian, S. Orrenius, and P. Nicotera. 1994. Different pro-oxidant levels stimulate growth, trigger apoptosis or produce necrosis of insulin-secreting RINmSF cells: The role of intracellular polyamines. *J. Biol. Chem.* **269**: 30553–30560.
22. Funk, A., J. Rudel, C. Fellbaum, and H. Hoffer. 1994. Specific in situ end labeling of apoptosis shows different rates of programmed cell death in non-Hodgkin lymphomas. *Verh. Dtsch. Ges. Pathol.* **78**: 318–320.
23. Gavrieli, Y., Y. Sherman, and S. A. Ben-Sasson. 1992. Identification of programmed cell death in-situ via specific labeling of nuclear DNA fragmentation. *J. Cell Biol.* **119**: 493–501.
24. Hartmann, A., S. Hunot, and E. C. Hirsch. 1998. CD95 (APO-1/Fas) and Parkinson's disease. *Ann. Neurol.* **44**: 425–426.
25. Ishitani, R., and D. M. Chuang. 1996. Glyceraldehyde phosphate dehydrogenase antisense oligodeoxynucleotides protect against cytotoxic arabinonucleoside-induced apoptosis in cultured cerebellar neurons. *PNAS* **93**: 9937–9941.
26. Ishitani, R., K. Sunaga, M. Tanaka, H. Aishita, and D. M. Chuang. 1997. Overexpression of glyceraldehyde-3-phosphate dehydrogenase is involved in low K<sup>+</sup>-induced apoptosis but not necrosis of cultured cerebellar granule cells. *Mol. Pharmacol.* **51**: 542–550.
27. Ishitani, R., M. Tanaka, S. Datsuyoshi, N. Katsube, and D. M. Chuang. 1998. Nuclear localization of overexpressed glyceraldehyde-3-phosphate dehydrogenase in cultured cerebellar neurons undergoing apoptosis. *Mol. Pharmacol.* **53**: 701–707.
28. Kass, G. E., J. E. Eriksson, M. Weis, S. Orrenius, and S. C. Chow. 1996. Chromatin condensation during apoptosis requires ATP. *Biochem. J.* **318**: 749–752.
29. Kerr, J. F. R., A. H. Wyllie, and A. R. Currie. 1972. Apoptosis, a basic biological phenomenon with wide-ranging implications in tissue kinetics. *Br. J. Cancer* **26**: 239–257.
30. Kingsbury, A. E., C. D. Marsden, and O. J. F. Foster. 1998. DNA fragmentation in human substantia nigra: Apoptosis or perimortem effect? *Mov. Disord.* **13**: 877–884.
31. Kluck, R. M., E. Bossy-Wetzel, D. R. Green, and D. D. Newmeyer. 1997. The release of cytochrome c from mitochondria: A primary site for Bcl-2 regulation of apoptosis. *Science* **275**: 1132–1136.
32. Kosel, S., R. Egensperger, U. V. Eitzen, P. Mehraein, and M. B. Graeber. 1997. On the question of apoptosis in the parkinsonian substantia nigra. *Acta Neuropathol.* **93**: 105–108.
33. Kosel, S., C. B. Lucking, R. Egensperger, P. Mehraein, and M. B. Graeber. 1996. Mitochondrial NADH dehydrogenase and CYP2D6 in Lewy-body parkinsonism. *J. Neurosci. Res.* **44**: 174–183.
34. Kressel, M., and P. Groscurth. 1994. Distinction of apoptotic and necrotic cell death by in situ labelling of fragmented DNA. *Cell Tissue Res.* **278**: 549–556.



35. Liu, X., C. N. Kim, J. Yang, R. Jemmerson, and X. Wang. 1996. Induction of apoptotic program in cell-free extracts: Requirement for dATP and cytochrome c. *Cell* **86**: 147–157.
36. Lucassen, P. J., W. C. J. Chung, W. Kamphorst, and D. F. Swaab. 1997. DNA damage distribution in the human brain as shown by in situ end labeling: Area-specific differences in aging and Alzheimer disease in the absence of apoptotic morphology. *J. Neuropath. Exp. Neurol.* **56**: 887–900.
37. Marzo, E., C. Brenner, N. Zamzami, J. M. Jurgensmeier, S. A. Susin, H. L. A. Vieira, M. C. Prevost, z. Xie, S. Matsuyama, J. C. Reed, and G. Kroemer. 1998. Bax and adenine nucleotide translocator cooperate in the mitochondrial control of apoptosis. *Science* **281**: 2027–2031.
38. Migheli, A., P. Cavalla, S. Marino, and D. Schiffer. 1994. A study of apoptosis in normal and pathologic nervous tissue after in situ end-labeling of DNA strand breaks. *J. Neuropath. Exp. Neurol.* **53**: 606–616.
39. Mizuno, Y., S. Ikebe, N. Hattori, Y. Nakagawa-Hattori, H. Mochizuki, M. Tanaka, and T. Ozawa. 1995. Role of mitochondria in the etiology and pathogenesis of Parkinson's disease. *Biochim. Biophys. Acta* **1271**: 265–274.
40. Mizuno, Y., K. Suzuki, and S. Ohta. 1990. Postmortem changes in mitochondrial respiratory enzymes in brain and a preliminary observation in Parkinson's disease. *J. Neurol. Sci.* **96**: 49–57.
41. Mochizuki, H., K. Goto, H. Mori, and Y. Mizuno. 1996. Histochemical detection of apoptosis in Parkinson's disease. *J. Neurol. Sci.* **137**: 120–123.
42. Mogi, M., M. Harada, T. Kondo, Y. Mizuno, H. Narabayashi, P. Riederer, and T. Nagatsu. 1996. The soluble form of Fas molecule is elevated in parkinsonian brain tissues. *Neurosci. Lett.* **220**: 195–198.
43. Mogi, M., M. Harada, H. Narabayashi, H. Inagaki, M. Minami, and T. Nagatsu. 1996. Interleukin (IL)-1 $\beta$ , IL-2, IL-4, IL-6 and transforming growth factor- $\alpha$  levels are elevated in ventricular cerebrospinal fluid in juvenile parkinsonism and Parkinson's disease. *Neurosci. Lett.* **211**: 13–16.
44. Nagata, S. 1999. Biddable death. *Nature Cell Biol.* **1**: E143–E145.
45. Nicholson, D. W. 1999. Caspase structure, proteolytic substrates, and function during apoptotic cell death. *Cell Death Differ.* **6**: 1028–1042.
46. Oberhammer, F., J. W. Wilson, C. Dive, I. D. Morris, J. A. Hickman, A. E. Wakeling, P. R. Walker, and M. Sikorska. 1993. Apoptotic death in epithelial cells: Cleavage of DNA to 300 and/or 50 kb fragments prior to or in the absence of internucleosomal fragmentation. *EMBO J.* **12**: 3679–3684.
47. Peitsch, M. C., B. Polzar, H. Stephan, et al. 1993. Characterization of the endogenous deoxyribonuclease involved in nuclear DNA degradation during apoptosis programmed cell death. *EMBO J.* **12**: 371–377.
48. Petito, C. K., and B. Roberts. 1995. Effect of postmortem interval on in situ end-labeling of DNA oligonucleosomes. *J. Neuropathol. Exp. Neurol.* **54**: 761–765.
49. Polyak, K., Y. Xia, J. L. Zweier, K. W. Kinzler, and B. Vogelstein. 1997. A model for p53-induced apoptosis. *Nature* **389**: 300–305.
50. Rossiter, J. P., R. J. Riopelle, and M. A. Bisby. 1996. Axotomy-induced apoptotic cell death of neonatal rat facial motoneurons: Time course analysis and relation to NADPH-diaphorase activity. *Exp. Neurol.* **138**: 33–44.
51. Sahara, S., M. Aoto, Y. Eguchi, N. Imamoto, Y. Yoneda, and Y. Tsujimoto. 1999. Acinus is a caspase 3-activated protein required for apoptotic chromatin condensation. *Nature* **401**: 168–173.
52. Sawa, A., A. A. Khan, L. D. Hester, and S. H. Snyder. 1997. Glyceraldehyde-3-phosphate dehydrogenase: Nuclear translocation participates in neuronal and nonneuronal cell death. *PNAS* **94**: 11669–11674.
53. Schapira, A. H. 1993. Mitochondrial complex I deficiency in Parkinson's disease. *Adv. Neurol.* **60**: 288–291.
54. Schapira, A. H. 1999. Mitochondrial involvement in Parkinson's disease, Huntington's disease, hereditary spastic paraplegia and Friedreich's ataxia. *Biochim. Biophys. Acta* **1410**: 159–170.
55. Shimizu, S., T. Ide, T. Yanagida, and Y. Tsujimoto. 2000. Electrophysiological study of a novel large pore formed by Bax and the voltage-dependent anion channel that is permeable to cytochrome c. *J. Biol. Chem.* **275**: 12321–12325.
56. Sirover, M. A. 1997. Role of the glycolytic protein, glyceraldehyde-3-phosphate dehydrogenase, in normal cell function and in cell pathology. *J. Cell. Biochem.* **66**: 133–140.
57. Susin, S. A., N. Zamzami, M. Castedo, E. Daugas, H. G. Wang, S. Geley, F. Fassy, J. C. Reed, and G. Kroemer. 1997. The central executioner of apoptosis: Multiple links between protease activation and mitochondria in Fas/Apo-1/CD95- and ceramide-induced apoptosis. *J. Exp. Med.* **186**: 25–37.
58. Tabor, S., K. Struhl, S. J. Scharf, and D. H. Gelfand. 1997. Enzymatic manipulation of DNA and RNA. In *Current Protocols in Molecular Biology*. Wiley, New York.
59. Tatton, N. A., and S. J. Kish. 1997. In situ detection of apoptotic nuclei in the substantia nigra compacta of 1-methyl-4-phenyl-1,2,3,6-tetrahydropyridine-treated mice using terminal deoxynucleotidyl transferase labelling and acridine orange staining. *Neuroscience* **77**: 1037–1048.
60. Tatton, N. A., A. Maclean-Fraser, W. G. Tatton, D. P. Perl, and C. W. Olanow. 1998. A fluorescent double-labeling method to detect and confirm apoptotic nuclei in Parkinson's disease. *Ann. Neurol.* **44**(Suppl. 1): S142–S148.
61. Tatton, N. A., and H. J. Rideout. 1999. Confocal microscopy as a tool to examine DNA fragmentation, chromatin condensation and other apoptotic changes in Parkinson's disease. *Parkinsonism Related Disord.* **5**: 179–186.
62. Tatton, W. G., W. Y. Ju, D. P. Holland, C. Tai, and M. Kwan. 1994. (–)-Deprenyl reduces PC12 cell apoptosis by inducing new protein synthesis. *J. Neurochem.* **63**: 1572–1575.
63. Tompkins, M. M., E. J. Basgall, E. Zamrini, and W. D. Hill. 1997. Apoptotic-like changes in Lewy-body-associated disorders and normal aging in substantia nigral neurons. *Am. J. Pathol.* **150**: 119–131.
64. Wadia, J. S., R. M. E. Chalmers-Redman, W. J. H. Ju, G. W. Carlile, J. L. Phillips, A. D. Fraser, and W. G. Tatton. 1998. Mitochondrial membrane potential and nuclear changes in apoptosis caused by serum and nerve growth factor withdrawal: Time course and modification by (–)-deprenyl. *J. Neurosci.* **18**: 932–947.
65. Walker, P. R., J. Leblanc, and M. Sikorska. 1997. Evidence that DNA fragmentation in apoptosis is initiated and propagated by single-strand breaks. *Cell Death Differ.* **4**: 506–515.
66. Walker, P. R., and M. Sikorska. 1994. Endonuclease activities, chromatin structure, and DNA degradation in apoptosis. *Biochem. Cell Biol.* **72**: 615–623.
67. Wolter, K. G., Y. T. Hsu, C. L. Smith, A. Nechushtan, X. G. Xi, and R. J. Youle. 1997. Movement of Bax from the cytosol to mitochondria during apoptosis. *J. Cell Biol.* **139**: 1281–1292.
68. Wullner, U., J. Kornhuber, M. Weller, J. B. Schulz, P. A. Loschmann, P. Riederer, and T. Klockgether. 1999. Cell death and apoptosis regulating proteins in Parkinson's disease—A cautionary note. *Acta Neuropathol.* **97**: 408–412.
69. Xiang, H., Y. Kinoshita, C. M. Knudson, S. J. Korsmeyer, P. A. Schwartzkroin, and R. S. Morrison. 1998. Bax involvement in p53-mediated neuronal cell death. *J. Neurosci.* **18**: 1363–1373.